Advances in Materials Science and Engineering

Nanotechnology for Energy and Environment

Guest Editors: J. M. P. Q. Delgado, Andreas Öchsner, and A. G. Barbosa de Lima

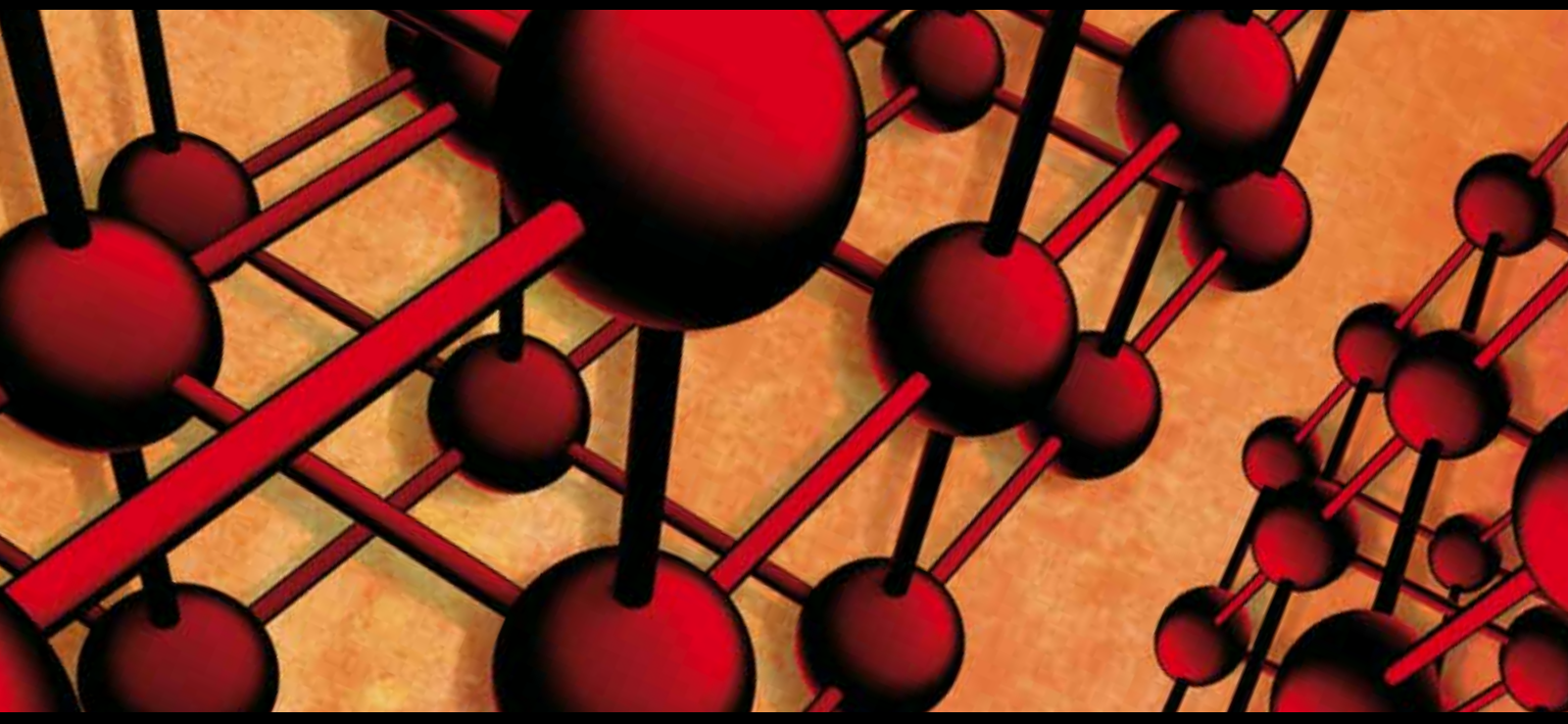

Nanotechnology for Energy and Environment

Advances in Materials Science and Engineering

Nanotechnology for Energy and Environment

Guest Editors: J. M. P. Q. Delgado, Andreas Öchsner,
and A. G. Barbosa de Lima

Editorial Board

Contents

Hindawi Publishing Corporation
Advances in Materials Science and Engineering
Volume 2014, Article ID 459108, 2 pages
http://dx.doi.org/10.1155/2014/459108

Editorial
Nanotechnology for Energy and Environment

J. M. P. Q. Delgado,[1] Andreas Öchsner,[2,3] and A. G. Barbosa de Lima[4]

[1] *Laboratory of Building Physics (LFC), Civil Engineering Department, Faculdade de Engenharia da Universidade do Porto, Rua Dr. Roberto Frias s/n, 4200-465 Porto, Portugal*
[2] *School of Engineering, Griffith University, Gold Coast Campus, Southport 4222, Australia*
[3] *School of Engineering, The University of Newcastle, Callaghan, NSW 2308, Australia*
[4] *Department of Mechanical Engineering, Federal University of Campina Grande, 58429-900 Campina Grande, PB, Brazil*

Correspondence should be addressed to J. M. P. Q. Delgado; jdelgado@fe.up.pt

Received 19 May 2014; Accepted 19 May 2014; Published 25 June 2014

Nanotechnology is the engineering of functional systems at the molecular scale. While nanomaterials have been a part of our everyday life for quite some time, the past two decades have witnessed a fast growth of the nanotechnology sector. Nanotechnology is being used in several applications to improve the environment and to produce more efficient and cost-effective energy, such as generating less pollution during the manufacture of materials, producing solar cells that generate electricity at a competitive cost, cleaning up organic chemicals polluting groundwater, and cleaning volatile organic compounds (VOCs) from air.

In this special issue the papers presented are devoted to the following. First is nanomaterials for building and construction, namely, a numerical and sensitivity analysis of the enthalpy and melting temperature effect on the inside building comfort sensation potential of the plastering mortar phase change materials (PCM). Building components with incorporated PCM are meant to increase heat storage capacity and enable stabilization of interior buildings surface temperatures whereby influencing the thermal comfort sensation and the stabilization of the interior ambient temperatures [1, 2]. Second is nanotechnology for water treatment, such as a review of the possible applications of the nanoparticles/fibers for the removal of pollutants from water/wastewater. The work presented overviews the availability and practice of different nanomaterials for removal of great number pollutants present in surface water, ground water, and industrial water. Several recommendations are made based on the current practices of nanotechnology applications in water industry. Third work presents the separation of TiO_2 photocatalyst nanoparticle. The results showed that flocculation of TiO_2 nanoparticles is influenced by ionic strength and pH. Fourth is nanotechnology for electrochemical conversion and energy storage, such as the progress update with the development of nanodielectric composites with electric field tunability for various high energy and high power electrical applications. Fifth is nanostructures, such as the numerical analysis of several zigzag and armchair single-walled carbon nanotubes (CNTs), to study the vibrational behaviour. The results presented showed that natural frequency of straight armchair and zigzag CNTs increases with the increase of the chiral number of both armchair and zigzag CNTs. It was also revealed that the natural frequency of CNTs with higher chirality decreases by introducing bending angles [3, 4]. Sixth is nanomaterials for solar cells, namely, the utilization of nanostructure graphene thin films as electron transfer layer in dye-sensitized solar cells. Those materials are of particular interest in the field of solar energy owing to their low cost and simplicity of fabrication. Seventh is nanocomposites, namely, the influence of processing type in the morphology of membranes obtained from PA6/MMT nanocomposites. Nanocomposites have an extensive use in the current process of membrane preparation, taking into account their unique features as membranes. Eighth paper presents the evaluation of thermomechanical behaviour during heating of nanocomposites of epoxy resin containing bentonite clay.

We hope that readers will find in this special issue not only accurate data and updated reviews on the nanotechnology field area but also important questions to be resolved. This special issue includes both theoretical and experimental developments, providing a self-contained major reference that is appealing to both the scientists and the engineers. At the same time, these topics will be going to the encounter of a variety of scientific and engineering disciplines, such as chemical, civil, agricultural, and mechanical engineering.

J. M. P. Q. Delgado
Andreas Öchsner
A. G. Barbosa de Lima

References

[1] P. Ahadi, "Applications of nanomaterials in construction with an approach to energy issue," *Advanced Materials Research*, vol. 261–263, pp. 509–514, 2011.

[2] A. V. Sá, M. Azenha, H. De Sousa, and A. Samagaio, "Thermal enhancement of plastering mortars with Phase Change Materials: experimental and numerical approach," *Energy and Buildings*, vol. 49, pp. 16–27, 2012.

[3] A. Ghavamian and A. Öchsner, "Numerical modeling of eigenmodes and eigenfrequencies of single- and multi-walled carbon nanotubes under the influence of atomic defects," *Computational Materials Science*, vol. 72, pp. 42–48, 2013.

[4] M. Farsadi, A. Öchsner, and M. Rahmandoust, "Numerical investigation of composite materials reinforced with waved carbon nanotubes," *Journal of Composite Materials*, vol. 47, no. 11, pp. 1425–1434, 2013.

Hindawi Publishing Corporation
Advances in Materials Science and Engineering
Volume 2014, Article ID 825910, 24 pages
http://dx.doi.org/10.1155/2014/825910

Review Article

A Review of Removal of Pollutants from Water/Wastewater Using Different Types of Nanomaterials

M. T. Amin, A. A. Alazba, and U. Manzoor

Alamoudi Water Research Chair, King Saud Universtiy, P.O. Box 2460, Riyadh 11451, Saudi Arabia

Correspondence should be addressed to M. T. Amin; mtamin@ksu.edu.sa

Received 2 January 2014; Revised 3 March 2014; Accepted 3 March 2014; Published 23 June 2014

Academic Editor: A. G. Barbosa de Lima

The rapidly increasing population, depleting water resources, and climate change resulting in prolonged droughts and floods have rendered drinking water a competitive resource in many parts of the world. The development of cost-effective and stable materials and methods for providing the fresh water in adequate amounts is the need of the water industry. Traditional water/wastewater treatment technologies remain ineffective for providing adequate safe water due to increasing demand of water coupled with stringent health guidelines and emerging contaminants. Nanotechnology-based multifunctional and highly efficient processes are providing affordable solutions to water/wastewater treatments that do not rely on large infrastructures or centralized systems. The aim of the present study is to review the possible applications of the nanoparticles/fibers for the removal of pollutants from water/wastewater. The paper will briefly overview the availability and practice of different nanomaterials (particles or fibers) for removal of viruses, inorganic solutes, heavy metals, metal ions, complex organic compounds, natural organic matter, nitrate, and other pollutants present in surface water, ground water, and/or industrial water. Finally, recommendations are made based on the current practices of nanotechnology applications in water industry for a stand-alone water purification unit for removing all types of contaminants from wastewater.

1. Introduction

Water has a broad impact on all aspects of human life including but not limited to health, food, energy, and economy. In addition to the environmental, economic, and social impacts of poor water supply and sanitation [1–4], the supply of fresh water is essential for the safety of children and the poor [5, 6]. It is estimated that 10–20 million people die every year due to waterborne and nonfatal infection causes death of more than 200 million people every year [7]. Every day, about 5,000–6,000 children die due to the water-related problem of diarrhea [8, 9]. There are currently more than 0.78 billion people around the world who do not have access to safe water resources [10] resulting in major health problems. It is estimated that more than one billion people in the world lack access to safe water and within couple of decades the current water supply will decrease by one-third.

The portion of total run-off which constitutes stable run-off flow is considered as the freshwater resource upon which humans depend. This stable fresh water flow has been estimated at 12,500–15,000 km^3 per year [11, 12], from which 4000 km^3 per year is considered to be the total freshwater for irrigation, industry, and domestic purposes [13], and which is estimated to increase to a range of 4300–5000 km^3 per year in 2025 [14–16]. Alternatively, only accessible fresh water is 0.5% of the world's 1.4 billion Km^3 of water which is furthermore poorly distributed across the globe [17].

There is limited possibility of an increase in the supply of fresh water due to competing demands of increasing populations throughout the world; also, water-related problems are expected to increase further due to climate changes and due to population growth over the next two decades [18]. It is estimated that worldwide population will increase by about 2.9 billion people between now and 2050 (according to UN's average projections) [15]. Shortage of fresh water supply is also a result of the exploitation of water resources for domestic, industry, and irrigation purposes in many

parts of the world [19]. The pressure on freshwater resources due to the increasing world's demand of food, energy, and so forth [20, 21] is increasing more and more due to population growth and threats of climate change. Polluting surface/ground water sources is another cause of reduced fresh water supplies [22–24]. Aquifers around the world are depleting and being polluted due to multiple problems of saltwater intrusion, soil erosion, inadequate sanitation, contamination of ground/surface waters by algal blooms, detergents, fertilizers, pesticides, chemicals, heavy metals, and so forth [25–28].

The occurrence of new/emerging microcontaminants (e.g., endocrine disrupting compounds (EDCs)) in polluted water/wastewater has rendered existing conventional water/wastewater treatment plants ineffective to meet the environmental standards. The discharge of these compounds into the aquatic environment has affected all living organisms. The traditional materials and treatment technologies like activated carbon, oxidation, activated sludge, nanofiltration (NF), and reverse osmosis (RO) membranes are not effective to treat complex and complicated polluted waters comprising pharmaceuticals, personal care products, surfactants, various industrial additives, and numerous chemicals purported. The conventional water treatment processes are not able to address adequately the removal of a wide spectrum of toxic chemicals and pathogenic microorganisms in raw water.

This is the right time to address water problems since aquifers around the world are depleting due to multiple factors such as saltwater intrusion and contamination from surface waters. Using better purification technologies can reduce problems of water shortages, health, energy, and climate change. A considerable saving of potable water can be achieved through reuse of wastewater which, in turn, requires the development materials and methods which are efficient, cost-effective, and reliable. Although dilution of complex wastewater effluents can help decreasing the load of micropollutants downstream [29, 30], however, much of them pass through conventional water treatment due to occurrence of these substances in micro- or even in nanograms per liter.

Biological treatment systems such as activated sludge and biological trickling filters are unable to remove a wide range of emerging contaminants and most of these compounds remain soluble in the effluent [31–33]. Physicochemical treatments such as coagulation, flocculation, or lime softening proved to be ineffective for removing different EDCs and pharmaceutical compounds in various studies [34–36]. Chlorination, though providing residual protection against regrowth of bacteria and pathogens [37, 38], results in undesirable tastes and odors [39] in addition to the forming of different disinfection by-products (DBPs) in portable drinking water [40–43]. Ozonation has been considered to be a less attractive alternative due to expensive costs and short lifetime. Both ultraviolet (UV) photolysis and ion exchange, though being advanced type of treatments, are not feasible alternatives for micropollutants removal [44].

Membrane processes like microfiltration, ultrafiltration, NF, and RO, which are pressure-driven filtration processes, are considered as some new highly effective processes [44–49]. These are considered as alternative methods of removing huge amounts of organic micropollutants [50–52]. Water/wastewater treatment by membrane techniques is cost-effective and technically feasible and can be better alternatives for the traditional treatment systems since their high efficiency in removal of pollutants meets the high environmental standards [53]. NF and RO have proved to be quite effective filtration technologies for removal of micropollutants [54, 55]. RO is relatively more effective than NF but higher energy consumption in RO makes it less attractive than NF where removal of pollutants is caused by different mechanisms including convection, diffusion (sieving), and charge effects [56]. Although NF based membrane processes are quite effective in removing huge loads of micropollutants [57], advanced materials and treatment methods are required to treat newly emerging micropollutants.

Since the water industry is required to produce drinking water of high quality, there is a clear need for the development of cost-effective and stable materials and methods to address the challenges of providing the fresh water in adequate amounts. There are inventions of new treatment methods; however, they need to be stable, economical, and more effective as compared with the already existing techniques. For this, traditional treatment technologies have to be modernized, that is, updated or modified or replaced by developing materials and methods which are efficient, cost-effective, and reliable. This is particularly important to achieve a considerable potable water savings through reuse of wastewater in addition to tackling the day-by-day worsening quality of drinking water.

Nanotechnology has been considered effective in solving water problems related to quality and quantity [58]. Nanomaterials (e.g., carbon nanotubes (CNTs) and dendrimers) are contributing to the development of more efficient treatment processes among the advanced water systems [59]. There are many aspects of nanotechnology to address the multiple problems of water quality in order to ensure the environmental stability. This study provides a unique perspective on basic research of nanotechnology for water/wastewater treatment and reuse by focusing on challenges of future research.

The paper has three main sections following the introduction which briefly discusses the traditional and current practices in water/wastewater treatment. Section 2 describes mainly the properties and types of nanomaterials and their importance in water/wastewater treatment. Section 3 discusses different types of nanomaterials focusing on membranes for treating a variety of pollutants in water/wastewater. The application of nanomaterials is reviewed based on their functions in unit operation processes. Section 4 provides a summary and outlook in the form of conclusions and recommendations for their full-scale application.

2. Nanotechnology for Water/Wastewater Purification

There are rising demands of clean water throughout the world as freshwater sources/resources are depleting due to

prolonged droughts, increasing population, climate changes threats, and strict water quality standards [60, 61]. Masses in developing countries are using unconventional water sources (e.g., stormwater, contaminated fresh water, brackish water) due to limited and depleting fresh water supplies. The existing water treatment systems, distribution systems, and disposable habits coupled with huge centralized schemes are no more sustainable. The current researches do not adequately address the practices that guarantee the availability of water for all users in accordance with the stringent water quality standards [62].

Several commercial and noncommercial technological developments are employed on daily basis but nanotechnology has proved to be one of the advanced ways for water/waste water treatment. Developments in nanoscale research have made it possible to invent economically feasible and environmentally stable treatment technologies for effectively treating water/wastewater meeting the ever increasing water quality standards. Advances in nanotechnology have provided the opportunities to meet the fresh water demands of the future generations. It is suggested that nanotechnology can adequately address many of the water quality issues by using different types of nanoparticles and/or nanofibers [63]. Nanotechnology uses materials of sizes smaller than 100 nm in at least one dimension (Figure 1) meaning at the level of atoms and molecules as compared with other disciplines such as chemistry, engineering, and materials science [64, 65].

At this scale, materials possess novel and significantly changed physical, chemical, and biological properties mainly due to their structure, higher surface area-to-volume ratio offering treatment and remediation, sensing and detection, and pollution prevention [66, 67]. These unique properties of nanomaterials, for example, high reactivity and strong sorption, are explored for application in water/wastewater treatment based on their functions in unit operations as highlighted in Table 1 [68].

Nanoparticles can penetrate deeper and thus can treat water/wastewater which is generally not possible by conventional technologies [69]. The higher surface area-to-volume ratio of nanomaterials enhances the reactivity with environmental contaminants.

In the context of treatment and remediation, nanotechnology has the potential to provide both water quality and quantity in the long run through the use of, for example, membranes enabling water reuse, desalination. In addition, it yields low-cost and real-time measurements through the development of continuous monitoring devices [70, 71]. Nanoparticles, having high absorption, interaction, and reaction capabilities, can behave as colloid by mixing mixed with aqueous suspensions and they can also display quantum size effects [72–76]. Energy conservation leading to cost savings is possible due to their small sizes; however, overall usage cost of the technology should be compared with other techniques in the market [77]. Figure 2 depicts some of the different types of nanomaterials that can be used in water/wastewater treatment [78–80].

Nanomaterials have effectively contributed to the development of more efficient and cost-effective water filtration processes since membrane technology is considered as one of the advanced water/wastewater treatment processes [81–91]. Nanoparticles have been frequently used in the manufacturing of membranes, allowing permeability control and fouling-resistance in various structures and relevant functionalities [92, 93]. Both polymeric and inorganic membranes are manufactured by either assembling nanoparticles into porous membranes or blending process [94–96]. The examples of nanomaterials used in this formation include, for example, metal oxide nanoparticles like TiO_2. CNTs have resulted in desired outputs of improved permeability, inactivation of bacteria, and so forth [97, 98].

Finally, nanofibrous media have also been used to improve the filtration systems due to their high permeability and small pore size properties [99]. They are synthesized by a new and efficient fabrication process, namely, electrospinning and may exhibit different properties depending on the selected polymers [100]. In short, the development of different nanomaterials like nanosorbents, nanocatalysts, zeolites, dendrimers, and nanostructured catalytic membranes has made it possible to disinfect disease causing microbes, removing toxic metals, and organic and inorganic solutes from water/wastewater. An attempt is made to highlight the factors that may influence the efficiency of the removal processes based on the available literature in the following section.

3. Pollutants Removal Using Different Nanomaterials

3.1. Disinfection. Biological contaminants can be classified into three categories, namely, microorganisms, natural organic matter (NOM), and biological toxins. Microbial contaminants include human pathogens and free living microbes [101–105]. The removal of cyanobacterial toxins is an issue in conventional water treatment systems [106, 107]. Many adsorbents including activated carbon have reasonably good removal efficiencies and again a number of factors influence the removal process [108–111].

Contamination from bacteria, protozoans, and viruses is possible in both ground and surface water. The toxicity of the standard chlorine chemical disinfection in addition to the carcinogenic and very harmful by-products formation is already mentioned. Chlorine dioxide is expensive and results in the production of hazardous substances like chlorite and chlorate in manufacturing process. Ozone, on the other hand, has no residual effects but produces unknown organic reaction products. For UV disinfection, longer exposure time is required for effectiveness and also there is no residual effect. Despite advances in disinfection technology, outbreaks from waterborne infections are still occurring. So, advanced disinfection technologies must, at least, eliminate the emerging pathogens, in addition to their suitability for large-scale adoption. There are many different types of nanomaterials such as Ag, titanium, and zinc capable of disinfecting waterborne disease-causing microbes. Due to their charge capacity, they possess antibacterial properties. TiO_2 photocatalysts and metallic and metal-oxide nanoparticles are among the most promising nanomaterials with antimicrobial properties.

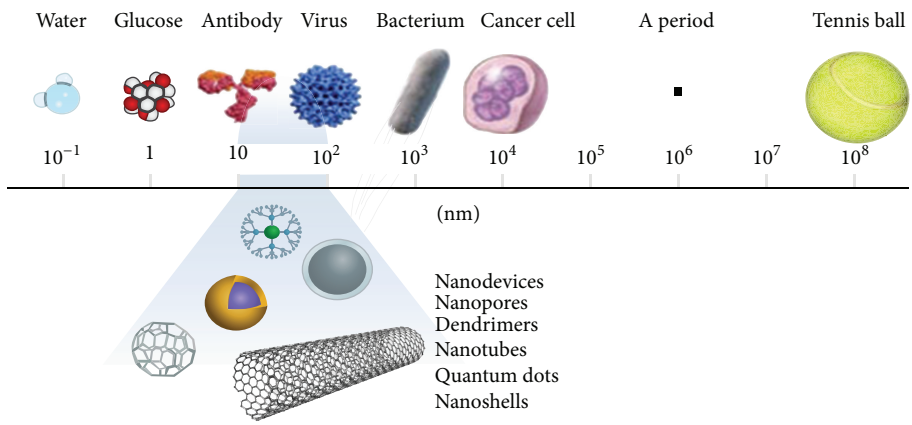

Figure 1: A size comparison of nanoparticle with other larger-sized materials.

Table 1: Examples of potential applications of nanotechnology in water/wastewater treatment.

Applications	Examples of nanomaterials	Some of novel properties
Adsorption	CNTs/nanoscale metal oxide and nanofibers	High specific surface area and assessable adsorption sites, selective and more adsorption sites, short intraparticle diffusion distance, tunable surface chemistry, easy reuse, and so forth.
Disinfection	Nanosilver/titanium dioxide (Ag/TiO_2) and CNTs	Strong antimicrobial activity, low toxicity and cost, high chemical stability ease of use, and so forth.
Photocatalysis	Nano-TiO_2 and Fullerene derivatives	Photocatalytic activity in solar spectrum, low human toxicity, high stability and selectivity, low cost, and so forth.
Membranes	Nano-Ag/TiO_2/Zeolites/Magnetite and CNTs	Strong antimicrobial activity, hydrophilicity low toxicity to humans, high mechanical and chemical stability, high permeability and selectivity, photocatalytic activity, and so forth.

The efficacy of metal ions in water disinfection has been highlighted by many researchers [112]. This part of the paper covers the application of these antimicrobial nanomaterials for water disinfection.

3.1.1. Silver Nanoparticles. Silver is the most widely used material due to its low toxicity and microbial inactivation in water [113–116] with well-reported antibacterial mechanism [117, 118]. Silver nanoparticles are derived from its salts like silver nitrate and silver chloride, and their effectiveness as biocides is documented in the literature [119–123]. Though the antibacterial effect is size dependent [124], smaller Ag nanoparticles (8 nm) were most effective, while larger particle size (11–23 nm) results in lower bactericidal activity [125]. Also, truncated triangular silver nanoplates exhibited better antibacterial effects than the spherical and rod-shaped nanoparticles indicating their shape dependency [126]. The mechanisms involved during the bactericidal effects of Ag nanoparticles include, for example, the formation of free radicals damaging the bacterial membranes [127, 128], interactions with DNA, adhesion to cell surface altering the membrane properties, and enzyme damage [122, 129, 130].

Immobilized nanoparticles have gained importance due to high antimicrobial activity [131]. Embedded Ag nanoparticles have been reported as very effective against both Gram-positive and Gram-negative bacteria [63]. In a study, the cellulose acetate fibers embedded with Ag nanoparticles by direct electrospinning method [132] were shown effective against both types of bacteria. Ag nanoparticles are also incorporated into different types of polymers for the production of antimicrobial nanofibers and nanocomposites [133–135]. Poly (ε-caprolactone-) based polyurethane nanofiber mats containing Ag nanoparticles were prepared as antimicrobial nanofilters in a study [136]. Different types of nanofibers containing Ag nanoparticles are prepared for antimicrobial application and exhibited very good antimicrobial properties [137–139]. Water filters prepared by polyurethane's foam coated with Ag nanofibers have shown good antibacterial properties against *Escherichia coli* (*E. coli*) [112].

There are other examples of low-cost potable microfilters prepared by incorporating Ag nanoparticles that can be used in remote areas in developing countries [140]. Ag nanoparticles also find their applications in water filtration membranes, for example, in polysulfone membranes [141], for biofouling reduction and have proved effective against variety of bacteria and viruses [142–148]. These Ag nanoparticles laden membranes had good antimicrobial activities against *E. coli*, *Pseudomonas*, and so forth [149, 150].

Finally, Ag nanocatalyst alone and incorporate with carbon covered in alumina has been demonstrated as efficient for degradation of microbial contaminants in water [151].

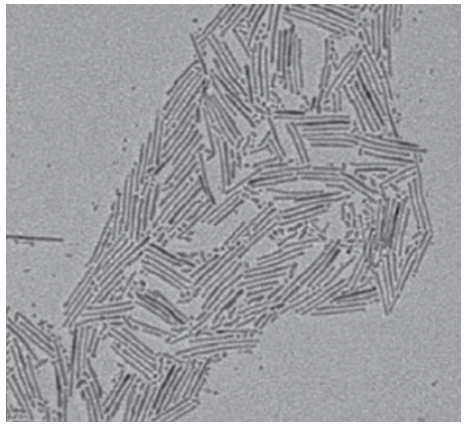

(a) TEM image of TiO_2 nanocrystals

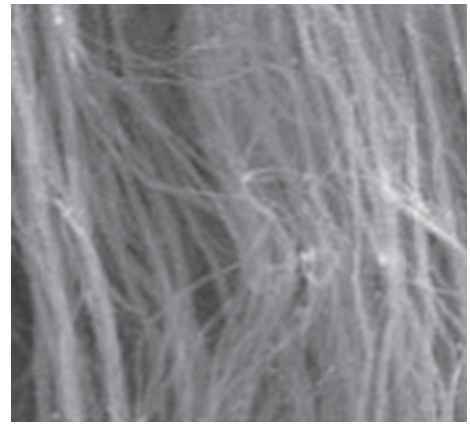

(b) SEM images of aligned CNTs

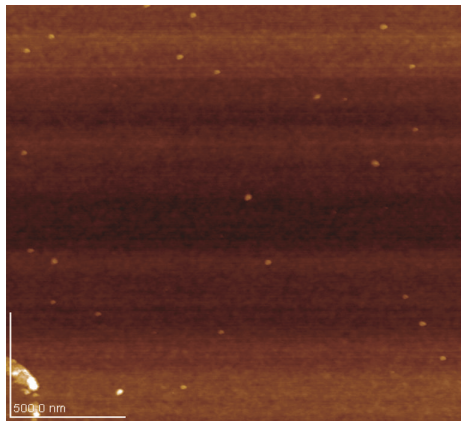

(c) AFM image of Zinc oxide (ZnO) nanoparticles

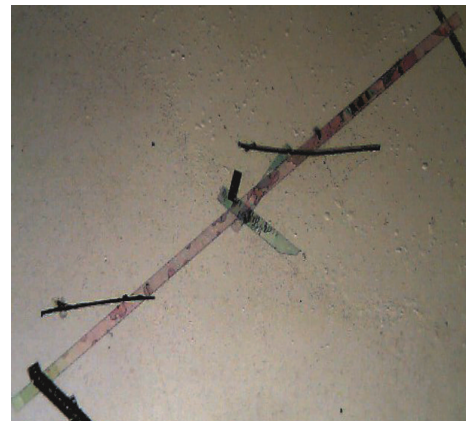

(d) Optical microscope image of Sn-doped ZnO nanobelts

Figure 2: Examples of different types of nanomaterials including particles, crystals, tube, and belts.

Although Ag nanoparticles have been used efficiently for inactivating bacteria and viruses as well as reducing membrane biofouling, their long-term efficacy against membrane biofouling has not been reported mainly due to loss of silver ions with time [152, 153]. So, further work to reduce this loss of silver ions is required for long-term control of membrane biofouling. Alternatively, doping of Ag nanoparticles with other metallic nanoparticles or its composites with metal-oxide nanoparticles can solve the issue and this could also lead to the parallel removal of inorganic/organic compounds from water/wastewater.

3.1.2. TiO_2 Nanoparticles. TiO_2 nanoparticles are among the emerging and most promising photocatalysts for water purification [154, 155]. The basic mechanism of a semiconductor-based photocatalysts like low-cost TiO_2 having good photoactivity and nontoxicity [156] involves the production of highly reactive oxidants, such as OH radicals, for disinfection of microorganisms, bacteria, fungi, algae, viruses, and so forth [157–165]. TiO_2, after 8 hours of simulated solar exposure, has been reported to reduce the viability of several waterborne pathogens such as protozoa, fungi, *E. coli*, and *Pseudomonas aeruginosa* [166]. A complete inactivation of fecal coliforms under sunlight is reported in a study expressing the photocatalytic disinfection efficiency of TiO_2 [167].

The limited photocatalytic capability of TiO_2, that is, only under UV light, has improved drastically by extending its optical absorbance to the visible-light region [168, 169]. This was achieved by doping transition metals [170] and anionic nonmetals such as nitrogen [171–180], carbon [181–187], sulfur [188–190], or fluorine [191] into TiO_2. Recently, Ag doping of TiO_2 has resulted in improved bacterial inactivation either by complete removal or decreased time of *E. coli* inactivation thereby enhancing disinfection under UV wavelengths and solar radiations [192–197].

As highlighted, the synthesis of visible-light-activated TiO_2 nanoparticles has attracted considerable interest [198], and TiO_2 nanoparticles and nanocrystallines irradiated with UV-visible light exhibited strong bactericidal activity against *E. coli* [199–202]. Metal-doped TiO_2 nanoparticles, sulfur, and iron in couple of studies have shown strong antibacterial effects against *E. coli* [203, 204]. TiO_2 was further modified by nanoparticles of transition metal oxides and nanostructured

TiO_2 photocatalysts showed great potential for water disinfection. For example, metal-ion-modified nitrogen-doped TiO_2 nanoparticle photocatalysts (palladium (Pd) in a study) have shown enhanced disinfection efficiency against *E. coli* (Gram-negative bacterium), *Pseudomonas aeruginosa*, and *Bacillus subtilis* spores due to photocatalytic oxidation under visible-light illumination [205, 206].

Nitrogen-doped TiO_2 nanoparticles catalysts have proved their efficiency for degradation of microbial contaminants in water [151]. Nanostructured TiO_2 films and membranes are capable of disinfecting microorganisms in addition to the decomposition of organic pollutants under UV and visible-light irradiation [207]. Due to its stability in water, TiO_2 can be incorporated in thin films or membrane filters for water filtration [208, 209]. TiO_2 nanorods and nanofilms exhibited a higher photocatalytic activity than commercial TiO_2 nanoparticles and TiO_2 thin films, respectively, for the photocatalytic inactivation of *E. coli* [191, 210, 211]. The inactivation mechanism of *E. coli* when using TiO_2 thin films was also investigated by many researchers [212, 213]. In a study, TiO_2 nanocomposites with multiwalled CNTs showed the complete inactivation of bacterial endospores (*Bacillus cereus*), compared to commercial TiO_2 nanoparticles [214]. Immobilized TiO_2 nanoparticle films successfully inactivated *E. coli K12* in surface and distilled water [215]. TiO_2 nanoparticles incorporated into an isotactic polypropylene polymeric matrix showed higher biocidal activity against *Enterococcus faecalis* and *Pseudomonas aeruginosa* [216].

The detailed review has demonstrated the antibacterial efficiency of TiO_2 nanoparticles, but the actual underlying mechanisms are not well defined especially under visible light. In addition, composites of TiO_2 nanoparticles by doping with other metallic nanoparticles have also shown their effectiveness, but the applications of using TiO_2 nanofibers and thin films need to be investigated for the effective removal of both inorganic/organic compounds in addition to the disinfection.

3.1.3. CNTs and Others. CNTs have proved to be very effective in removing bacterial pathogens. CNTs (one of nanosorbents) which have been used for removal of biological impurities have received special attention for their excellent capabilities of removing biological contaminants from water [63]. CNTs possess antimicrobial characteristics against a wide range of microorganisms including bacteria such as *E. coli* and *Salmonella* [217–222] and viruses [223, 224]. The adsorption of cyanobacterial toxins on CNTs is also higher when compared with carbon-based adsorbents mainly due to large specific surface area, external diameter of CNTs, large composition of mesoporous volume, and so forth [225–228].

Researchers have attributed the antimicrobial effects of CNTs to their unique physical, cytotoxic, and surface functionalizing properties [229], their fibrous shape [230, 231], the size and length of the tubes, and number of layers (single- or multiwalled) [155, 232]. The mechanisms of killing bacteria by CNTs are also due to the production of oxidative stress, disturbances to cell membrane, and so forth [233]. Although single-walled CNTs are more detrimental against microorganisms than multiwalled CNTs [234], dispersivity of CNTs is a more important parameter than length [235]. Many researchers observed an extremely high adsorption rate of bacteria by single-walled CNTs, in addition to their high sorption capacities by many researchers [236–244].

Filtration membranes containing radially aligned CNTs are very effective in removing both bacteria and viruses in very short time due to size exclusion and depth filtration [245–247] and thus enable such filters to be used as cost-effective and point-of-use water disinfection devices. CNTs can also reduce membrane biofouling and a nanocomposite membrane of single-walled CNTs and polyvinyl-N-carbazole showed high inactivation of bacteria upon direct contact in a study [248]. Another example of controlling the biofouling in thin film nanocomposite membranes is the single-walled CNTs covalently bonded to thin film composite membrane surface which have exhibited moderate antibacterial properties [249].

Among the other nanomaterials for microbial disinfection, bifunctional ferrous oxide (Fe_3O_4) @Ag and Fe_3O_4 @TiO_2 nanoparticles were employed successfully against pathogenic bacteria including *E. coli*, *Staphylococcus epidermidis*, and *Bacillus subtilis* thus covering both Gram-positive and Gram-negative bacteria as well as spores [250, 251]. Magnesium oxide nanoparticles were also used effectively as biocides against both Gram-positive and Gram-negative bacteria and bacterial spores [252, 253].Nanotungsten oxide and palladium-incorporated ZnO nanoparticles have shown good antibacterial properties at removal of *E. coli* from water [254, 255]. Nitrogen-doped ZnO and Zirconium oxide nanoparticles also have proved good antibacterial nanostructured materials [151, 256].

3.2. Desalination. Desalination is considered an important alternative for obtaining fresh water source. Though expensive, membrane based desalination processes cover most of the desalination capability out of which only RO accounts for 41% [257]. Parameters that control the desalination cost include maximizing the flux of water through membrane to minimize the fouling. Recent developments in membrane technology have resulted in energy efficiency in RO plants [258]. NF has also been evaluated for desalinating seawater [259].

Nanomaterials are very useful in developing more efficient and cheaper nanostructured and reactive membranes for water/wastewater treatment and desalination such as CNT filters [260]. Nanomaterials offer opportunities to control the cost of desalination and increase its energy efficiency and among these are CNTs [261, 262], zeolites [263, 264], and graphene [265–267]. The controlled synthesis of both the length and diameters of CNTs has enabled them to be used in RO membranes to achieve high water fluxes [268–270].

Thin film nanocomposite membranes containing Ag and TiO_2 nanoparticles exhibited good salt rejection [150, 271]. Membrane permeability and salt rejection are shown to be effected by the number of coatings in TiO_2/Al_2O_3 (aluminium oxide) composite ceramic membranes coated by iron

oxide nanoparticles (Fe_2O_3) [272, 273]. A high sodium chloride rejection was obtained by using alumina ceramic membranes fabricated with silica nanoparticles [274]. Zeolite-based membranes for RO have exhibited high flux with excellent ion rejection characteristics [275, 276]. Studies also have indicated the potential of graphene membranes for water desalination with higher fluxes than polymeric RO membranes [277].

Other nanostructures such as lyotropic liquid crystals and aquaporins also have exhibited high flux and selective water transportation [278–280]. Zeolite-polyamide thin film nanocomposite membranes offered new ways of designing NF and RO membranes with increased water permeability and high salt rejection [275, 281]. The use of nanozeolites in thin film nanocomposite membranes has resulted in enhanced permeability and salt rejection [282, 283].

By grafting functional groups, such as carboxyl, at opening of CNTs, membranes have better selective rejection of some components but this has resulted in reduced permeability rendering CNTs incapable for desalination [281, 284, 285]. Hinds concluded a uniform CNT diameter of less than 0.8 nm for high salt rejection [286]. Nanocomposite membranes may serve as ideal membranes for desalination but a basic understanding of transport mechanism along with proper pore size selection by keeping the uniformity is required for economically feasible and commercially acceptable desalination membranes. The effects of real seawater feed on the efficiency of different nanomaterials need to be investigated in terms of long-term operation and maintenance of membrane performance.

3.3. Removal of Heavy Metals and Ions. Different types of nanomaterials have been introduced for removal of heavy metals from water/wastewater such as nanosorbents including CNTs, zeolites, and dendrimers and they have exceptional adsorption properties [63]. The ability of CNTs to adsorb heavy metals is reviewed by many researchers [287] such as Cd^{2+} [288], Cr^{3+} [289], Pb^{2+} [290], and Zn^{2+} [291] and metalloids such as arsenic (As) compounds [292]. Composites of CNTs with Fe and cerium oxide (CeO_2) have also been reported to remove heavy metal ions in few studies [293–295]. Cerium oxide nanoparticles supported on CNTs are used effectively to adsorb arsenic [289]. Fast adsorption kinetics of CNTs is mainly due to the highly accessible adsorption sites and the short intraparticle diffusion distance [287].

Metal based nanomaterials proved to be better in removing heavy metals than activated carbon [296], for example, adsorption of arsenic by using TiO_2 nanoparticles and nanosized magnetite [297, 298]. The utilization of photocatalysts such as TiO_2 nanoparticles has been investigated in detail to reduce toxic metal ions in water [299]. In a study, the effectiveness of nanocrystalline TiO_2 in removing different forms of arsenic is elaborated and it has shown to be more effective photocatalyst than commercially available TiO_2 nanoparticles with a maximum removal efficiency of arsenic at about neutral pH value [300]. A nanocomposite of TiO_2 nanoparticles anchored on graphene sheet was also used to reduce Cr(VI) to Cr(III) in sunlight [301]. Similar Cr treatment was carried out by using palladium nanoparticles in another study [302].

The capability of removing heavy metals like As is also investigated by using iron oxide nanomaterials (Fe_2O_3 and Fe_3O_4) as cost-effective adsorbents by many researchers [303–305]. Arsenic removal was also investigated by using high specific surface area of Fe_3O_4 nanocrystals [306]. Polymer-grafted Fe_2O_3 nanocomposite was effectively used to remove divalent heavy metal ions for copper, nickel, and cobalt over a pH range of 3 to 7 [307].

Bisphosphonate-modified magnetite nanoparticles were also used to remove the radioactive metal toxins, uranium dioxide (UO_2^{2+}) with high efficiency from water [308]. Studies have shown that zero-valent iron or iron nanoparticles (nZVI or Fe^0) are very effective for the transformation of heavy metal ions such as As(III), As(V), Pb(II), Cu(II), Ni(II), and Cr(VI) [309–313]. Reduction of Cr(VI) to Cr(III) was also done by using nZVI and bimetallic nZVI nanoparticles in a study [314].

Novel self-assembled 3D flower-like iron oxide nanostructures were also used to successfully adsorb both As(V) and Cr(VI) [315]. The 3D nanostructures of CeO_2 are used as good adsorbents for both As and Cr [316]. The efficiency of NaP1 zeolites was evaluated for removal of heavy metals (Cr(III), Ni(II), Zn(II), Cu(II), and Cd(II)) from wastewater [317, 318]. Dendritic polymers were also used for treatment of toxic metal ions [319]. The applicability of self-assembled monolayers on mesoporous supports for removing toxic metal ions novel was also evaluated by many researchers [320–322]. Biopolymers have been used for heavy metal remediation from aqueous wastes [323, 324]. Chitosan nanoparticles for the sorption of Pb(II) were also used in one study [325].

NF is reviewed for the removal of cations and arsenic from ground/surface waters [326] and it has been shown very effective to remove uranium (VI) from sea water [327]. Novel nanofilter membranes prepared by assembling positive poly (allylamine hydrochloride) and negative poly (styrene sulfonate) onto porous alumina exhibited a high retention of Ca^{2+} and Mg^{2+} [85]. The incorporation of iron (hydr)oxide nanoparticles into porous carbon materials has made it possible to remove both inorganics and organics thus enabling such filters to be used as point-of-use applications [328, 329]. A dendrimer-UF system was used for the removal of Cu^{2+} and the complete removal from water was obtained [330]. Finally, there are commercial products for efficient removal of arsenic and these include iron oxide nanoparticles and polymers and nanocrystalline titanium dioxide medium in the form of beads [331, 332].

3.4. Removal of Organic Contaminants. NOM constitutes a diverse group of hydrophobic (humic and fulvic acids) and hydrophilic organic compounds and it contributes significantly towards water contamination [333–339]. A variety of carbon-based adsorbents have been used for the removal of NOM from raw water and several factors affect this sorption of NOM [340–343].

3.4.1. CNTs. Different types of nanomaterial like nanosorbents such as CNTs, polymeric materials (e.g., dendrimers), and zeolites have exceptional adsorption properties and are applied for removal of organics from water/wastewater [63]. CNTs have received special attention due to their exceptional water treatment capabilities and adsorption of organics on CNTs is widely studied and extensively reviewed [287]. The removal of NOM by CNTs is higher when compared with carbon-based adsorbents mainly due to large surface areas and other factors [344, 345]. CNTs are also effective to remove polycyclic aromatic organic compounds [346–348] and atrazine [345].

Nanoporous activated carbon fibers, prepared by electrospinning of CNTs, showed much higher organic sorption equilibrium constants for benzene, toluene, xylene, and ethylbenzene than granular activated carbon [349]. The sorption of 1,2-dichlorobenzene by CNTs has been shown as effective in one study [350]. Compared with activated carbon, both single- and multiwalled CNTs displayed higher adsorption capacities for trihalomethanes [293, 351]. Multiwalled CNTs have been used as sorbents for chlorophenols, herbicides, DDTs, and so forth [352–355]. Finally, novel polymers with functionalized CNTs showed effective removal of organic pollutants from water [295].

3.4.2. TiO_2 Nanoparticles. Metal oxide nanomaterials such as TiO_2 in addition to CeO_2 have also been used as catalysts for fast and comparatively complete degradation of organic pollutants in ozonation processes [356, 357]. Photocatalysts like TiO_2 nanoparticles are used effectively for the treatment of water contaminated with organic pollutants like polychlorinated biphenyls (PCBs), benzenes, and chlorinated alkanes [299]. Removal of total organic carbon from wastewater was enhanced by the addition of TiO_2 nanoparticles in a study [358]. TiO_2 nanoparticles were also used in a "falling film" reactor for the degradation of microcystins in water [159]. Multiwalled CNTs functionalized with Fe nanoparticles have been proved effective sorbents for aromatic compounds like benzene and toluene [359].

Decomposition of organic compounds can be enhanced by noble metal doping into TiO_2 due to enhanced hydroxyl radical production and so forth [360–362]. For example, the doping Si into TiO_2 nanoparticles was effective to improve its efficiency due to the increase in surface area and crystallinity [363, 364]. TiO_2 nanocrystals modified with noble metal deposits and so forth were used for the degradation of methylene blue in the visible-light range [198, 365, 366]. Nitrogen- and Fe(III-) doped TiO_2 nanoparticles were better in degrading azo dyes and phenol, respectively, than commercially available TiO_2 nanoparticles [367, 368]. TiO_2 nanoparticles deposited onto porous Al_2O_3 were used effectively for the removal of TOC in a study [369]. TiO_2 nanocomposites with mesoporous silica were also used for the treatment of aromatic pollutants [370–373]. A composite of nanosized SO_4^{2-}/TiO_2 was used for the degradation of 4-nitrophenol in one study [374]. TiO_2 nanotubes have been used effectively to degrade toluene better than bulk structural materials [375] and were found to be more efficient than TiO_2 nanoparticles for degrading organic compounds [376]. A commercial product (Purifics Photo-Cat system) has been shown highly efficient at removing organics [377–379].

3.4.3. Zero-Valent Iron. Nanocatalysts including semiconductor materials, zero-valence metal, and bimetallic nanoparticles have been used for degradation of environmental contaminants such as PCBs, pesticides, and azo dyes due to their higher surface area and shape dependent properties [380]. Magnetic nanosorbents also have proved effective in organic contaminants removal [381]. Iron oxide nanomaterials have shown better removal capabilities of organic pollutants than bulk materials [303, 382, 383]. Fe_2O_3 nanoparticles have also been used for the removal of colored humic acids from wastewater [384]. Chlorinated organic compounds and PCBs have been transformed successfully using nZVI [385–387] as well as inorganic ions such as nitrate and perchlorate [388, 389].

Particles of nZVI have been proved effective in degradation of toxic chlorinated organic compounds, for example, 2,2′-dichlorobiphenyl in a few remediation studies [390, 391]. The stabilized nZVI particles could also be an effective way for in situ remediation of groundwater or industrial effluents [392]. The nZVI and bimetallic nZVI have emerged as effective redox media for reducing a variety of organic pollutants such as PCBs, pesticides, organic dyes, chlorinated alkanes, and alkenes and inorganic anions (e.g., nitrates) in water/wastewater due to larger surface areas and reactivity [393, 394]. Bimetallic Ni^0/Fe^0 and Pd^0/Fe^0 nanoparticles were more effective than commercial microscale Fe for reductive dehalogenation of chlorinated organics and brominated methanes, hydrodechlorination of chlorinated aliphatics, chlorinated aromatics, and PCBs as reported by many researchers [395–402].

3.4.4. Other Nanomaterials. In a study, nanostructured ZnO semiconductor films were used for degradation of organic contaminants (4-chlorocatechol) [403]. The nanocatalyst of Ag and amidoxime fibers was used efficiently for degradation of organic dyes [404]. A bimetallic nanocomposite of Pd-Cu/γ-alumina was used for the reduction of nitrate in one study [405]. Traces of halogenated organic compounds were biodegraded using hydrogen and the Pd based nanoparticles [301, 406]. Pd nanoparticles and bimetallic Pd/Au (gold) nanoparticles were used effectively for hydrodechlorination of trichloroethylene (TCE) [407, 408]. Mineralization of organic dyes was accelerated in one study by using films of manganese oxide (MnO_2) nanoparticles and hydrogen peroxide [409]. Similarly, MnO_2 hierarchical hollow nanostructures were used for the removal of organic pollutant in waste water [410]. The immobilized nanoparticles of metallo-porphyrinogens have also been successfully used for the reductive dehalogenation of chlorinated organic compounds (TCE and carbon tetrachloride) [411]. The applicability of self-assembled monolayers on mesoporous supports for removing anions and radionuclides was also evaluated by many researchers [412, 413]. Molecularly imprinted nanospheres were used for the removal of micropollutants

from hospital waste water [414]. Finally, single-enzyme nanoparticles could be used for decontaminating a broad range of organic contaminants as highlighted in one study [415].

3.4.5. Membranes. The immobilization of metallic nanoparticles in membrane has also been proved effective for degradation and dechlorination of toxic contaminants [416]. Inorganic membranes containing nano-TiO_2 or modified nano-TiO_2 have been used effectively for reductive degradation of contaminants, particularly chlorinated compounds [417, 418]. The use of TiO_2 immobilized on a polyethylene support and a TiO_2 slurry in combination with polymeric membranes has proved very effective in degrading 1,2-dichlorobenzene and pharmaceuticals, respectively [419, 420].

Polyethersulfone composite membranes with nano-TiO_2 as additive showed higher fluxes and enhanced antifouling properties [421–423]. Ceramic composite membrane made of TiO_2 nanoparticles inside a tubular Al_2O_3 substrate showed improved water quality and flux compared to Al_2O_3 membranes [424]. By doping TiO_2 nanoparticles to the Al_2O_3 membrane, it was possible to control the membrane fouling by decreased adsorption of oil droplets to membrane surface in the treatment of oily wastewater [425]. Nanostructured composite of TiO_2 and Fe_2O_3 incorporated into ultrafiltration membranes successfully reduced the fouling burden and improved the permeate flux [369].

Cellulose acetate membrane laden with nZVI was found effective in dechlorination of TCE [426]. A reactive membrane of bimetallic nZVI and Pt^0 nanoparticles was found to be very effective at reducing TCE [427]. Bimetallic Fe/Ni and Fe/Pd nanoparticles incorporated in nZVI as polymer–inorganic porous composite membranes have been successfully used for the reductive degradation of halogenated organic solvents [428–430]. Polyvinylidene fluoride film containing Pd and Pd/Fe was used effectively for dechlorination of PCB's in one study [431] leading to the development of a membrane reactor for dechlorination of a wider range of compounds [391, 432]. Alumina-zirconia-titania ceramic membrane coated with Fe_2O_3 nanoparticles was observed to reduce the dissolved organic carbon better than the uncoated membrane enhancing the degradation of NOM [273, 433]. Finally, ceramic composite membranes of TiO_2 and CNTs have resulted in enhanced membrane permeability and photocatalytic activity [434–436].

NF is reviewed for the removal of NOM and nitrates from ground/surface waters [326] and it has been reported to improve the water quality with a substantial reduction in organic contaminants [437]. Cost-effective nanostructured and reactive membranes are fabricated using different nanomaterials to develop more efficient water purification methods and in a study ceramic membrane of Al_2O_3 nanoparticles alone and doped with Fe, Mn, and La showed selectivity towards three different synthetic dyes [84]. An improved antifouling performance and flux increase was also observed in silica-incorporated membranes [438].

In the context of improving the UF processes for water treatment containing organic and inorganic solutes, dendritic polymers are used as water-soluble ligands for radionuclides and inorganic anions [439, 440]. Nearly complete reduction of 4-nitrophenol was seen when using a composite membrane composed of alumina and polymers through layer-by-layer adsorption of polyelectrolytes and citrate-stabilized Au nanoparticles [89]. Finally, the addition of metal oxide nanoparticles including silica, TiO_2, alumina, and zeolites to polymeric ultrafiltration membranes has helped reducing fouling [441–445].

4. Conclusions and Perspectives

Safe water has become a competitive resource in many parts of the world due to increasing population, prolonged droughts, climate change, and so forth. Nanomaterials have unique characteristics, for example, large surface areas, size, shape, and dimensions, that make them particularly attractive for water/wastewater treatment applications such as disinfection, adsorption, and membrane separations. The review of the literature has shown that water/wastewater treatment using nanomaterials is a promising field for current and future research.

Surface modifications of different nanomaterials like nanoscale TiO_2, nZVI by coupling with a second catalytic metal can result in enhanced water/wastewater quality when applied for this purpose by increasing the selectivity and reactivity of the selected materials. Surface modification may lead to the enhanced photocatalytic activity of the selected compounds due to the short lifetime of reactive oxygen species and increase the affinity of modified nanomaterials towards many emerging water contaminants. Bimetallic nanoparticles have also proved effective for remediation of water contaminants. However, further studies are required for understanding the mechanism of degradation on bimetallic nanoparticles responsible for the improved efficiency. For real field applications, however, an improved understanding of the process mechanism is very important for the successful applications of innovative nanocomposites for water/wastewater treatment.

Electrospinning offers the way to modify the surface properties of nanomaterials and different nanofibrous filters have successfully been used as antifouling water filtration membranes. They have extremely high surface-to-volume ratio and porosity, are very active against waterborne pathogens, less toxic with minimum health risks, and provide solutions to ensure safe water. It is very easy to dope functional nanomaterials to form multifunctional media/membrane filters with increased reactivity and selectivity for different contaminants. Although these electrospun nanofibers are prepared by simple and cost-effective method, their manufacturing at industrial scale is still a challenge and it is vital to consider the subject from an engineering aspect. The use of nanofibrous composites membranes for water/wastewater treatment is very limited and a stand-alone system (Figure 3) is proposed for removing all types of contaminants including bacteria/viruses, heavy metals and ions, and complex organic compounds.

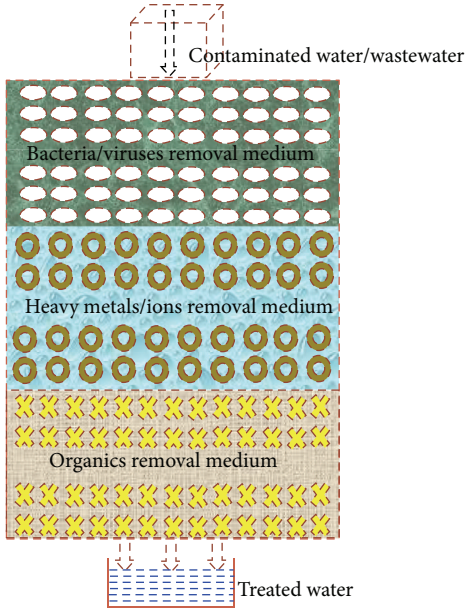

Figure 3: Schematic of a proposed composite nanofibrous media/membrane filters for complete removal of contaminants from water/wastewater.

The use of nanofibers and composite nanostructures membranes can help degrade a wide range of organic and inorganic contaminants in real field applications. The better understanding of the formation of nanocomposites membranes will certainly be a step towards improving the performance of multifunctional nanocomposites membranes. The pattern of nanoparticles within the host matrices of membranes and changes in the structures and properties of both nanomaterials and host matrices could be among the priority concerns in the real field applications of the nanofibrous membranes for water/wastewater treatment.

Conflict of Interests

The authors declare that there is no conflict of interests regarding the publication of this paper.

Acknowledgment

This project was supported by the NSTIP strategic technologies program, Grant no. 11-WAT1875-02, Kingdom of Saudi Arabia.

References

[1] D. D. Mara, "Water, sanitation and hygiene for the health of developing nations," *Public Health*, vol. 117, no. 6, pp. 452–456, 2003.

[2] M. Moore, P. Gould, and B. S. Keary, "Global urbanization and impact on health," *International Journal of Hygiene and Environmental Health*, vol. 206, no. 4-5, pp. 269–278, 2003.

[3] D. M. Johnson, D. R. Hokanson, Q. Zhang, K. D. Czupinski, and J. Tang, "Feasibility of water purification technology in rural areas of developing countries," *Journal of Environmental Management*, vol. 88, no. 3, pp. 416–427, 2008.

[4] M. A. Montgomery and M. Elimelech, "Water and sanitation in developing countries: Including health in the equation," *Environmental Science and Technology*, vol. 41, no. 1, pp. 17–24, 2007.

[5] J. Theron and T. E. Cloete, "Emerging waterborne infections: contributing factors, agents, and detection tools," *Critical Reviews in Microbiology*, vol. 28, no. 1, pp. 1–26, 2002.

[6] K. Eshelby, "Dying for a drink," *British Medical Journal*, vol. 334, no. 7594, pp. 610–612, 2007.

[7] P. Leonard, S. Hearty, J. Brennan et al., "Advances in biosensors for detection of pathogens in food and water," *Enzyme and Microbial Technology*, vol. 32, no. 1, pp. 3–13, 2003.

[8] N. J. Ashbolt, "Microbial contamination of drinking water and disease outcomes in developing regions," *Toxicology*, vol. 198, no. 1–3, pp. 229–238, 2004.

[9] G. Hutton, L. Haller, and J. Bartram, *Economic and Health Effects of Increasing Coverage of Low Cost Household Drinking Water Supply and Sanitation Interventions*, World Health Organization, 2007.

[10] World Health Organization and UNICEF, *Progress on Sanitation and Drinking-Water*, World Health Organization, Geneva, Switzerland, 2013.

[11] M. I. L'vovich, *World Water Resources and Their Future*, American Geophysical Union, Washington, DC, USA, 1979.

[12] S. L. Postel, G. C. Daily, and P. R. Ehrlich, "Human appropriation of renewable fresh water," *Science*, vol. 271, no. 5250, pp. 785–788, 1996.

[13] P. H. Gleick, *P. I. for S. in D., Environment, and Security, and S. E. Institute, Water in Crisis: A Guide to the World's Fresh Water Resources*, Oxford University Press, 1993.

[14] I. A. Shiklomanov, "Appraisal and assessment of world water resources," *Water International*, vol. 25, no. 1, pp. 11–32, 2000.

[15] J. Rockström, "Water for food and nature in drought-prone tropics: vapour shift in rain-fed agriculture," *Philosophical Transactions of the Royal Society B: Biological Sciences*, vol. 358, no. 1440, pp. 1997–2009, 2003.

[16] D. Seckler, D. Molden, and R. Sakthivadivel, *The Concept of Efficiency in Water Resources Management and Policy*, 2003.

[17] H. El-Dessouky and H. Ettouney, "Teaching desalination—a multidiscipline engineering science," *Heat Transfer Engineering*, vol. 23, no. 5, pp. 1–3, 2002.

[18] C. J. Vörösmarty, P. Green, J. Salisbury, and R. B. Lammers, "Global water resources: Vulnerability from climate change and population growth," *Science*, vol. 289, no. 5477, pp. 284–288, 2000.

[19] M. A. Shannon, P. W. Bohn, M. Elimelech, J. G. Georgiadis, B. J. Marĩas, and A. M. Mayes, "Science and technology for water purification in the coming decades," *Nature*, vol. 452, no. 7185, pp. 301–310, 2008.

[20] H. C. J. Godfray, J. R. Beddington, I. R. Crute et al., "Food security: the challenge of feeding 9 billion people," *Science*, vol. 327, no. 5967, pp. 812–818, 2010.

[21] K. Mulder, N. Hagens, and B. Fisher, "Burning water: a comparative analysis of the energy return on water invested," *Ambio*, vol. 39, no. 1, pp. 30–39, 2010.

[22] K. E. Kemper, "Groundwater-from development to management," *Hydrogeology Journal*, vol. 12, no. 1, pp. 3–5, 2004.

[23] J. A. Foley, R. DeFries, G. P. Asner et al., "Global consequences of land use," *Science*, vol. 309, no. 5734, pp. 570–574, 2005.

[24] S. E. Coetser, R. G. M. Heath, and N. Ndombe, "Diffuse pollution associated with the mining sectors in South Africa: a first-order assessment," *Water Science and Technology*, vol. 55, no. 3, pp. 9–16, 2007.

[25] L. Ritter, K. Solomon, P. Sibley et al., "Sources, pathways, and relative risks of contaminants in surface water and groundwater: a perspective prepared for the Walkerton inquiry," *Journal of Toxicology and Environmental Health—Part A*, vol. 65, no. 1, pp. 1–142, 2002.

[26] J. Fawell and M. J. Nieuwenhuijsen, "Contaminants in drinking water," *British Medical Bulletin*, vol. 68, pp. 199–208, 2003.

[27] S. Rodriguez-Mozaz, M. J. López De Alda, and D. Barceló, "Monitoring of estrogens, pesticides and bisphenol A in natural waters and drinking water treatment plants by solid-phase extraction-liquid chromatography-mass spectrometry," *Journal of Chromatography A*, vol. 1045, no. 1-2, pp. 85–92, 2004.

[28] I. R. Falconer and A. R. Humpage, "Health risk assessment of cyanobacterial (blue-green algal) toxins in drinking water," *International Journal of Environmental Research and Public Health*, vol. 2, no. 1, pp. 43–50, 2005.

[29] J. C. Bowman, J. L. Zhou, and J. W. Readman, "Sediment-water interactions of natural oestrogens under estuarine conditions," *Marine Chemistry*, vol. 77, no. 4, pp. 263–276, 2002.

[30] I. M. Verstraeten, T. Heberer, J. R. Vogel, T. Speth, S. Zuehlke, and U. Duennbier, "Occurrence of endocrine-disrupting and other wastewater compunds during water treatment with case studies from Lincoln, Nebraska and Berlin, Germany," *Practice Periodical of Hazardous, Toxic, and Radioactive Waste Management*, vol. 7, no. 4, pp. 253–263, 2003.

[31] H. Ozaki, "Rejection of micropollutants by membrane filtration," in *Proceedings of the Regional Symposium on Membrane Science and Technology*, Johor, Malaysia, 2004.

[32] M. R. Servos, D. T. Bennie, B. K. Burnison et al., "Distribution of estrogens, 17β-estradiol and estrone, in Canadian municipal wastewater treatment plants," *Science of the Total Environment*, vol. 336, no. 1–3, pp. 155–170, 2005.

[33] T. Urase and T. Kikuta, "Separate estimation of adsorption and degradation of pharmaceutical substances and estrogens in the activated sludge process," *Water Research*, vol. 39, no. 7, pp. 1289–1300, 2005.

[34] M. Petrovic, A. Diaz, F. Ventura, and D. Barceló, "Occurrence and removal of estrogenic short-chain ethoxy nonylphenolic compounds and their halogenated derivatives during drinking water production," *Environmental Science and Technology*, vol. 37, no. 19, pp. 4442–4448, 2003.

[35] P. Westerhoff, Y. Yoon, S. Snyder, and E. Wert, "Fate of endocrine-disruptor, pharmaceutical, and personal care product chemicals during simulated drinking water treatment processes," *Environmental Science and Technology*, vol. 39, no. 17, pp. 6649–6663, 2005.

[36] N. Vieno, T. Tuhkanen, and L. Kronberg, "Removal of pharmaceuticals in drinking water treatment: Effect of chemical coagulation," *Environmental Technology*, vol. 27, no. 2, pp. 183–192, 2006.

[37] U. Szewzyk, R. Szewzyk, W. Manz, and K.-H. Schleifer, "Microbiogical safety of drinking water," *Annual Review of Microbiology*, vol. 54, pp. 81–127, 2000.

[38] W. Zhang and F. A. DiGiano, "Comparison of bacterial regrowth in distribution systems using free chlorine and chloramine: A statistical study of causative factors," *Water Research*, vol. 36, no. 6, pp. 1469–1482, 2002.

[39] I. H. Suffet, J. Ho, D. Chou, D. Khiari, and J. Mallevialle, "Taste-and- odor problems observed during drinking water treatment," in *Advances in Taste-and-Odor Treatment and Control*, I. H. Suffet, J. Mallevialle, and E. Kawczynski, Eds., American Water Works Association, 1995.

[40] G. Becher, "Drinking water chlorination and health," *Acta Hydrochimica et Hydrobiologica*, vol. 27, no. 2, pp. 100–102, 1999.

[41] R. M. Hozalski, L. Zhang, and W. A. Arnold, "Reduction of haloacetic acids by Fe0: implications for treatment and fate," *Environmental Science and Technology*, vol. 35, no. 11, pp. 2258–2263, 2001.

[42] R. Sadiq and M. J. Rodriguez, "Disinfection by-products (DBPs) in drinking water and predictive models for their occurrence: a review," *Science of the Total Environment*, vol. 321, no. 1–3, pp. 21–46, 2004.

[43] K. Gopal, S. S. Tripathy, J. L. Bersillon, and S. P. Dubey, "Chlorination byproducts, their toxicodynamics and removal from drinking water," *Journal of Hazardous Materials*, vol. 140, no. 1-2, pp. 1–6, 2007.

[44] C. Adams, Y. Wang, K. Loftin, and M. Meyer, "Removal of antibiotics from surface and distilled water in conventional water treatment processes," *Journal of Environmental Engineering*, vol. 128, no. 3, pp. 253–260, 2002.

[45] H. Strathmann, "Membrane separation processes: current relevance and future opportunities," *AIChE Journal*, vol. 47, no. 5, pp. 1077–1087, 2001.

[46] B. Van der Bruggen and C. Vandecasteele, "Distillation vs. membrane filtration: overview of process evolutions in seawater desalination," *Desalination*, vol. 143, no. 3, pp. 207–218, 2002.

[47] A. L. Ahmad, B. S. Ooi, A. W. Mohammad, and J. P. Choudhury, "Development of a highly hydrophilic nanofiltration membrane for desalination and water treatment," *Desalination*, vol. 168, no. 1–3, pp. 215–221, 2004.

[48] J.-J. Qin, M. H. Oo, and K. A. Kekre, "Nanofiltration for recovering wastewater from a specific dyeing facility," *Separation and Purification Technology*, vol. 56, no. 2, pp. 199–203, 2007.

[49] K. Walha, R. B. Amar, L. Firdaous, F. Quéméneur, and P. Jaouen, "Brackish groundwater treatment by nanofiltration, reverse osmosis and electrodialysis in Tunisia: performance and cost comparison," *Desalination*, vol. 207, no. 1–3, pp. 95–106, 2007.

[50] M. Mulder, "The use of membrane processes in environmental problems. An introduction," in *Membrane Processes in Separation and Purification*, J. G. Crespo and K. W. Böddeker, Eds., pp. 229–262, Springer, 1994.

[51] Y. Kiso, T. Kon, T. Kitao, and K. Nishimura, "Rejection properties of alkyl phthalates with nanofiltration membranes," *Journal of Membrane Science*, vol. 182, no. 1-2, pp. 205–214, 2001.

[52] M. Bodzek, M. Dudziak, and K. Luks-Betlej, "Application of membrane techniques to water purification. Removal of phthalates," *Desalination*, vol. 162, no. 1–3, pp. 121–128, 2004.

[53] G. Owen, M. Bandi, J. A. Howell, and S. J. Churchouse, "Economic assessment of membrane processes for water and waste water treatment," *Journal of Membrane Science*, vol. 102, no. 1–3, pp. 77–91, 1995.

[54] Y. Yoon, P. Westerhoff, J. Yoon, and S. A. Snyder, "Removal of 17β estradiol and fluoranthene by nanofiltration and ultrafiltration," *Journal of Environmental Engineering*, vol. 130, no. 12, pp. 1460–1467, 2004.

[55] Y. Yoon, P. Westerhoff, S. A. Snyder, and E. C. Wert, "Nanofiltration and ultrafiltration of endocrine disrupting compounds, pharmaceuticals and personal care products," *Journal of Membrane Science*, vol. 270, no. 1-2, pp. 88–100, 2006.

[56] L. Braeken, B. Bettens, K. Boussu et al., "Transport mechanisms of dissolved organic compounds in aqueous solution during nanofiltration," *Journal of Membrane Science*, vol. 279, no. 1-2, pp. 311–319, 2006.

[57] N. Bolong, A. F. Ismail, M. R. Salim, and T. Matsuura, "A review of the effects of emerging contaminants in wastewater and options for their removal," *Desalination*, vol. 238, no. 1–3, pp. 229–246, 2009.

[58] J.-Y. Bottero, J. Rose, and M. R. Wiesner, "Nanotechnologies: tools for sustainability in a new wave of water treatment processes," *Integrated Environmental Assessment and Management*, vol. 2, no. 4, pp. 391–395, 2006.

[59] S. O. Obare and G. J. Meyer, "Nanostructured materials for environmental remediation of organic contaminants in water," *Journal of Environmental Science and Health—Part A*, vol. 39, no. 10, pp. 2549–2582, 2004.

[60] E. J. Lee and K. J. Schwab, "Deficiencies in drinking water distribution systems in developing countries," *Journal of Water and Health*, vol. 3, no. 2, pp. 109–127, 2005.

[61] C. L. Moe and R. D. Rheingans, "Global challenges in water, sanitation and health," *Journal of Water and Health*, vol. 4, no. 1, pp. 41–58, 2006.

[62] W. J. Weber Jr., "Distributed optimal technology networks: a concept and strategy for potable water sustainability," *Water Science and Technology*, vol. 46, no. 6-7, pp. 241–246, 2002.

[63] N. Savage and M. S. Diallo, "Nanomaterials and water purification: opportunities and challenges," *Journal of Nanoparticle Research*, vol. 7, no. 4-5, pp. 331–342, 2005.

[64] T. Masciangioli and W. X. Zhang, "Peer reviewed: environmental technologies at the nanoscale," *Environmental Science & Technology*, vol. 37, no. 5, pp. 102A–108A, 2003.

[65] J. C. T. Eijkel and A. van den Berg, "Nanofluidics: what is it and what can we expect from it?" *Microfluidics and Nanofluidics*, vol. 1, no. 3, pp. 249–267, 2005.

[66] D. G. Rickerby and M. Morrison, "Nanotechnology and the environment: a European perspective," *Science and Technology of Advanced Materials*, vol. 8, no. 1-2, pp. 19–24, 2007.

[67] A. Vaseashta, M. Vaclavikova, S. Vaseashta, G. Gallios, P. Roy, and O. Pummakarnchana, "Nanostructures in environmental pollution detection, monitoring, and remediation," *Science and Technology of Advanced Materials*, vol. 8, no. 1-2, pp. 47–59, 2007.

[68] X. Qu, P. J. J. Alvarez, and Q. Li, "Applications of nanotechnology in water and wastewater treatment," *Water Research*, vol. 47, no. 12, pp. 3931–3946, 2013.

[69] P. Gautam, D. Madathil, and A. N. Brijesh Nair, "Nanotechnology in waste water treatment: a review," *International Journal of ChemTech Research*, vol. 5, no. 5, pp. 2303–2308, 2013.

[70] J. Riu, A. Maroto, and F. X. Rius, "Nanosensors in environmental analysis," *Talanta*, vol. 69, no. 2, pp. 288–301, 2006.

[71] J. Theron, J. A. Walker, and T. E. Cloete, "Nanotechnology and water treatment: applications and emerging opportunities," *Critical Reviews in Microbiology*, vol. 34, no. 1, pp. 43–69, 2008.

[72] A. P. Alivisatos, "Perspectives on the physical chemistry of semiconductor nanocrystals," *The Journal of Physical Chemistry*, vol. 100, no. 31, pp. 13226–13239, 1996.

[73] A. P. Alivisatos, "Semiconductor clusters, nanocrystals, and quantum dots," *Science*, vol. 271, no. 5251, pp. 933–937, 1996.

[74] J. Z. Zhang, "Ultrafast studies of electron dynamics in semiconductor and metal colloidal nanoparticles: effects of size and surface," *Accounts of Chemical Research*, vol. 30, no. 10, pp. 423–429, 1997.

[75] S. V. Gaponenko, *Optical Properties of Semiconductor Nanocrystals*, Cambridge University Press, Cambridge, UK, 1998.

[76] S. J. Rosenthal, "Bar-coding biomolecules with fluorescent nanocrystals," *Nature Biotechnology*, vol. 19, no. 7, pp. 621–622, 2001.

[77] R. A. Crane and T. B. Scott, "Nanoscale zero-valent iron: future prospects for an emerging water treatment technology," *Journal of Hazardous Materials*, vol. 211-212, pp. 112–125, 2012.

[78] J. Fei and J. Li, "Metal oxide nanomaterials for water treatment," in *Nanotechnologies for the Life Sciences*, Wiley-VCH Verlag GmbH & Co. KGaA, 2007.

[79] U. Manzoor, M. Islam, L. Tabassam, and S. U. Rahman, "Quantum confinement effect in ZnO nanoparticles synthesized by co-precipitate method," *Physica E*, vol. 41, no. 9, pp. 1669–1672, 2009.

[80] S. Zia, M. Amin, U. Manzoor, and A. S. Bhatti, "Ultra-long multicolor belts and unique morphologies of tin-doped zinc oxide nanostructures," *Applied Physics A: Materials Science and Processing*, vol. 115, no. 1, pp. 275–281, 2014.

[81] D. Bhattacharyya, J. A. Hestekin, P. Brushaber, L. Cullen, L. G. Bachas, and S. K. Sikdar, "Novel poly-glutamic acid functionalized microfiltration membranes for sorption of heavy metals at high capacity," *Journal of Membrane Science*, vol. 141, no. 1, pp. 121–135, 1998.

[82] S. M. C. Ritchie, L. G. Bachas, T. Olin, S. K. Sikdar, and D. Bhattacharyya, "Surface modification of silica- and cellulose-based microfiltration membranes with functional polyamino acids for heavy metal sorption," *Langmuir*, vol. 15, no. 19, pp. 6346–6357, 1999.

[83] S. M. C. Ritchie, K. E. Kissick, L. G. Bachas, S. K. Sikdar, C. Parikh, and D. Bhattacharyya, "Polycysteine and other polyamino acid functionalized microfiltration membranes for heavy metal capture," *Environmental Science and Technology*, vol. 35, no. 15, pp. 3252–3258, 2001.

[84] K. A. DeFriend, M. R. Wiesner, and A. R. Barron, "Alumina and aluminate ultrafiltration membranes derived from alumina nanoparticles," *Journal of Membrane Science*, vol. 224, no. 1-2, pp. 11–28, 2003.

[85] B. W. Stanton, J. J. Harris, M. D. Miller, and M. L. Bruening, "Ultrathin, multilayered polyelectrolyte films as nanofiltration membranes," *Langmuir*, vol. 19, no. 17, pp. 7038–7042, 2003.

[86] A. M. Hollman and D. Bhattacharyya, "Pore assembled multilayers of charged polypeptides in microporous membranes for ion separation," *Langmuir*, vol. 20, no. 13, pp. 5418–5424, 2004.

[87] A. N. Chatterjee, D. M. Cannon Jr., E. N. Gatimu, J. V. Sweedler, N. R. Aluru, and P. W. Bohn, "Modeling and simulation of ionic currents in three-dimensional microfluidic devices with nanofluidic interconnects," *Journal of Nanoparticle Research*, vol. 7, no. 4-5, pp. 507–516, 2005.

[88] J. Xu, A. Dozier, and D. Bhattacharyya, "Synthesis of nanoscale bimetallic particles in polyelectrolyte membrane matrix for reductive transformation of halogenated organic compounds," *Journal of Nanoparticle Research*, vol. 7, no. 4-5, pp. 449–467, 2005.

[89] D. M. Dotzauer, J. Dai, L. Sun, and M. L. Bruening, "Catalytic membranes prepared using layer-by-layer adsorption of polyelectrolyte/metal nanoparticle films in porous supports," *Nano Letters*, vol. 6, no. 10, pp. 2268–2272, 2006.

[90] M. Arkas, R. Allabashi, D. Tsiourvas, E.-M. Mattausch, and R. Perfler, "Organic/inorganic hybrid filters based on dendritic and cyclodextrin "nanosponges" for the removal of organic

pollutants from water," *Environmental Science and Technology*, vol. 40, no. 8, pp. 2771–2777, 2006.

[91] R. Allabashi, M. Arkas, G. Hörmann, and D. Tsiourvas, "Removal of some organic pollutants in water employing ceramic membranes impregnated with cross-linked silylated dendritic and cyclodextrin polymers," *Water Research*, vol. 41, no. 2, pp. 476–486, 2007.

[92] M. M. Cortalezzi, J. Rose, G. F. Wells, J.-Y. Bottero, A. R. Barron, and M. R. Wiesner, "Ceramic membranes derived from ferroxane nanoparticles: a new route for the fabrication of iron oxide ultrafiltration membranes," *Journal of Membrane Science*, vol. 227, no. 1-2, pp. 207–217, 2003.

[93] J.-F. Li, Z.-L. Xu, H. Yang, L.-Y. Yu, and M. Liu, "Effect of TiO_2 nanoparticles on the surface morphology and performance of microporous PES membrane," *Applied Surface Science*, vol. 255, no. 9, pp. 4725–4732, 2009.

[94] A. Bottino, G. Capannelli, and A. Comite, "Preparation and characterization of novel porous PVDF-ZrO2 composite membranes," *Desalination*, vol. 146, no. 1-3, pp. 35–40, 2002.

[95] S. H. Kim, S.-Y. Kwak, B.-H. Sohn, and T. H. Park, "Design of TiO_2 nanoparticle self-assembled aromatic polyamide thin-film-composite (TFC) membrane as an approach to solve biofouling problem," *Journal of Membrane Science*, vol. 211, no. 1, pp. 157–165, 2003.

[96] J.-H. Li, Y.-Y. Xu, L.-P. Zhu, J.-H. Wang, and C.-H. Du, "Fabrication and characterization of a novel TiO_2 nanoparticle self-assembly membrane with improved fouling resistance," *Journal of Membrane Science*, vol. 326, no. 2, pp. 659–666, 2009.

[97] J. Kim, S. H. R. Davies, M. J. Baumann, V. V. Tarabara, and S. J. Masten, "Effect of ozone dosage and hydrodynamic conditions on the permeate flux in a hybrid ozonation-ceramic ultrafiltration system treating natural waters," *Journal of Membrane Science*, vol. 311, no. 1-2, pp. 165–172, 2008.

[98] S.-R. Chae, S. Wang, Z. D. Hendren, M. R. Wiesner, Y. Watanabe, and C. K. Gunsch, "Effects of fullerene nanoparticles on *Escherichia coli* K12 respiratory activity in aqueous suspension and potential use for membrane biofouling control," *Journal of Membrane Science*, vol. 329, no. 1-2, pp. 68–74, 2009.

[99] R. S. Barhate and S. Ramakrishna, "Nanofibrous filtering media: filtration problems and solutions from tiny materials," *Journal of Membrane Science*, vol. 296, no. 1-2, pp. 1–8, 2007.

[100] A. Frenot and I. S. Chronakis, "Polymer nanofibers assembled by electrospinning," *Current Opinion in Colloid and Interface Science*, vol. 8, no. 1-2, pp. 64–75, 2003.

[101] I. C. Escobar, A. A. Randall, and J. S. Taylor, "Bacterial growth in distribution systems: effect of assimilable organic carbon and biodegradable dissolved organic carbon," *Environmental Science and Technology*, vol. 35, no. 17, pp. 3442–3447, 2001.

[102] I. Majsterek, P. Sicinska, M. Tarczynska, M. Zalewski, and Z. Walter, "Toxicity of microcystin from cyanobacteria growing in a source of drinking water," *Comparative Biochemistry and Physiology—C Toxicology and Pharmacology*, vol. 139, no. 1-3, pp. 175–179, 2004.

[103] D. Berry, C. Xi, and L. Raskin, "Microbial ecology of drinking water distribution systems," *Current Opinion in Biotechnology*, vol. 17, no. 3, pp. 297–302, 2006.

[104] N. R. Dugan and D. J. Williams, "Cyanobacteria passage through drinking water filters during perturbation episodes as a function of cell morphology, coagulant and initial filter loading rate," *Harmful Algae*, vol. 5, no. 1, pp. 26–35, 2006.

[105] S. Srinivasan, G. W. Harrington, I. Xagoraraki, and R. Goel, "Factors affecting bulk to total bacteria ratio in drinking water distribution systems," *Water Research*, vol. 42, no. 13, pp. 3393–3404, 2008.

[106] W.-J. Huang, B.-L. Cheng, and Y.-L. Cheng, "Adsorption of microcystin-LR by three types of activated carbon," *Journal of Hazardous Materials*, vol. 141, no. 1, pp. 115–122, 2007.

[107] F. Al Momani, D. W. Smith, and M. Gamal El-Din, "Degradation of cyanobacteria toxin by advanced oxidation processes," *Journal of Hazardous Materials*, vol. 150, no. 2, pp. 238–249, 2008.

[108] P. Pendleton, R. Schumann, and S. H. Wong, "Microcystin-LR adsorption by activated carbon," *Journal of Colloid and Interface Science*, vol. 240, no. 1, pp. 1–8, 2001.

[109] D.-K. Lee, S.-C. Kim, I.-C. Cho, S.-J. Kim, and S.-W. Kim, "Photocatalytic oxidation of microcystin-LR in a fluidized bed reactor having TiO_2-coated activated carbon," *Separation and Purification Technology*, vol. 34, no. 1–3, pp. 59–66, 2004.

[110] H. Yan, A. Gong, H. He, J. Zhou, Y. Wei, and L. Lv, "Adsorption of microcystins by carbon nanotubes," *Chemosphere*, vol. 62, no. 1, pp. 142–148, 2006.

[111] H. Wang, L. Ho, D. M. Lewis, J. D. Brookes, and G. Newcombe, "Discriminating and assessing adsorption and biodegradation removal mechanisms during granular activated carbon filtration of microcystin toxins," *Water Research*, vol. 41, no. 18, pp. 4262–4270, 2007.

[112] P. Jain and T. Pradeep, "Potential of silver nanoparticle-coated polyurethane foam as an antibacterial water filter," *Biotechnology and Bioengineering*, vol. 90, no. 1, pp. 59–63, 2005.

[113] J. A. Spadaro, T. J. Berger, S. D. Barranco, S. E. Chapin, and R. O. Becker, "Antibacterial effects of silver electrodes with weak direct current," *Antimicrobial agents and chemotherapy*, vol. 6, no. 5, pp. 637–642, 1974.

[114] G. Zhao and S. E. Stevens Jr., "Multiple parameters for the comprehensive evaluation of the susceptibility of *Escherichia coli* to the silver ion," *BioMetals*, vol. 11, no. 1, pp. 27–32, 1998.

[115] Y. Inoue, M. Hoshino, H. Takahashi et al., "Bactericidal activity of Ag-zeolite mediated by reactive oxygen species under aerated conditions," *Journal of Inorganic Biochemistry*, vol. 92, no. 1, pp. 37–42, 2002.

[116] V. S. Kumar, B. M. Nagaraja, V. Shashikala et al., "Highly efficient Ag/C catalyst prepared by electro-chemical deposition method in controlling microorganisms in water," *Journal of Molecular Catalysis A: Chemical*, vol. 223, no. 1-2, pp. 313–319, 2004.

[117] Q. L. Feng, J. Wu, G. Q. Chen, F. Z. Cui, T. N. Kim, and J. O. Kim, "A mechanistic study of the antibacterial effect of silver ions on *Escherichia coli* and Staphylococcus aureus," *Journal of Biomedical Materials Research*, vol. 52, no. 4, pp. 662–668, 2000.

[118] M. Yamanaka, K. Hara, and J. Kudo, "Bactericidal actions of a silver ion solution on *Escherichia coli*, studied by energy-filtering transmission electron microscopy and proteomic analysis," *Applied and Environmental Microbiology*, vol. 71, no. 11, pp. 7589–7593, 2005.

[119] I. Sondi and B. Salopek-Sondi, "Silver nanoparticles as antimicrobial agent: a case study on *E. coli* as a model for Gram-negative bacteria," *Journal of Colloid and Interface Science*, vol. 275, no. 1, pp. 177–182, 2004.

[120] C. Baker, A. Pradhan, L. Pakstis, D. J. Pochan, and S. I. Shah, "Synthesis and antibacterial properties of silver nanoparticles," *Journal of Nanoscience and Nanotechnology*, vol. 5, no. 2, pp. 244–249, 2005.

[121] A. Panáček, L. Kvítek, R. Prucek et al., "Silver colloid nanoparticles: synthesis, characterization, and their antibacterial activity," *The Journal of Physical Chemistry B*, vol. 110, no. 33, pp. 16248–16253, 2006.

[122] J. S. Kim, E. Kuk, K. N. Yu et al., "Antimicrobial effects of silver nanoparticles," *Nanomedicine: Nanotechnology, Biology, and Medicine*, vol. 3, no. 1, pp. 95–101, 2007.

[123] S. Shrivastava, T. Bera, A. Roy, G. Singh, P. Ramachandrarao, and D. Dash, "Characterization of enhanced antibacterial effects of novel silver nanoparticles," *Nanotechnology*, vol. 18, no. 22, Article ID 225103, 2007.

[124] J. R. Morones, J. L. Elechiguerra, A. Camacho et al., "The bactericidal effect of silver nanoparticles," *Nanotechnology*, vol. 16, no. 10, pp. 2346–2353, 2005.

[125] S. Makhluf, R. Dror, Y. Nitzan, Y. Abramovich, R. Jelinek, and A. Gedanken, "Microwave-assisted synthesis of nanocrystalline MgO and its use as a bacteriocide," *Advanced Functional Materials*, vol. 15, no. 10, pp. 1708–1715, 2005.

[126] S. Pal, Y. K. Tak, and J. M. Song, "Does the antibacterial activity of silver nanoparticles depend on the shape of the nanoparticle? A study of the gram-negative bacterium *Escherichia coli*," *Applied and Environmental Microbiology*, vol. 73, no. 6, pp. 1712–1720, 2007.

[127] Z.-M. Xiu, J. Ma, and P. J. J. Alvarez, "Differential effect of common ligands and molecular oxygen on antimicrobial activity of silver nanoparticles versus silver ions," *Environmental Science and Technology*, vol. 45, no. 20, pp. 9003–9008, 2011.

[128] Z.-M. Xiu, Q.-B. Zhang, H. L. Puppala, V. L. Colvin, and P. J. J. Alvarez, "Negligible particle-specific antibacterial activity of silver nanoparticles," *Nano Letters*, vol. 12, no. 8, pp. 4271–4275, 2012.

[129] S. Y. Liau, D. C. Read, W. J. Pugh, J. R. Furr, and A. D. Russell, "Interaction of silver nitrate with readily identifiable groups: relationship to the antibacterial action of silver ions," *Letters in Applied Microbiology*, vol. 25, no. 4, pp. 279–283, 1997.

[130] M. Danilczuk, A. Lund, J. Sadlo, H. Yamada, and J. Michalik, "Conduction electron spin resonance of small silver particles," *Spectrochimica Acta—Part A: Molecular and Biomolecular Spectroscopy*, vol. 63, no. 1, pp. 189–191, 2006.

[131] A. Esteban-Cubillo, C. Pecharromán, E. Aguilar, J. Santarén, and J. S. Moya, "Antibacterial activity of copper monodispersed nanoparticles into sepiolite," *Journal of Materials Science*, vol. 41, no. 16, pp. 5208–5212, 2006.

[132] W. K. Son, J. H. Youk, T. S. Lee, and W. H. Park, "Preparation of antimicrobial ultrafine cellulose acetate fibers with silver nanoparticles," *Macromolecular Rapid Communications*, vol. 25, no. 18, pp. 1632–1637, 2004.

[133] L. Balogh, D. R. Swanson, D. A. Tomalia, G. L. Hagnauer, and A. T. McManus, "Dendrimer-Silver Complexes and Nanocomposites as Antimicrobial Agents," *Nano Letters*, vol. 1, no. 1, pp. 18–21, 2001.

[134] Y. Chen, L. Wang, S. Jiang, and H. Yu, "Study on Novel Antibacterial Polymer Materials (I) Preparation of Zeolite Antibacterial Agents and Antibacterial Polymer Composite and Their Antibacterial Properties," *Journal of Polymer Materials*, vol. 20, no. 3, pp. 279–284, 2003.

[135] M. Botes and T. E. Cloete, "The potential of nanofibers and nanobiocides in water purification," *Critical Reviews in Microbiology*, vol. 36, no. 1, pp. 68–81, 2010.

[136] H. J. Jeon, J. S. Kim, T. G. Kim, J. H. Kim, W.-R. Yu, and J. H. Youk, "Preparation of poly(ε-caprolactone)-based polyurethane nanofibers containing silver nanoparticles," *Applied Surface Science*, vol. 254, no. 18, pp. 5886–5890, 2008.

[137] N. L. Lala, R. Ramaseshan, L. Bojun et al., "Fabrication of nanofibers with antimicrobial functionality used as filters: protection against bacterial contaminants," *Biotechnology and Bioengineering*, vol. 97, no. 6, pp. 1357–1365, 2007.

[138] C.-Y. Chen and C.-L. Chiang, "Preparation of cotton fibers with antibacterial silver nanoparticles," *Materials Letters*, vol. 62, no. 21-22, pp. 3607–3609, 2008.

[139] K. Vimala, K. Samba Sivudu, Y. Murali Mohan, B. Sreedhar, and K. Mohana Raju, "Controlled silver nanoparticles synthesis in semi-hydrogel networks of poly(acrylamide) and carbohydrates: a rational methodology for antibacterial application," *Carbohydrate Polymers*, vol. 75, no. 3, pp. 463–471, 2009.

[140] M. Peter-Varbanets, C. Zurbrügg, C. Swartz, and W. Pronk, "Decentralized systems for potable water and the potential of membrane technology," *Water Research*, vol. 43, no. 2, pp. 245–265, 2009.

[141] K. Zodrow, L. Brunet, S. Mahendra et al., "Polysulfone ultrafiltration membranes impregnated with silver nanoparticles show improved biofouling resistance and virus removal," *Water Research*, vol. 43, no. 3, pp. 715–723, 2009.

[142] H. J. Lee, S. Y. Yeo, and S. H. Jeong, "Antibacterial effect of nanosized silver colloidal solution on textile fabrics," *Journal of Materials Science*, vol. 38, no. 10, pp. 2199–2204, 2003.

[143] Y. Lv, H. Liu, Z. Wang et al., "Silver nanoparticle-decorated porous ceramic composite for water treatment," *Journal of Membrane Science*, vol. 331, no. 1-2, pp. 50–56, 2009.

[144] N. Ma, X. Fan, X. Quan, and Y. Zhang, "Ag-TiO_2/HAP/Al_2O_3 bioceramic composite membrane: fabrication, characterization and bactericidal activity," *Journal of Membrane Science*, vol. 336, no. 1-2, pp. 109–117, 2009.

[145] N. Ma, X. Quan, Y. Zhang, S. Chen, and H. Zhao, "Integration of separation and photocatalysis using an inorganic membrane modified with Si-doped TiO_2 for water purification," *Journal of Membrane Science*, vol. 335, no. 1-2, pp. 58–67, 2009.

[146] B. De Gusseme, T. Hennebel, E. Christiaens et al., "Virus disinfection in water by biogenic silver immobilized in polyvinylidene fluoride membranes," *Water Research*, vol. 45, no. 4, pp. 1856–1864, 2011.

[147] H. Ma, B. S. Hsiao, and B. Chu, "Thin-film nanofibrous composite membranes containing cellulose or chitin barrier layers fabricated by ionic liquids," *Polymer*, vol. 52, no. 12, pp. 2594–2599, 2011.

[148] M. S. Mauter, Y. Wang, K. C. Okemgbo, C. O. Osuji, E. P. Giannelis, and M. Elimelech, "Antifouling ultrafiltration membranes via post-fabrication grafting of biocidal nanomaterials," *ACS Applied Materials and Interfaces*, vol. 3, no. 8, pp. 2861–2868, 2011.

[149] W.-L. Chou, D.-G. Yu, and M.-C. Yang, "The preparation and characterization of silver-loading cellulose acetate hollow fiber membrane for water treatment," *Polymers for Advanced Technologies*, vol. 16, no. 8, pp. 600–607, 2005.

[150] S. Y. Lee, H. J. Kim, R. Patel, S. J. Im, J. H. Kim, and B. R. Min, "Silver nanoparticles immobilized on thin film composite polyamide membrane: characterization, nanofiltration, antifouling properties," *Polymers for Advanced Technologies*, vol. 18, no. 7, pp. 562–568, 2007.

[151] S. Chaturvedi, P. N. Dave, and N. K. Shah, "Applications of nano-catalyst in new era," *Journal of Saudi Chemical Society*, vol. 16, no. 3, pp. 307–325, 2012.

[152] D.-G. Yu, M.-Y. Teng, W.-L. Chou, and M.-C. Yang, "Characterization and inhibitory effect of antibacterial PAN-based hollow fiber loaded with silver nitrate," *Journal of Membrane Science*, vol. 225, no. 1-2, pp. 115–123, 2003.

[153] J. S. Taurozzi, H. Arul, V. Z. Bosak et al., "Effect of filler incorporation route on the properties of polysulfone-silver nanocomposite membranes of different porosities," *Journal of Membrane Science*, vol. 325, no. 1, pp. 58–68, 2008.

[154] A. A. Adesina, "Industrial exploitation of photocatalysis: progress, perspectives and prospects," *Catalysis Surveys from Asia*, vol. 8, no. 4, pp. 265–273, 2004.

[155] Q. Li, S. Mahendra, D. Y. Lyon et al., "Antimicrobial nanomaterials for water disinfection and microbial control: potential applications and implications," *Water Research*, vol. 42, no. 18, pp. 4591–4602, 2008.

[156] K. Hashimoto, H. Irie, and A. Fujishima, "TiO_2 photocatalysis: a historical overview and future prospects," *Japanese Journal of Applied Physics, Part 1: Regular Papers and Short Notes and Review Papers*, vol. 44, no. 12, pp. 8269–8285, 2005.

[157] H. Einaga, S. Futamura, and T. Ibusuki, "Photocatalytic decomposition of benzene over TiO_2 in a humidified airstream," *Physical Chemistry Chemical Physics*, vol. 1, no. 20, pp. 4903–4908, 1999.

[158] A. Fujishima, T. N. Rao, and D. A. Tryk, "Titanium dioxide photocatalysis," *Journal of Photochemistry and Photobiology C: Photochemistry Reviews*, vol. 1, no. 1, pp. 1–21, 2000.

[159] G. S. Shephard, S. Stockenström, D. De Villiers, W. J. Engelbrecht, and G. F. S. Wessels, "Degradation of microcystin toxins in a falling film photocatalytic reactor with immobilized titanium dioxide catalyst," *Water Research*, vol. 36, no. 1, pp. 140–146, 2002.

[160] J. A. Ibáñez, M. I. Litter, and R. A. Pizarro, "Photocatalytic bactericidal effect of TiO_2 on Enterobacter cloacae. Comparative study with other Gram (-) bacteria," *Journal of Photochemistry and Photobiology A: Chemistry*, vol. 157, no. 1, pp. 81–85, 2003.

[161] H.-L. Liu and T. C.-K. Yang, "Photocatalytic inactivation of *Escherichia coli* and Lactobacillus helveticus by ZnO and TiO_2 activated with ultraviolet light," *Process Biochemistry*, vol. 39, no. 4, pp. 475–481, 2003.

[162] M. Cho, H. Chung, W. Choi, and J. Yoon, "Linear correlation between inactivation of *E. coli* and OH radical concentration in TiO_2 photocatalytic disinfection," *Water Research*, vol. 38, no. 4, pp. 1069–1077, 2004.

[163] M. Cho, H. Chung, W. Choi, and J. Yoon, "Different inactivation behaviors of MS-2 phage and *Escherichia coli* in TiO_2 photocatalytic disinfection," *Applied and Environmental Microbiology*, vol. 71, no. 1, pp. 270–275, 2005.

[164] P. Hajkova, P. Spatenka, J. Horsky, I. Horska, and A. Kolouch, "Photocatalytic effect of TiO_2 films on viruses and bacteria," *Plasma Processes and Polymers*, vol. 4, no. 1, pp. S397–S401, 2007.

[165] L. Zan, W. Fa, T. Peng, and Z.-K. Gong, "Photocatalysis effect of nanometer TiO_2 and TiO_2-coated ceramic plate on Hepatitis B virus," *Journal of Photochemistry and Photobiology B: Biology*, vol. 86, no. 2, pp. 165–169, 2007.

[166] J. Lonnen, S. Kilvington, S. C. Kehoe, F. Al-Touati, and K. G. McGuigan, "Solar and photocatalytic disinfection of protozoan, fungal and bacterial microbes in drinking water," *Water Research*, vol. 39, no. 5, pp. 877–883, 2005.

[167] S. Gelover, L. A. Gómez, K. Reyes, and M. Teresa Leal, "A practical demonstration of water disinfection using TiO_2 films and sunlight," *Water Research*, vol. 40, no. 17, pp. 3274–3280, 2006.

[168] M. Ni, M. K. H. Leung, D. Y. C. Leung, and K. Sumathy, "A review and recent developments in photocatalytic water-splitting using TiO_2 for hydrogen production," *Renewable and Sustainable Energy Reviews*, vol. 11, no. 3, pp. 401–425, 2007.

[169] A. Fujishima, X. Zhang, and D. A. Tryk, "TiO_2 photocatalysis and related surface phenomena," *Surface Science Reports*, vol. 63, no. 12, pp. 515–582, 2008.

[170] V. Subramanian, E. Wolf, and P. V. Kamat, "Semiconductor-metal composite nanostructures. To what extent do metal nanoparticles improve the photocatalytic activity of TiO_2 films?" *Journal of Physical Chemistry B*, vol. 105, no. 46, pp. 11439–11446, 2001.

[171] R. Asahi, T. Morikawa, T. Ohwaki, K. Aoki, and Y. Taga, "Visible-light photocatalysis in nitrogen-doped titanium oxides," *Science*, vol. 293, no. 5528, pp. 269–271, 2001.

[172] C. Burda, Y. Lou, X. Chen, A. C. S. Samia, J. Stout, and J. L. Gole, "Enhanced nitrogen doping in TiO_2 nanoparticles," *Nano Letters*, vol. 3, no. 8, pp. 1049–1051, 2003.

[173] H. Irie, Y. Watanabe, and K. Hashimoto, "Nitrogen-concentration dependence on photocatalytic activity of TiO_2-xNx powders," *Journal of Physical Chemistry B*, vol. 107, no. 23, pp. 5483–5486, 2003.

[174] O. Diwald, T. L. Thompson, T. Zubkov, E. G. Goralski, S. D. Walck, and J. T. Yates Jr., "Photochemical activity of nitrogen-doped rutile TiO_2 (110) in visible light," *Journal of Physical Chemistry B*, vol. 108, no. 19, pp. 6004–6008, 2004.

[175] S. Yang and L. Gao, "New method to prepare nitrogen-doped titanium dioxide and its photocatalytic activities irradiated by visible light," *Journal of the American Ceramic Society*, vol. 87, no. 9, pp. 1803–1805, 2004.

[176] C. Di Valentin, G. Pacchioni, and A. Selloni, "Origin of the different photoactivity of N-doped anatase and rutile TiO_2," *Physical Review B—Condensed Matter and Materials Physics*, vol. 70, no. 8, Article ID 85116, 2004.

[177] S. Livraghi, A. Votta, M. C. Paganini, and E. Giamello, "The nature of paramagnetic species in nitrogen doped TiO_2 active in visible light photocatalysis," *Chemical Communications*, no. 4, pp. 498–500, 2005.

[178] S. Livraghi, M. C. Paganini, E. Giamello, A. Selloni, C. Di Valentin, and G. Pacchioni, "Origin of photoactivity of nitrogen-doped titanium dioxide under visible light," *Journal of the American Chemical Society*, vol. 128, no. 49, pp. 15666–15671, 2006.

[179] Y. Liu, J. Li, X. Qiu, and C. Burda, "Novel TiO_2 nanocatalysts for wastewater purification: tapping energy from the sun," *Water Science and Technology*, vol. 54, no. 8, pp. 47–54, 2006.

[180] M.-S. Wong, W.-C. Chu, D.-S. Sun et al., "Visible-light-induced bactericidal activity of a nitrogen-doped titanium photocatalyst against human pathogens," *Applied and Environmental Microbiology*, vol. 72, no. 9, pp. 6111–6116, 2006.

[181] S. U. M. Khan, M. Al-Shahry, and W. B. Ingler Jr., "Efficient photochemical water splitting by a chemically modified n-TiO_2," *Science*, vol. 297, no. 5590, pp. 2243–2245, 2002.

[182] S. Sakthivel and H. Kisch, "Daylight photocatalysis by carbon-modified titanium dioxide," *Angewandte Chemie—International Edition*, vol. 42, no. 40, pp. 4908–4911, 2003.

[183] K. Noworyta and J. Augustynski, "Spectral photoresponses of carbon-doped TiO_2 film electrodes," *Electrochemical and Solid-State Letters*, vol. 7, no. 6, pp. E31–E33, 2004.

[184] L. Lin, W. Lin, Y. X. Zhu et al., "Uniform carbon-covered titania and its photocatalytic property," *Journal of Molecular Catalysis A: Chemical*, vol. 236, no. 1-2, pp. 46–53, 2005.

[185] M. E. Rincón, M. E. Trujillo-Camacho, and A. K. Cuentas-Gallegos, "Sol-gel titanium oxides sensitized by nanometric

carbon blacks: comparison with the optoelectronic and photocatalytic properties of physical mixtures," *Catalysis Today*, vol. 107-108, pp. 606–611, 2005.

[186] H. Wang and J. P. Lewis, "Effects of dopant states on photoactivity in carbon-doped TiO_2," *Journal of Physics Condensed Matter*, vol. 17, no. 21, pp. L209–L213, 2005.

[187] D. Mitoraj, A. Jańczyk, M. Strus et al., "Visible light inactivation of bacteria and fungi by modified titanium dioxide," *Photochemical and Photobiological Sciences*, vol. 6, no. 6, pp. 642–648, 2007.

[188] T. Umebayashi, T. Yamaki, H. Itoh, and K. Asai, "Band gap narrowing of titanium dioxide by sulfur doping," *Applied Physics Letters*, vol. 81, no. 3, pp. 454–456, 2002.

[189] T. Ohno, T. Mitsui, and M. Matsumura, "Photocatalytic activity of S-doped TiO_2 photocatalyst under visible light," *Chemistry Letters*, vol. 32, no. 4, pp. 364–365, 2003.

[190] T. Yamamoto, F. Yamashita, I. Tanaka, E. Matsubara, and A. Muramatsu, "Electronic states of sulfur doped TiO_2 by first principles calculations," *Materials Transactions*, vol. 45, no. 7, pp. 1987–1990, 2004.

[191] J. C. Yu, J. Yu, W. Ho, Z. Jiang, and L. Zhang, "Effects of F-doping on the photocatalytic activity and microstructures of nanocrystalline TiO_2 powders," *Chemistry of Materials*, vol. 14, no. 9, pp. 3808–3816, 2002.

[192] M. Sökmen, F. Candan, and Z. Sümer, "Disinfection of *E. coli* by the Ag-TiO_2/UV system: lipidperoxidation," *Journal of Photochemistry and Photobiology A: Chemistry*, vol. 143, no. 2-3, pp. 241–244, 2001.

[193] H. M. Sung-Suh, J. R. Choi, H. J. Hah, S. M. Koo, and Y. C. Bae, "Comparison of Ag deposition effects on the photocatalytic activity of nanoparticulate TiO_2 under visible and UV light irradiation," *Journal of Photochemistry and Photobiology A: Chemistry*, vol. 163, no. 1-2, pp. 37–44, 2004.

[194] V. Vamathevan, R. Amal, D. Beydoun, G. Low, and S. McEvoy, "Silver metallisation of titania particles: effects on photoactivity for the oxidation of organics," *Chemical Engineering Journal*, vol. 98, no. 1-2, pp. 127–139, 2004.

[195] X. Zhang, M. Zhou, and L. Lei, "Preparation of an Ag-TiO_2 photocatalyst coated on activated carbon by MOCVD," *Materials Chemistry and Physics*, vol. 91, no. 1, pp. 73–79, 2005.

[196] K. Page, R. G. Palgrave, I. P. Parkin, M. Wilson, S. L. P. Savin, and A. V. Chadwick, "Titania and silver-titania composite films on glass—potent antimicrobial coatings," *Journal of Materials Chemistry*, vol. 17, no. 1, pp. 95–104, 2007.

[197] M. V. Liga, E. L. Bryant, V. L. Colvin, and Q. Li, "Virus inactivation by silver doped titanium dioxide nanoparticles for drinking water treatment," *Water Research*, vol. 45, no. 2, pp. 535–544, 2011.

[198] E. Bae and W. Choi, "Highly enhanced photoreductive degradation of perchlorinated compounds on dye-sensitized metal/TiO_2 under visible light," *Environmental Science and Technology*, vol. 37, no. 1, pp. 147–152, 2003.

[199] J. C. Ireland, P. Klostermann, E. W. Rice, and R. M. Clark, "Inactivation of *Escherichia coli* by titanium dioxide photocatalytic oxidation," *Applied and Environmental Microbiology*, vol. 59, no. 5, pp. 1668–1670, 1993.

[200] C. Wei, W.-Y. Lin, Z. Zalnal et al., "Bactericidal activity of TiO_2 photocatalyst in aqueous media: toward a solar-assisted water disinfection system," *Environmental Science and Technology*, vol. 28, no. 5, pp. 934–938, 1994.

[201] M. Bekbölet and C. V. Araz, "Inactivation of *Escherichia coli* by photocatalytic oxidation," *Chemosphere*, vol. 32, no. 5, pp. 959–965, 1996.

[202] P.-C. Maness, S. Smolinski, D. M. Blake, Z. Huang, E. J. Wolfrum, and W. A. Jacoby, "Bactericidal activity of photocatalytic TiO_2 reaction: toward an understanding of its killing mechanism," *Applied and Environmental Microbiology*, vol. 65, no. 9, pp. 4094–4098, 1999.

[203] J. C. Yu, W. Ho, J. Yu, H. Yip, K. W. Po, and J. Zhao, "Efficient visible-light-induced photocatalytic disinfection on sulfur-doped nanocrystalline titania," *Environmental Science and Technology*, vol. 39, no. 4, pp. 1175–1179, 2005.

[204] T. A. Egerton, S. A. M. Kosa, and P. A. Christensen, "Photoelectrocatalytic disinfection of *E. coli* suspensions by iron doped TiO_2," *Physical Chemistry Chemical Physics*, vol. 8, no. 3, pp. 398–406, 2006.

[205] P. Wu, R. Xie, and J. K. Shang, "Enhanced visible-light photocatalytic disinfection of bacterial spores by palladium-modified nitrogen-doped titanium oxide," *Journal of the American Ceramic Society*, vol. 91, no. 9, pp. 2957–2962, 2008.

[206] P. Wu, R. Xie, J. A. Imlay, and J. K. Shang, "Visible-light-induced photocatalytic inactivation of bacteria by composite photocatalysts of palladium oxide and nitrogen-doped titanium oxide," *Applied Catalysis B: Environmental*, vol. 88, no. 3-4, pp. 576–581, 2009.

[207] H. Choi, S. R. Al-Abed, and D. D. Dionysiou, "Nanostructured titanium oxide film- and membrane-based photocatalysis for water treatment," in *Nanotechnology Applications for Clean Water*, N. Savage, M. Diallo, J. Duncan, A. Street, and R. Sustich, Eds., chapter 3, pp. 39–46, William Andrew, Boston, Mass, USA, 2009.

[208] L. Belháčová, J. Krýsa, J. Geryk, and J. Jirkovský, "Inactivation of microorganisms in a flow-through photoreactor with an immobilized TiO_2 layer," *Journal of Chemical Technology and Biotechnology*, vol. 74, no. 2, pp. 149–154, 1999.

[209] S.-Y. Kwak, S. H. Kim, and S. S. Kim, "Hybrid organic/inorganic reverse osmosis (RO) membrane for bactericidal anti-fouling. 1. Preparation and characterization of TiO_2 nanoparticle self-assembled aromatic polyamide thin-film-composite (TFC) membrane," *Environmental Science and Technology*, vol. 35, no. 11, pp. 2388–2394, 2001.

[210] J. Joo, S. G. Kwon, T. Yu et al., "Large-scale synthesis of TiO_2 nanorods via nonhydrolytic sol-gel ester elimination reaction and their application to photocatalytic inactivation of *E. coli*," *Journal of Physical Chemistry B*, vol. 109, no. 32, pp. 15297–15302, 2005.

[211] K.-J. Shieh, M. Li, Y.-H. Lee, S.-D. Sheu, Y.-T. Liu, and Y.-C. Wang, "Antibacterial performance of photocatalyst thin film fabricated by defection effect in visible light," *Nanomedicine: Nanotechnology, Biology, and Medicine*, vol. 2, no. 2, pp. 121–126, 2006.

[212] K. Sunada, T. Watanabe, and K. Hashimoto, "Studies on photokilling of bacteria on TiO_2 thin film," *Journal of Photochemistry and Photobiology A: Chemistry*, vol. 156, no. 1–3, pp. 227–233, 2003.

[213] J. Kiwi and V. Nadtochenko, "Evidence for the mechanism of photocatalytic degradation of the bacterial wall membrane at the TiO_2 interface by ATR-FTIR and laser kinetic spectroscopy," *Langmuir*, vol. 21, no. 10, pp. 4631–4641, 2005.

[214] S.-H. Lee, S. Pumprueg, B. Moudgil, and W. Sigmund, "Inactivation of bacterial endospores by photocatalytic nanocomposites," *Colloids and Surfaces B: Biointerfaces*, vol. 40, no. 2, pp. 93–98, 2005.

[215] D. M. A. Alrousan, P. S. M. Dunlop, T. A. McMurray, and J. A. Byrne, "Photocatalytic inactivation of *E. coli* in surface water

using immobilised nanoparticle TiO_2 films," *Water Research*, vol. 43, no. 1, pp. 47–54, 2009.

[216] A. Kubacka, M. Ferrer, M. L. Cerrada et al., "Boosting TiO_2-anatase antimicrobial activity: polymer-oxide thin films," *Applied Catalysis B: Environmental*, vol. 89, no. 3-4, pp. 441–447, 2009.

[217] Y. Zhu, T. Ran, Y. Li, J. Guo, and W. Li, "Dependence of the cytotoxicity of multi-walled carbon nanotubes on the culture medium," *Nanotechnology*, vol. 17, no. 18, article 024, pp. 4668–4674, 2006.

[218] S. Deng, V. K. K. Upadhyayula, G. B. Smith, and M. C. Mitchell, "Adsorption equilibrium and kinetics of microorganisms on single-wall carbon nanotubes," *IEEE Sensors Journal*, vol. 8, no. 6, pp. 954–962, 2008.

[219] D. Nepal, S. Balasubramanian, A. L. Simonian, and V. A. Davis, "Strong antimicrobial coatings: single-walled carbon nanotubes armored with biopolymers," *Nano Letters*, vol. 8, no. 7, pp. 1896–1901, 2008.

[220] V. K. K. Upadhyayula, S. Deng, M. C. Mitchell, G. B. Smith, V. K. Nair, and S. Ghoshroy, "Adsorption kinetics of *Escherichia coli* and Staphylococcus aureus on single-walled carbon nanotube aggregates," *Water Science and Technology*, vol. 58, no. 1, pp. 179–184, 2008.

[221] V. K. K. Upadhyayula, S. Ghoshroy, V. S. Nair, G. B. Smith, M. C. Mitchell, and S. Deng, "Single-walled carbon nanotubes as fluorescence biosensors for pathogen recognition in water systems," *Research Letters in Nanotechnology*, vol. 2008, Article ID 156358, 5 pages, 2008.

[222] T. Akasaka and F. Watari, "Capture of bacteria by flexible carbon nanotubes," *Acta Biomaterialia*, vol. 5, no. 2, pp. 607–612, 2009.

[223] A. S. Brady-Estévez, S. Kang, and M. Elimelech, "A single-walled-carbon-nanotube filter for removal of viral and bacterial pathogens," *Small*, vol. 4, no. 4, pp. 481–484, 2008.

[224] S. T. Mostafavi, M. R. Mehrnia, and A. M. Rashidi, "Preparation of nanofilter from carbon nanotubes for application in virus removal from water," *Desalination*, vol. 238, no. 1–3, pp. 271–280, 2009.

[225] R. Q. Long and R. T. Yang, "Carbon nanotubes as superior sorbent for dioxin removal," *Journal of the American Chemical Society*, vol. 123, no. 9, pp. 2058–2059, 2001.

[226] H. Yan, G. Pan, H. Zou, X. Li, and H. Chen, "Effective removal of microcystins using carbon nanotubes embedded with bacteria," *Chinese Science Bulletin*, vol. 49, no. 16, pp. 1694–1698, 2004.

[227] C. Ye, Q. Gong, F. Lu, and J. Liang, "Adsorption of middle molecular weight toxins on carbon nanotubes," *Acta Physico—Chimica Sinica*, vol. 23, no. 9, pp. 1321–1324, 2007.

[228] E. C. de Albuquerque Jr., M. O. A. Méndez, A. dos Reis Coutinho, and T. T. Franco, "Removal of cyanobacteria toxins from drinking water by adsorption on activated carbon fibers," *Materials Research*, vol. 11, no. 3, pp. 371–380, 2008.

[229] V. K. K. Upadhyayula, S. Deng, M. C. Mitchell, and G. B. Smith, "Application of carbon nanotube technology for removal of contaminants in drinking water: a review," *Science of the Total Environment*, vol. 408, no. 1, pp. 1–13, 2009.

[230] S. Kang, M. Pinault, L. D. Pfefferle, and M. Elimelech, "Single-walled carbon nanotubes exhibit strong antimicrobial activity," *Langmuir*, vol. 23, no. 17, pp. 8670–8673, 2007.

[231] S. Kang, M. Herzberg, D. F. Rodrigues, and M. Elimelech, "Antibacterial effects of carbon nanotubes: size does matter!," *Langmuir*, vol. 24, no. 13, pp. 6409–6413, 2008.

[232] P. Wick, P. Manser, L. K. Limbach et al., "The degree and kind of agglomeration affect carbon nanotube cytotoxicity," *Toxicology Letters*, vol. 168, no. 2, pp. 121–131, 2007.

[233] C. D. Vecitis, K. R. Zodrow, S. Kang, and M. Elimelech, "Electronic-structure-dependent bacterial cytotoxicity of single-walled carbon nanotubes," *ACS Nano*, vol. 4, no. 9, pp. 5471–5479, 2010.

[234] S. Kang, M. S. Mauter, and M. Elimelech, "Physicochemical determinants of multiwalled carbon nanotube bacterial cytotoxicity," *Environmental Science and Technology*, vol. 42, no. 19, pp. 7528–7534, 2008.

[235] L. R. Arias and L. Yang, "Inactivation of bacterial pathogens by carbon nanotubes in suspensions," *Langmuir*, vol. 25, no. 5, pp. 3003–3012, 2009.

[236] G. Jia, H. Wang, L. Yan et al., "Cytotoxicity of carbon nanomaterials: single-wall nanotube, multi-wall nanotube, and fullerene," *Environmental Science and Technology*, vol. 39, no. 5, pp. 1378–1383, 2005.

[237] K. Donaldson, R. Aitken, L. Tran et al., "Carbon nanotubes: a review of their properties in relation to pulmonary toxicology and workplace safety," *Toxicological Sciences*, vol. 92, no. 1, pp. 5–22, 2006.

[238] H. Dumortier, S. Lacotte, G. Pastorin et al., "Functionalized carbon nanotubes are non-cytotoxic and preserve the functionality of primary immune cells," *Nano Letters*, vol. 6, no. 7, pp. 1522–1528, 2006.

[239] M. Endo, T. Hayashi, and Y.-A. Kim, "Large-scale production of carbon nanotubes and their applications," *Pure and Applied Chemistry*, vol. 78, no. 9, pp. 1703–1713, 2006.

[240] J. B. Nuzzo, "The biological threat to U.S. water supplies: toward a national water security policy," *Biosecurity and Bioterrorism*, vol. 4, no. 2, pp. 147–159, 2006.

[241] J. J. Niu, J. N. Wang, Y. Jiang, L. F. Su, and J. Ma, "An approach to carbon nanotubes with high surface area and large pore volume," *Microporous and Mesoporous Materials*, vol. 100, no. 1–3, pp. 1–5, 2007.

[242] S. Kar, R. C. Bindal, S. Prabhakar, P. K. Tewari, K. Dasgupta, and D. Sathiyamoorthy, "Potential of carbon nanotubes in water purification: an approach towards the development of an integrated membrane system," *International Journal of Nuclear Desalination*, vol. 3, no. 2, pp. 143–150, 2008.

[243] M. L. Jugan, L. Oziol, M. Bimbot et al., "In vitro assessment of thyroid and estrogenic endocrine disruptors in wastewater treatment plants, rivers and drinking water supplies in the greater Paris area (France)," *Science of the Total Environment*, vol. 407, no. 11, pp. 3579–3587, 2009.

[244] H. Liu, J. Ru, J. Qu, R. Dai, Z. Wang, and C. Hu, "Removal of persistent organic pollutants from micro-polluted drinking water by triolein embedded absorbent," *Bioresource Technology*, vol. 100, no. 12, pp. 2995–3002, 2009.

[245] A. S. Brady-Estévez, M. H. Schnoor, S. Kang, and M. Elimelech, "SWNT-MWNT hybrid filter attains high viral removal and bacterial inactivation," *Langmuir*, vol. 26, no. 24, pp. 19153–19158, 2010.

[246] C. D. Vecitis, M. H. Schnoor, M. S. Rahaman, J. D. Schiffman, and M. Elimelech, "Electrochemical multiwalled carbon nanotube filter for viral and bacterial removal and inactivation," *Environmental Science and Technology*, vol. 45, no. 8, pp. 3672–3679, 2011.

[247] M. S. Rahaman, C. D. Vecitis, and M. Elimelech, "Electrochemical carbon-nanotube filter performance toward virus removal

and inactivation in the presence of natural organic matter," *Environmental Science and Technology*, vol. 46, no. 3, pp. 1556–1564, 2012.

[248] F. Ahmed, C. M. Santos, R. A. M. V. Vergara, M. C. R. Tria, R. Advincula, and D. F. Rodrigues, "Antimicrobial applications of electroactive PVK-SWNT nanocomposites," *Environmental Science and Technology*, vol. 46, no. 3, pp. 1804–1810, 2012.

[249] A. Tiraferri, C. D. Vecitis, and M. Elimelech, "Covalent binding of single-walled carbon nanotubes to polyamide membranes for antimicrobial surface properties," *ACS Applied Materials and Interfaces*, vol. 3, no. 8, pp. 2869–2877, 2011.

[250] P. Gong, H. Li, X. He et al., "Preparation and antibacterial activity of Fe3O4@Ag nanoparticles," *Nanotechnology*, vol. 18, no. 28, Article ID 285604, 2007.

[251] W.-J. Chen, P.-J. Tsai, and Y.-C. Chen, "Functional Fe3O4/TiO2 core/shell magnetic nanoparticles as photokilling agents for pathogenic bacteria," *Small*, vol. 4, no. 4, pp. 485–491, 2008.

[252] O. B. Koper, J. S. Klabunde, G. L. Marchin, K. J. Klabunde, P. Stoimenov, and L. Bohra, "Nanoscale powders and formulations with biocidal activity toward spores and vegetative cells of Bacillus species, viruses, and toxins," *Current Microbiology*, vol. 44, no. 1, pp. 49–55, 2002.

[253] P. K. Stoimenov, R. L. Klinger, G. L. Marchin, and K. J. Klabunde, "Metal oxide nanoparticles as bactericidal agents," *Langmuir*, vol. 18, no. 17, pp. 6679–6686, 2002.

[254] M. A. Gondal, M. A. Dastageer, and A. Khalil, "Synthesis of nano-WO3 and its catalytic activity for enhanced antimicrobial process for water purification using laser induced photocatalysis," *Catalysis Communications*, vol. 11, no. 3, pp. 214–219, 2009.

[255] A. Khalil, M. A. Gondal, and M. A. Dastageer, "Augmented photocatalytic activity of palladium incorporated ZnO nanoparticles in the disinfection of *Escherichia coli* microorganism from water," *Applied Catalysis A: General*, vol. 402, no. 1-2, pp. 162–167, 2011.

[256] H. Bai, Z. liu, and D. D. Sun, "Hierarchical ZnO nanostructured membrane for multifunctional environmental applications," *Colloids and Surfaces A: Physicochemical and Engineering Aspects*, vol. 410, pp. 11–17, 2012.

[257] T. Humplik, J. Lee, S. C. O'Hern et al., "Nanostructured materials for water desalination," *Nanotechnology*, vol. 22, no. 29, Article ID 292001, 2011.

[258] C. Fritzmann, J. Löwenberg, T. Wintgens, and T. Melin, "State-of-the-art of reverse osmosis desalination," *Desalination*, vol. 216, no. 1–3, pp. 1–76, 2007.

[259] M. S. Mohsen, J. O. Jaber, and M. D. Afonso, "Desalination of brackish water by nanofiltration and reverse osmosis," *Desalination*, vol. 157, no. 1–3, p. 167, 2003.

[260] A. Srivastava, O. N. Srivastava, S. Talapatra, R. Vajtai, and P. M. Ajayan, "Carbon nanotube filters," *Nature Materials*, vol. 3, no. 9, pp. 610–614, 2004.

[261] J. K. Holt, H. G. Park, Y. Wang et al., "Fast mass transport through sub-2-nanometer carbon nanotubes," *Science*, vol. 312, no. 5776, pp. 1034–1037, 2006.

[262] F. Fornasiero, G. P. Hyung, J. K. Holt et al., "Ion exclusion by sub-2-nm carbon nanotube pores," *Proceedings of the National Academy of Sciences of the United States of America*, vol. 105, no. 45, pp. 17250–17255, 2008.

[263] L. Li, J. Dong, T. M. Nenoff, and R. Lee, "Desalination by reverse osmosis using MFI zeolite membranes," *Journal of Membrane Science*, vol. 243, no. 1-2, pp. 401–404, 2004.

[264] L. Li, N. Liu, B. McPherson, and R. Lee, "Influence of counter ions on the reverse osmosis through MFI zeolite membranes: implications for produced water desalination," *Desalination*, vol. 228, no. 1–3, pp. 217–225, 2008.

[265] K. Sint, B. Wang, and P. Král, "Selective ion passage through functionalized graphene nanopores," *Journal of the American Chemical Society*, vol. 130, no. 49, pp. 16448–16449, 2008.

[266] D.-E. Jiang, V. R. Cooper, and S. Dai, "Porous graphene as the ultimate membrane for gas separation," *Nano Letters*, vol. 9, no. 12, pp. 4019–4024, 2009.

[267] J. Bai, X. Zhong, S. Jiang, Y. Huang, and X. Duan, "Graphene nanomesh," *Nature Nanotechnology*, vol. 5, no. 3, pp. 190–194, 2010.

[268] C. L. Pint, S. T. Pheasant, M. Pasquali, K. E. Coulter, H. K. Schmidt, and R. H. Hauge, "Synthesis of high aspect-ratio carbon nanotube "flying carpets" from nanostructured flake substrates," *Nano Letters*, vol. 8, no. 7, pp. 1879–1883, 2008.

[269] N. Arjmandi, P. Sasanpour, and B. Rashidian, "CVD synthesis of small-diameter Single-Walled carbon nanotubes on silicon," *Scientia Iranica*, vol. 16, no. 1 D, pp. 61–64, 2009.

[270] C. Song and B. Corry, "Intrinsic ion selectivity of narrow hydrophobic pores," *Journal of Physical Chemistry B*, vol. 113, no. 21, pp. 7642–7649, 2009.

[271] H. S. Lee, S. J. Im, J. H. Kim, H. J. Kim, J. P. Kim, and B. R. Min, "Polyamide thin-film nanofiltration membranes containing TiO_2 nanoparticles," *Desalination*, vol. 219, no. 1–3, pp. 48–56, 2008.

[272] M. M. Cortalezzi, J. Rose, A. R. Barron, and M. R. Wiesner, "Characteristics of ultrafiltration ceramic membranes derived from alumoxane nanoparticles," *Journal of Membrane Science*, vol. 205, no. 1-2, pp. 33–43, 2002.

[273] B. S. Karnik, S. H. Davies, M. J. Baumann, and S. J. Masten, "Fabrication of catalytic membranes for the treatment of drinking water using combined ozonation and ultrafiltration," *Environmental Science and Technology*, vol. 39, no. 19, pp. 7656–7661, 2005.

[274] M. C. Duke, S. Mee, and J. C. D. da Costa, "Performance of porous inorganic membranes in non-osmotic desalination," *Water Research*, vol. 41, no. 17, pp. 3998–4004, 2007.

[275] B.-H. Jeong, E. M. V. Hoek, Y. Yan et al., "Interfacial polymerization of thin film nanocomposites: a new concept for reverse osmosis membranes," *Journal of Membrane Science*, vol. 294, no. 1-2, pp. 1–7, 2007.

[276] L. Li and R. Lee, "Purification of produced water by ceramic membranes: material screening, process design and economics," *Separation Science and Technology*, vol. 44, no. 15, pp. 3455–3484, 2009.

[277] M. E. Suk and N. R. Aluru, "Water transport through ultrathin graphene," *Journal of Physical Chemistry Letters*, vol. 1, no. 10, pp. 1590–1594, 2010.

[278] X. Gong, J. Li, H. Lu et al., "A charge-driven molecular water pump," *Nature Nanotechnology*, vol. 2, no. 11, pp. 709–712, 2007.

[279] C. C. Striemer, T. R. Gaborski, J. L. McGrath, and P. M. Fauchet, "Charge- and size-based separation of macromolecules using ultrathin silicon membranes," *Nature*, vol. 445, no. 7129, pp. 749–753, 2007.

[280] G. Zuo, R. Shen, S. Ma, and W. Guo, "Transport properties of single-file water molecules inside a carbon nanotube biomimicking water channel," *ACS Nano*, vol. 4, no. 1, pp. 205–210, 2010.

[281] E. M. V. Hoek and A. K. Ghosh, "Nanotechnology-Based Membranes for Water Purification," in *Nanotechnology Applications*

for Clean Water, N. Savage, M. Diallo, J. Duncan, A. Street, and R. Sustich, Eds., chapter 4, pp. 47–58, William Andrew, Boston, Mass, USA, 2009.

[282] M. L. Lind, A. K. Ghosh, A. Jawor et al., "Influence of zeolite crystal size on zeolite-polyamide thin film nanocomposite membranes," *Langmuir*, vol. 25, no. 17, pp. 10139–10145, 2009.

[283] M. L. Lind, D. E. Suk, T.-V. Nguyen, and E. M. V. Hoek, "Tailoring the structure of thin film nanocomposite membranes to achieve seawater RO membrane performance," *Environmental Science and Technology*, vol. 44, no. 21, pp. 8230–8235, 2010.

[284] P. Nednoor, N. Chopra, V. Gavalas, L. G. Bachas, and B. J. Hinds, "Reversible biochemical switching of ionic transport through aligned carbon nanotube membranes," *Chemistry of Materials*, vol. 17, no. 14, pp. 3595–3599, 2005.

[285] M. S. Mauter and M. Elimelech, "Environmental applications of carbon-based nanomaterials," *Environmental Science and Technology*, vol. 42, no. 16, pp. 5843–5859, 2008.

[286] B. Hinds, "Dramatic transport properties of carbon nanotube membranes for a robust protein channel mimetic platform," *Current Opinion in Solid State and Materials Science*, vol. 16, no. 1, pp. 1–9, 2012.

[287] G. P. Rao, C. Lu, and F. Su, "Sorption of divalent metal ions from aqueous solution by carbon nanotubes: a review," *Separation and Purification Technology*, vol. 58, no. 1, pp. 224–231, 2007.

[288] Y.-H. Li, J. Ding, Z. Luan et al., "Competitive adsorption of $Pb2^{+}$, $Cu2^{+}$ and Cd 2^{+} ions from aqueous solutions by multiwalled carbon nanotubes," *Carbon*, vol. 41, no. 14, pp. 2787–2792, 2003.

[289] Z.-C. Di, J. Ding, X.-J. Peng, Y.-H. Li, Z.-K. Luan, and J. Liang, "Chromium adsorption by aligned carbon nanotubes supported ceria nanoparticles," *Chemosphere*, vol. 62, no. 5, pp. 861–865, 2006.

[290] Y.-H. Li, Z. Di, J. Ding, D. Wu, Z. Luan, and Y. Zhu, "Adsorption thermodynamic, kinetic and desorption studies of $Pb2^{+}$ on carbon nanotubes," *Water Research*, vol. 39, no. 4, pp. 605–609, 2005.

[291] C. Lu, H. Chiu, and C. Liu, "Removal of zinc(II) from aqueous solution by purified carbon nanotubes: kinetics and equilibrium studies," *Industrial and Engineering Chemistry Research*, vol. 45, no. 8, pp. 2850–2855, 2006.

[292] X. Peng, Z. Luan, J. Ding, Z. Di, Y. Li, and B. Tian, "Ceria nanoparticles supported on carbon nanotubes for the removal of arsenate from water," *Materials Letters*, vol. 59, no. 4, pp. 399–403, 2005.

[293] C. Lu, Y.-L. Chung, and K.-F. Chang, "Adsorption of trihalomethanes from water with carbon nanotubes," *Water Research*, vol. 39, no. 6, pp. 1183–1189, 2005.

[294] C. Lu and H. Chiu, "Adsorption of zinc(II) from water with purified carbon nanotubes," *Chemical Engineering Science*, vol. 61, no. 4, pp. 1138–1145, 2006.

[295] K. L. Salipira, B. B. Mamba, R. W. Krause, T. J. Malefetse, and S. H. Durbach, "Carbon nanotubes and cyclodextrin polymers for removing organic pollutants from water," *Environmental Chemistry Letters*, vol. 5, no. 1, pp. 13–17, 2007.

[296] Y. C. Sharma, V. Srivastava, V. K. Singh, S. N. Kaul, and C. H. Weng, "Nano-adsorbents for the removal of metallic pollutants from water and wastewater," *Environmental Technology*, vol. 30, no. 6, pp. 583–609, 2009.

[297] E. A. Deliyanni, D. N. Bakoyannakis, A. I. Zouboulis, and K. A. Matis, "Sorption of As(V) ions by akaganéite-type nanocrystals," *Chemosphere*, vol. 50, no. 1, pp. 155–163, 2003.

[298] J. T. Mayo, C. Yavuz, S. Yean et al., "The effect of nanocrystalline magnetite size on arsenic removal," *Science and Technology of Advanced Materials*, vol. 8, no. 1-2, pp. 71–75, 2007.

[299] K. Kabra, R. Chaudhary, and R. L. Sawhney, "Treatment of hazardous organic and inorganic compounds through aqueous-phase photocatalysis: a review," *Industrial and Engineering Chemistry Research*, vol. 43, no. 24, pp. 7683–7696, 2004.

[300] M. E. Pena, G. P. Korfiatis, M. Patel, L. Lippincott, and X. Meng, "Adsorption of As(V) and As(III) by nanocrystalline titanium dioxide," *Water Research*, vol. 39, no. 11, pp. 2327–2337, 2005.

[301] K. Zhang, K. C. Kemp, and V. Chandra, "Homogeneous anchoring of TiO_2 nanoparticles on graphene sheets for waste water treatment," *Materials Letters*, vol. 81, pp. 127–130, 2012.

[302] M. A. Omole, I. K'Owino, and O. A. Sadik, "Nanostructured materials for improving water quality: potentials and risks," in *Nanotechnology Applications for Clean Water*, N. Savage, M. Diallo, J. Duncan, A. Street, and R. Sustich, Eds., chapter 17, pp. 233–247, William Andrew, Boston, Mass, USA, 2009.

[303] C. H. Lai and C. Y. Chen, "Removal of metal ions and humic acid from water by iron-coated filter media," *Chemosphere*, vol. 44, no. 5, pp. 1177–1184, 2001.

[304] M. S. Onyango, Y. Kojima, H. Matsuda, and A. Ochieng, "Adsorption kinetics of arsenic removal from groundwater by iron-modified zeolite," *Journal of Chemical Engineering of Japan*, vol. 36, no. 12, pp. 1516–1522, 2003.

[305] L. C. A. Oliveira, D. I. Petkowicz, A. Smaniotto, and S. B. C. Pergher, "Magnetic zeolites: a new adsorbent for removal of metallic contaminants from water," *Water Research*, vol. 38, no. 17, pp. 3699–3704, 2004.

[306] C. T. Yavuz, J. T. Mayo, W. W. Yu et al., "Low-field magnetic separation of monodisperse Fe3O4 nanocrystals," *Science*, vol. 314, no. 5801, pp. 964–967, 2006.

[307] M. Takafuji, S. Ide, H. Ihara, and Z. Xu, "Preparation of poly(1-vinylimidazole)-grafted magnetic nanoparticles and their application for removal of metal ions," *Chemistry of Materials*, vol. 16, no. 10, pp. 1977–1983, 2004.

[308] L. Wang, Z. Yang, J. Gao et al., "A biocompatible method of decorporation: bisphosphonate-modified magnetite nanoparticles to remove uranyl ions from blood," *Journal of the American Chemical Society*, vol. 128, no. 41, pp. 13358–13359, 2006.

[309] S. M. Ponder, J. G. Darab, and T. E. Mallouk, "Remediation of Cr(VI) and Pb(II) aqueous solutions using supported, nanoscale zero-valent iron," *Environmental Science and Technology*, vol. 34, no. 12, pp. 2564–2569, 2000.

[310] S. R. Kanel, B. Manning, L. Charlet, and H. Choi, "Removal of arsenic(III) from groundwater by nanoscale zero-valent iron," *Environmental Science and Technology*, vol. 39, no. 5, pp. 1291–1298, 2005.

[311] S. R. Kanel, J.-M. Greneche, and H. Choi, "Arsenic(V) removal from groundwater using nano scale zero-valent iron as a colloidal reactive barrier material," *Environmental Science and Technology*, vol. 40, no. 6, pp. 2045–2050, 2006.

[312] G. C. C. Yang and H.-L. Lee, "Chemical reduction of nitrate by nanosized iron: kinetics and pathways," *Water Research*, vol. 39, no. 5, pp. 884–894, 2005.

[313] X.-Q. Li and W.-X. Zhang, "Iron nanoparticles: the core-shell structure and unique properties for Ni(II) sequestration," *Langmuir*, vol. 22, no. 10, pp. 4638–4642, 2006.

[314] W. Zhang, "Nanoscale iron particles for environmental remediation: an overview," *Journal of Nanoparticle Research*, vol. 5, no. 3-4, pp. 323–332, 2003.

[315] L. S. Zhong, J. S. Hu, H. P. Liang, A. M. Cao, W. G. Song, and L. J. Wan, "Self-assembled 3D flowerlike iron oxide nanostructures and their application in water treatment," *Advanced Materials*, vol. 18, no. 18, pp. 2426–2431, 2006.

[316] L.-S. Zhong, J.-S. Hu, A.-M. Cao, Q. Liu, W.-G. Song, and L.-J. Wan, "3D flowerlike ceria micro/nanocomposite structure and its application for water treatment and CO removal," *Chemistry of Materials*, vol. 19, no. 7, pp. 1648–1655, 2007.

[317] N. Moreno, X. Querol, C. Ayora, C. F. Pereira, and M. Janssen-Jurkovicová, "Utilization of zeolites synthesized from coal fly ash for the purification of acid mine waters," *Environmental Science and Technology*, vol. 35, no. 17, pp. 3526–3534, 2001.

[318] E. Álvarez-Ayuso, A. García-Sánchez, and X. Querol, "Purification of metal electroplating waste waters using zeolites," *Water Research*, vol. 37, no. 20, pp. 4855–4862, 2003.

[319] M. S. Diallo, S. Christie, P. Swaminathan et al., "Dendritic chelating agents. 1. Cu(II) binding to ethylene diamine core poly(amidoamine) dendrimers in aqueous solutions," *Langmuir*, vol. 20, no. 7, pp. 2640–2651, 2004.

[320] S. V. Mattigod, X. Feng, G. E. Fryxell, J. Liu, and M. Gong, "Separation of complexed mercury from aqueous wastes using self-assembled mercaptan on mesoporous silica," *Separation Science and Technology*, vol. 34, no. 12, pp. 2329–2345, 1999.

[321] W. Yantasee, Y. Lin, G. E. Fryxell, B. J. Busche, and J. C. Birnbaum, "Removal of heavy metals from aqueous solution using novel nanoengineered sorbents: self-assembled carbamoylphosphonic acids on mesoporous silica," *Separation Science and Technology*, vol. 38, no. 15, pp. 3809–3825, 2003.

[322] S. V. Mattigod, G. E. Fryxell, X. Feng, K. E. Parker, and E. M. Piers, "Removal of mercury from aqueous streams of fossil fuel power plants using novel functionalized nanoporous sorbents," in *Coal Combustion Byproducts and Environmental Issues*, K. S. Sajwan, I. Twardowska, T. Punshon, and A. K. Alva, Eds., pp. 99–104, Springer, New York, NY, USA, 2006.

[323] J. Kostal, A. Mulchandani, and W. Chen, "Tunable biopolymers for heavy metal removal," *Macromolecules*, vol. 34, no. 7, pp. 2257–2261, 2001.

[324] J. Kostal, A. Mulchandani, K. E. Gropp, and W. Chen, "A temperature responsive biopolymer for mercury remediation," *Environmental Science and Technology*, vol. 37, no. 19, pp. 4457–4462, 2003.

[325] L. Qi and Z. Xu, "Lead sorption from aqueous solutions on chitosan nanoparticles," *Colloids and Surfaces A: Physicochemical and Engineering Aspects*, vol. 251, no. 1–3, pp. 183–190, 2004.

[326] B. Van Der Bruggen and C. Vandecasteele, "Removal of pollutants from surface water and groundwater by nanofiltration: overview of possible applications in the drinking water industry," *Environmental Pollution*, vol. 122, no. 3, pp. 435–445, 2003.

[327] A. Favre-Reguillon, G. Lebuzit, J. Foos, A. Guy, M. Draye, and M. Lemaire, "Selective concentration of uranium from seawater by nanofiltration," *Industrial and Engineering Chemistry Research*, vol. 42, no. 23, pp. 5900–5904, 2003.

[328] K. D. Hristovski, H. Nguyen, and P. K. Westerhoff, "Removal of arsenate and 17α-ethinyl estradiol (EE2) by iron (hydr)oxide modified activated carbon fibers," *Journal of Environmental Science and Health—Part A Toxic/Hazardous Substances and Environmental Engineering*, vol. 44, no. 4, pp. 354–361, 2009.

[329] K. D. Hristovski, P. K. Westerhoff, T. Möller, and P. Sylvester, "Effect of synthesis conditions on nano-iron (hydr)oxide impregnated granulated activated carbon," *Chemical Engineering Journal*, vol. 146, no. 2, pp. 237–243, 2009.

[330] M. S. Diallo, S. Christie, P. Swaminathan, J. H. Johnson Jr., and W. A. Goddard III, "Dendrimer enhanced ultrafiltration.1. Recovery of Cu(II) from aqueous solutions using PAMAM dendrimers with ethylene diamine core and terminal NH2 groups," *Environmental Science and Technology*, vol. 39, no. 5, pp. 1366–1377, 2005.

[331] M. J. Aragon, R. L. Everett, M. D. Siegel et al., "Arsenic pilot plant operation and results," SAND 2007-6059, Sandia National Laboratories, Anthony, NM, USA, 2007.

[332] P. Sylvester, P. Westerhoff, T. Möller, M. Badruzzaman, and O. Boyd, "A hybrid sorbent utilizing nanoparticles of hydrous iron oxide for arsenic removal from drinking water," *Environmental Engineering Science*, vol. 24, no. 1, pp. 104–112, 2007.

[333] C. Charnock and O. Kjønnø, "Assimilable organic carbon and biodegradable dissolved organic carbon in Norwegian raw and drinking waters," *Water Research*, vol. 34, no. 10, pp. 2629–2642, 2000.

[334] J. Frias, F. Ribas, and F. Lucena, "Effects of different nutrients on bacterial growth in a pilot distribution system," *Antonie van Leeuwenhoek, International Journal of General and Molecular Microbiology*, vol. 80, no. 2, pp. 129–138, 2001.

[335] F. Li, A. Yuasa, K. Ebie, Y. Azuma, T. Hagishita, and Y. Matsui, "Factors affecting the adsorption capacity of dissolved organic matter onto activated carbon: modified isotherm analysis," *Water Research*, vol. 36, no. 18, pp. 4592–4604, 2002.

[336] M. J. Lehtola, T. Juhna, I. T. Miettinen, T. Vartiainen, and P. J. Martikainen, "Formation of biofilms in drinking water distribution networks, a case study in two cities in Finland and Latvia," *Journal of Industrial Microbiology and Biotechnology*, vol. 31, no. 11, pp. 489–494, 2004.

[337] B. Schreiber, T. Brinkmann, V. Schmalz, and E. Worch, "Adsorption of dissolved organic matter onto activated carbon—the influence of temperature, absorption wavelength, and molecular size," *Water Research*, vol. 39, no. 15, pp. 3449–3456, 2005.

[338] A. Matilainen, N. Vieno, and T. Tuhkanen, "Efficiency of the activated carbon filtration in the natural organic matter removal," *Environment International*, vol. 32, no. 3, pp. 324–331, 2006.

[339] C. Lu and F. Su, "Adsorption of natural organic matter by carbon nanotubes," *Separation and Purification Technology*, vol. 58, no. 1, pp. 113–121, 2007.

[340] S. A. Dastgheib, T. Karanfil, and W. Cheng, "Tailoring activated carbons for enhanced removal of natural organic matter from natural waters," *Carbon*, vol. 42, no. 3, pp. 547–557, 2004.

[341] P. A. Quinlivan, L. Li, and D. R. U. Knappe, "Effects of activated carbon characteristics on the simultaneous adsorption of aqueous organic micropollutants and natural organic matter," *Water Research*, vol. 39, no. 8, pp. 1663–1673, 2005.

[342] W. Cheng, S. A. Dastgheib, and T. Karanfil, "Adsorption of dissolved natural organic matter by modified activated carbons," *Water Research*, vol. 39, no. 11, pp. 2281–2290, 2005.

[343] H. Hyung and J.-H. Kim, "Natural organic matter (NOM) adsorption to multi-walled carbon nanotubes: effect of NOM characteristics and water quality parameters," *Environmental Science and Technology*, vol. 42, no. 12, pp. 4416–4421, 2008.

[344] N. B. Saleh, L. D. Pfefferle, and M. Elimelech, "Aggregation kinetics of multiwalled carbon nanotubes in aquatic systems: measurements and environmental implications," *Environmental Science and Technology*, vol. 42, no. 21, pp. 7963–7969, 2008.

[345] X. M. Yan, B. Y. Shi, J. J. Lu, C. H. Feng, D. S. Wang, and H. X. Tang, "Adsorption and desorption of atrazine on carbon

nanotubes," *Journal of Colloid and Interface Science*, vol. 321, no. 1, pp. 30–38, 2008.

[346] T. G. Hedderman, S. M. Keogh, G. Chambers, and H. J. Byrne, "In-depth study into the interaction of single walled carbon nanotubes with anthracene and p-terphenyl," *Journal of Physical Chemistry B*, vol. 110, no. 9, pp. 3895–3901, 2006.

[347] K. Yang, L. Zhu, and B. Xing, "Adsorption of polycyclic aromatic hydrocarbons by carbon nanomaterials," *Environmental Science and Technology*, vol. 40, no. 6, pp. 1855–1861, 2006.

[348] S. Gotovac, C.-M. Yang, Y. Hattori, K. Takahashi, H. Kanoh, and K. Kaneko, "Adsorption of polyaromatic hydrocarbons on single wall carbon nanotubes of different functionalities and diameters," *Journal of Colloid and Interface Science*, vol. 314, no. 1, pp. 18–24, 2007.

[349] C. L. Mangun, Z. Yue, J. Economy, S. Maloney, P. Kemme, and D. Cropek, "Adsorption of organic contaminants from water using tailored ACFs," *Chemistry of Materials*, vol. 13, no. 7, pp. 2356–2360, 2001.

[350] X. Peng, Y. Li, Z. Luan et al., "Adsorption of 1,2-dichlorobenzene from water to carbon nanotubes," *Chemical Physics Letters*, vol. 376, no. 1-2, pp. 154–158, 2003.

[351] C. Lu, Y.-L. Chung, and K.-F. Chang, "Adsorption thermodynamic and kinetic studies of trihalomethanes on multiwalled carbon nanotubes," *Journal of Hazardous Materials*, vol. 138, no. 2, pp. 304–310, 2006.

[352] Y.-Q. Cai, Y.-E. Cai, S.-F. Mou, and Y.-Q. Lu, "Multi-walled carbon nanotubes as a solid-phase extraction adsorbent for the determination of chlorophenols in environmental water samples," *Journal of Chromatography A*, vol. 1081, no. 2, pp. 245–247, 2005.

[353] Q. Zhou, J. Xiao, and W. Wang, "Using multi-walled carbon nanotubes as solid phase extraction adsorbents to determine dichlorodiphenyltrichloroethane and its metabolites at trace level in water samples by high performance liquid chromatography with UV detection," *Journal of Chromatography A*, vol. 1125, no. 2, pp. 152–158, 2006.

[354] Q. Zhou, J. Xiao, W. Wang, G. Liu, Q. Shi, and J. Wang, "Determination of atrazine and simazine in environmental water samples using multiwalled carbon nanotubes as the adsorbents for preconcentration prior to high performance liquid chromatography with diode array detector," *Talanta*, vol. 68, no. 4, pp. 1309–1315, 2006.

[355] M. Zhou, P. R. Nemade, X. Lu et al., "New type of membrane material for water desalination based on a cross-linked bicontinuous cubic lyotropic liquid crystal assembly," *Journal of the American Chemical Society*, vol. 129, no. 31, pp. 9574–9575, 2007.

[356] J. Nawrocki and B. Kasprzyk-Hordern, "The efficiency and mechanisms of catalytic ozonation," *Applied Catalysis B: Environmental*, vol. 99, no. 1-2, pp. 27–42, 2010.

[357] C. A. Orge, J. J. M. Órfão, M. F. R. Pereira, A. M. Duarte de Farias, R. C. R. Neto, and M. A. Fraga, "Ozonation of model organic compounds catalysed by nanostructured cerium oxides," *Applied Catalysis B: Environmental*, vol. 103, no. 1-2, pp. 190–199, 2011.

[358] N. Chitose, S. Ueta, S. Seino, and T. A. Yamamoto, "Radiolysis of aqueous phenol solutions with nanoparticles. 1. Phenol degradation and TOC removal in solutions containing TiO_2 induced by UV, γ-ray and electron beams," *Chemosphere*, vol. 50, no. 8, pp. 1007–1013, 2003.

[359] J. Jin, R. Li, H. Wang, H. Chen, K. Liang, and J. Ma, "Magnetic Fe nanoparticle functionalized water-soluble multi-walled carbon nanotubules towards the preparation of sorbent for aromatic compounds removal," *Chemical Communications*, no. 4, pp. 386–388, 2007.

[360] X. Han, Q. Kuang, M. Jin, Z. Xie, and L. Zheng, "Synthesis of titania nanosheets with a high percentage of exposed (001) facets and related photocatalytic properties," *Journal of the American Chemical Society*, vol. 131, no. 9, pp. 3152–3153, 2009.

[361] N. Murakami, Y. Kurihara, T. Tsubota, and T. Ohno, "Shape-controlled anatase titanium(IV) oxide particles prepared by hydrothermal treatment of peroxo titanic acid in the presence of polyvinyl alcohol," *Journal of Physical Chemistry C*, vol. 113, no. 8, pp. 3062–3069, 2009.

[362] S. Liu, J. Yu, and M. Jaroniec, "Anatase TiO_2 with dominant high-energy 001 facets: synthesis, properties, and applications," *Chemistry of Materials*, vol. 23, no. 18, pp. 4085–4093, 2011.

[363] S. Iwamoto, W. Tanakulrungsank, M. Inoue, K. Kagawa, and P. Praserthdam, "Synthesis of large-surface area silica-modified titania ultrafine particles by the glycothermal method," *Journal of Materials Science Letters*, vol. 19, no. 16, pp. 1439–1443, 2000.

[364] S. Iwamoto, S. Iwamoto, M. Inoue, H. Yoshida, T. Tanaka, and K. Kagawa, "XANES and XPS study of silica-modified titanias prepared by the glycothermal method," *Chemistry of Materials*, vol. 17, no. 3, pp. 650–655, 2005.

[365] H. Liu and L. Gao, "Synthesis and properties of CdSe-sensitized rutile TiO_2 nanocrystals as a visible light-responsive photocatalyst," *Journal of the American Ceramic Society*, vol. 88, no. 4, pp. 1020–1022, 2005.

[366] L. Wu, J. C. Yu, and X. Fu, "Characterization and photocatalytic mechanism of nanosized CdS coupled TiO_2 nanocrystals under visible light irradiation," *Journal of Molecular Catalysis A: Chemical*, vol. 244, no. 1-2, pp. 25–32, 2006.

[367] Y. Liu, X. Chen, J. Li, and C. Burda, "Photocatalytic degradation of azo dyes by nitrogen-doped TiO_2 nanocatalysts," *Chemosphere*, vol. 61, no. 1, pp. 11–18, 2005.

[368] M. S. Nahar, K. Hasegawa, and S. Kagaya, "Photocatalytic degradation of phenol by visible light-responsive iron-doped TiO_2 and spontaneous sedimentation of the TiO_2 particles," *Chemosphere*, vol. 65, no. 11, pp. 1976–1982, 2006.

[369] D. Sun, T. T. Meng, T. H. Loong, and T. J. Hwa, "Removal of natural organic matter from water using a nano-structured photocatalyst coupled with filtration membrane," *Water Science and Technology*, vol. 49, no. 1, pp. 103–110, 2004.

[370] A. Tuel and L. G. Hubert-Pfalzgraf, "Nanometric monodispersed titanium oxide particles on mesoporous silica: synthesis, characterization, and catalytic activity in oxidation reactions in the liquid phase," *Journal of Catalysis*, vol. 217, no. 2, pp. 343–353, 2003.

[371] M.-J. López-Muñoz, R. V. Grieken, J. Aguado, and J. Marugán, "Role of the support on the activity of silica-supported TiO_2 photocatalysts: structure of the TiO_2/SBA-15 photocatalysts," *Catalysis Today*, vol. 101, no. 3-4, pp. 307–314, 2005.

[372] X. Zhang, F. Zhang, and K.-Y. Chan, "Synthesis of titania-silica mixed oxide mesoporous materials, characterization and photocatalytic properties," *Applied Catalysis A: General*, vol. 284, no. 1-2, pp. 193–198, 2005.

[373] M. Pratap Reddy, A. Venugopal, and M. Subrahmanyam, "Hydroxyapatite-supported Ag-TiO_2 as *Escherichia coli* disinfection photocatalyst," *Water Research*, vol. 41, no. 2, pp. 379–386, 2007.

[374] S. K. Samantaray, P. Mohapatra, and K. Parida, "Physicochemical characterisation and photocatalytic activity of nanosized SO42-/TiO2 towards degradation of 4-nitrophenol," *Journal of Molecular Catalysis A: Chemical*, vol. 198, no. 1-2, pp. 277–287, 2003.

[375] Y. Chen, J. C. Crittenden, S. Hackney, L. Sutter, and D. W. Hand, "Preparation of a novel TiO_2-based p-n junction nanotube photocatalyst," *Environmental Science and Technology*, vol. 39, no. 5, pp. 1201–1208, 2005.

[376] J. M. Macak, M. Zlamal, J. Krysa, and P. Schmuki, "Self-organized TiO_2 nanotube layers as highly efficient photocatalysts," *Small*, vol. 3, no. 2, pp. 300–304, 2007.

[377] N. M. Al-Bastaki, "Performance of advanced methods for treatment of wastewater: UV/TiO_2, RO and UF," *Chemical Engineering and Processing: Process Intensification*, vol. 43, no. 7, pp. 935–940, 2004.

[378] M. J. Benotti, B. D. Stanford, E. C. Wert, and S. A. Snyder, "Evaluation of a photocatalytic reactor membrane pilot system for the removal of pharmaceuticals and endocrine disrupting compounds from water," *Water Research*, vol. 43, no. 6, pp. 1513–1522, 2009.

[379] P. Westerhoff, H. Moon, D. Minakata, and J. Crittenden, "Oxidation of organics in retentates from reverse osmosis wastewater reuse facilities," *Water Research*, vol. 43, no. 16, pp. 3992–3998, 2009.

[380] X. Zhao, L. Lv, B. Pan, W. Zhang, S. Zhang, and Q. Zhang, "Polymer-supported nanocomposites for environmental application: a review," *Chemical Engineering Journal*, vol. 170, no. 2-3, pp. 381–394, 2011.

[381] A. F. C. Campos, R. Aquino, T. A. P. G. Cotta, F. A. Tourinho, and J. Depeyrot, "Using speciation diagrams to improve synthesis of magnetic nanosorbents for environmental applications," *Bulletin of Materials Science*, vol. 34, no. 7, pp. 1357–1361, 2011.

[382] P. Li, D. E. Miser, S. Rabiei, R. T. Yadav, and M. R. Hajaligol, "The removal of carbon monoxide by iron oxide nanoparticles," *Applied Catalysis B: Environmental*, vol. 43, no. 2, pp. 151–162, 2003.

[383] R. Wu, J. Qu, and Y. Chen, "Magnetic powder MnO-Fe_2O_3 composite—A novel material for the removal of azo-dye from water," *Water Research*, vol. 39, no. 4, pp. 630–638, 2005.

[384] S. Qiao, D. D. Sun, J. H. Tay, and C. Easton, "Photocatalytic oxidation technology for humic acid removal using a nanostructured TiO_2/Fe_2O_3 catalyst," *Water Science and Technology*, vol. 47, no. 1, pp. 211–217, 2003.

[385] C.-B. Wang and W.-X. Zhang, "Synthesizing nanoscale iron particles for rapid and complete dechlorination of TCE and PCBs," *Environmental Science and Technology*, vol. 31, no. 7, pp. 2154–2156, 1997.

[386] W.-X. Zhang, C.-B. Wang, and H.-L. Lien, "Treatment of chlorinated organic contaminants with nanoscale bimetallic particles," *Catalysis Today*, vol. 40, no. 4, pp. 387–395, 1998.

[387] R. Cheng, J.-L. Wang, and W.-X. Zhang, "Comparison of reductive dechlorination of p-chlorophenol using Fe0 and nanosized Fe0," *Journal of Hazardous Materials*, vol. 144, no. 1-2, pp. 334–339, 2007.

[388] S. Choe, Y.-Y. Chang, K.-Y. Hwang, and J. Khim, "Kinetics of reductive denitrification by nanoscale zero-valent iron," *Chemosphere*, vol. 41, no. 8, pp. 1307–1311, 2000.

[389] J. Cao, D. Elliott, and W.-X. Zhang, "Perchlorate reduction by nanoscale iron particles," *Journal of Nanoparticle Research*, vol. 7, no. 4-5, pp. 499–506, 2005.

[390] S. Parra, S. E. Stanca, I. Guasaquillo, and K. Ravindranathan Thampi, "Photocatalytic degradation of atrazine using suspended and supported TiO_2," *Applied Catalysis B: Environmental*, vol. 51, no. 2, pp. 107–116, 2004.

[391] J. Xu and D. Bhattacharyya, "Modeling of Fe/Pd nanoparticle-based functionalized membrane reactor for PCB dechlorination at room temperature," *Journal of Physical Chemistry C*, vol. 112, no. 25, pp. 9133–9144, 2008.

[392] Y. Xu and D. Zhao, "Reductive immobilization of chromate in water and soil using stabilized iron nanoparticles," *Water Research*, vol. 41, no. 10, pp. 2101–2108, 2007.

[393] B. Schrick, J. L. Blough, A. D. Jones, and T. E. Mallouk, "Hydrodechlorination of trichloroethylene to hydrocarbons using bimetallic nickel-iron nanoparticles," *Chemistry of Materials*, vol. 14, no. 12, pp. 5140–5147, 2002.

[394] J. T. Nurmi, P. G. Tratnyek, V. Sarathy et al., "Characterization and properties of metallic iron nanoparticles: spectroscopy, electrochemistry, and kinetics," *Environmental Science and Technology*, vol. 39, no. 5, pp. 1221–1230, 2005.

[395] H.-L. Lien and W.-X. Zhang, "Transformation of chlorinated methanes by nanoscale iron particles," *Journal of Environmental Engineering*, vol. 125, no. 11, pp. 1042–1047, 1999.

[396] S.-F. Cheng and S.-C. Wu, "The enhancement methods for the degradation of TCE by zero-valent metals," *Chemosphere*, vol. 41, no. 8, pp. 1263–1270, 2000.

[397] S.-F. Cheng and S.-C. Wu, "Feasibility of using metals to remediate water containing TCE," *Chemosphere*, vol. 43, no. 8, pp. 1023–1028, 2001.

[398] H.-L. Lien and W.-X. Zhang, "Nanoscale iron particles for complete reduction of chlorinated ethenes," *Colloids and Surfaces A: Physicochemical and Engineering Aspects*, vol. 191, no. 1-2, pp. 97–105, 2001.

[399] F. He and D. Zhao, "Preparation and characterization of a new class of starch-stabilized bimetallic nanoparticles for degradation of chlorinated hydrocarbons in water," *Environmental Science and Technology*, vol. 39, no. 9, pp. 3314–3320, 2005.

[400] B.-W. Zhu, T.-T. Lim, and J. Feng, "Reductive dechlorination of 1,2,4-trichlorobenzene with palladized nanoscale Fe0 particles supported on chitosan and silica," *Chemosphere*, vol. 65, no. 7, pp. 1137–1145, 2006.

[401] J. Wei, X. Xu, Y. Liu, and D. Wang, "Catalytic hydrodechlorination of 2,4-dichlorophenol over nanoscale Pd/Fe: reaction pathway and some experimental parameters," *Water Research*, vol. 40, no. 2, pp. 348–354, 2006.

[402] T.-T. Lim, J. Feng, and B.-W. Zhu, "Kinetic and mechanistic examinations of reductive transformation pathways of brominated methanes with nano-scale Fe and Ni/Fe particles," *Water Research*, vol. 41, no. 4, pp. 875–883, 2007.

[403] P. V. Kamat, R. Huehn, and R. Nicolaescu, "A "sense and shoot" approach for photocatalytic degradation of organic contaminants in water," *Journal of Physical Chemistry B*, vol. 106, no. 4, pp. 788–794, 2002.

[404] Z.-C. Wu, Y. Zhang, T.-X. Tao, L. Zhang, and H. Fong, "Silver nanoparticles on amidoxime fibers for photo-catalytic degradation of organic dyes in waste water," *Applied Surface Science*, vol. 257, no. 3, pp. 1092–1097, 2010.

[405] B. P. Chaplin, E. Roundy, K. A. Guy, J. R. Shapley, and C. I. Werth, "Effects of natural water ions and humic acid on catalytic nitrate reduction kinetics using an alumina supported Pd-Cu catalyst," *Environmental Science and Technology*, vol. 40, no. 9, pp. 3075–3081, 2006.

[406] H. Hildebrand, K. Mackenzie, and F.-D. Kopinke, "Novel nano-catalysts for wastewater treatment," *Global Nest Journal*, vol. 10, no. 1, pp. 47–53, 2008.

[407] M. O. Nutt, J. B. Hughes, and M. S. Wong, "Designing Pd-on-Au bimetallic nanoparticle catalysts for trichloroethene hydrodechlorination," *Environmental Science and Technology*, vol. 39, no. 5, pp. 1346–1353, 2005.

[408] M. O. Nutt, K. N. Heck, P. Alvarez, and M. S. Wong, "Improved Pd-on-Au bimetallic nanoparticle catalysts for aqueous-phase trichloroethene hydrodechlorination," *Applied Catalysis B: Environmental*, vol. 69, no. 1-2, pp. 115–125, 2006.

[409] L. Espinal, S. L. Suib, and J. F. Rusling, "Electrochemical catalysis of styrene epoxidation with films of MnO_2 nanoparticles and H_2O_2," *Journal of the American Chemical Society*, vol. 126, no. 24, pp. 7676–7682, 2004.

[410] J. Fei, Y. Cui, X. Yan et al., "Controlled preparation of MnO2 hierarchical hollow nanostructures and their application in water treatment," *Advanced Materials*, vol. 20, no. 3, pp. 452–456, 2008.

[411] I. Dror, D. Baram, and B. Berkowitz, "Use of nanosized catalysts for transformation of chloro-organic pollutants," *Environmental Science and Technology*, vol. 39, no. 5, pp. 1283–1290, 2005.

[412] S. D. Kelly, K. M. Kemner, G. E. Fryxell, J. Liu, S. V. Mattigod, and K. F. Ferris, "X-ray-absorption fine-structure spectroscopy study of the interactions between contaminant tetrahedral anions and self-assembled monolayers on mesoporous supports," *Journal of Physical Chemistry B*, vol. 105, no. 27, pp. 6337–6346, 2001.

[413] G. E. Fryxell, Y. Lin, S. Fiskum et al., "Actinide sequestration using self-assembled monolayers on mesoporous supports," *Environmental Science and Technology*, vol. 39, no. 5, pp. 1324–1331, 2005.

[414] T. Schreiber, A. Weber, K. Niedergall et al., "Water treatment by molecularly imprinted polymer nanoparticles," in *Proceedings of the MRS Spring Meeting & Exhibit*, pp. Q04–Q07, April 2009.

[415] J. Kim and J. W. Grate, "Nano-biotechnology in using enzymes for environmental remediation: single-enzyme nanoparticles," in *Nanotechnology and the Environment: Applications and Implications*, B. Karn, T. Masciangioli, W. Zhang, V. Colvin, and P. Alivisatos, Eds., vol. 890, pp. 220–225, American Chemical Society, Washington, DC, USA, 2004.

[416] J. Xu, L. Bachas, and D. Bhattacharyya, "Synthesis of nanostructured bimetallic particles in polyligand-functionalized membranes for remediation applications," in *Nanotechnology Applications for Clean Water*, N. Savage, M. Diallo, J. Duncan, A. Street, and R. Sustich, Eds., chapter 22, pp. 311–335, William Andrew, Boston, Mass, USA, 2009.

[417] H. Choi, E. Stathatos, and D. D. Dionysiou, "Sol-gel preparation of mesoporous photocatalytic TiO_2 films and TiO_2/Al_2O_3 composite membranes for environmental applications," *Applied Catalysis B: Environmental*, vol. 63, no. 1-2, pp. 60–67, 2006.

[418] L. Wu and S. M. C. Ritchie, "Enhanced dechlorination of trichloroethylene by membrane-supported Pd-coated iron nanoparticles," *Environmental Progress*, vol. 27, no. 2, pp. 218–224, 2008.

[419] H. F. Lin, R. Ravikrishna, and K. T. Valsaraj, "Reusable adsorbents for dilute solution separation. 6. Batch and continuous reactors for the adsorption and degradation of 1,2-dichlorobenzene from dilute wastewater streams using titania as a photocatalyst," *Separation and Purification Technology*, vol. 28, no. 2, pp. 87–102, 2002.

[420] R. Molinari, L. Palmisano, E. Drioli, and M. Schiavello, "Studies on various reactor configurations for coupling photocatalysis and membrane processes in water purification," *Journal of Membrane Science*, vol. 206, no. 1-2, pp. 399–415, 2002.

[421] Y. Yang, H. Zhang, P. Wang, Q. Zheng, and J. Li, "The influence of nano-sized TiO_2 fillers on the morphologies and properties of PSF UF membrane," *Journal of Membrane Science*, vol. 288, no. 1-2, pp. 231–238, 2007.

[422] A. Rahimpour, S. S. Madaeni, A. H. Taheri, and Y. Mansourpanah, "Coupling TiO_2 nanoparticles with UV irradiation for modification of polyethersulfone ultrafiltration membranes," *Journal of Membrane Science*, vol. 313, no. 1-2, pp. 158–169, 2008.

[423] G. Wu, S. Gan, L. Cui, and Y. Xu, "Preparation and characterization of PES/TiO_2 composite membranes," *Applied Surface Science*, vol. 254, no. 21, pp. 7080–7086, 2008.

[424] G. C. C. Yang and C.-J. Li, "Preparation of tubular TiO_2/Al_2O_3 composite membranes and their performance in electrofiltration of oxide-CMP wastewater," *Desalination*, vol. 200, no. 1–3, pp. 74–76, 2006.

[425] Q. Zhang, Y. Fan, and N. Xu, "Effect of the surface properties on filtration performance of Al2O3-TiO2 composite membrane," *Separation and Purification Technology*, vol. 66, no. 2, pp. 306–312, 2009.

[426] L. Wu, M. Shamsuzzoha, and S. M. C. Ritchie, "Preparation of cellulose acetate supported zero-valent iron nanoparticles for the dechlorination of trichloroethylene in water," *Journal of Nanoparticle Research*, vol. 7, no. 4-5, pp. 469–476, 2005.

[427] D. E. Meyer, K. Wood, L. G. Bachas, and D. Bhattacharyya, "Degradation of chlorinated organics by membrane-immobilized nanosized metals," *Environmental Progress*, vol. 23, no. 3, pp. 232–242, 2004.

[428] L. Wu and S. M. C. Ritchie, "Removal of trichloroethylene from water by cellulose acetate supported bimetallic Ni/Fe nanoparticles," *Chemosphere*, vol. 63, no. 2, pp. 285–292, 2006.

[429] J. Xu and D. Bhattacharyya, "Fe/Pd nanoparticle immobilization in microfiltration membrane pores: synthesis, characterization, and application in the dechlorination of polychlorinated biphenyls," *Industrial and Engineering Chemistry Research*, vol. 46, no. 8, pp. 2348–2359, 2007.

[430] V. V. Tarabara, "Multifunctional nanomaterial-enabled membranes for water treatment," in *Nanotechnology Applications for Clean Water*, N. Savage, M. Diallo, J. Duncan, A. Street, and R. Sustich, Eds., chapter 5, pp. 59–75, William Andrew, Boston, Mass, USA, 2009.

[431] J. Xu and D. Bhattacharyya, "Membrane-based bimetallic nanoparticles for environmental remediation: synthesis and reactive properties," *Environmental Progress*, vol. 24, no. 4, pp. 358–366, 2005.

[432] K. Venkatachalam, X. Arzuaga, N. Chopra et al., "Reductive dechlorination of 3,3′,4,4′-tetrachlorobiphenyl (PCB77) using palladium or palladium/iron nanoparticles and assessment of the reduction in toxic potency in vascular endothelial cells," *Journal of Hazardous Materials*, vol. 159, no. 2-3, pp. 483–491, 2008.

[433] B. S. Karnik, S. H. R. Davies, K. C. Chen, D. R. Jaglowski, M. J. Baumann, and S. J. Masten, "Effects of ozonation on the permeate flux of nanocrystalline ceramic membranes," *Water Research*, vol. 39, no. 4, pp. 728–734, 2005.

[434] H. Verweij, M. C. Schillo, and J. Li, "Fast mass transport through carbon nanotube membranes," *Small*, vol. 3, no. 12, pp. 1996–2004, 2007.

[435] G. C. C. Yang and C.-M. Tsai, "Preparation of carbon fibers/carbon/alumina tubular composite membranes and their applications in treating Cu-CMP wastewater by a novel electrochemical process," *Journal of Membrane Science*, vol. 321, no. 2, pp. 232–239, 2008.

[436] Y. Yao, G. Li, K. A. Gray, and R. M. Lueptow, "Single-walled carbon nanotube-facilitated dispersion of particulate TiO_2 on ZrO_2 ceramic membrane filters," *Langmuir*, vol. 24, no. 14, pp. 7072–7075, 2008.

[437] S. Peltier, M. Cotte, D. Gatel, L. Herremans, and J. Cavard, "Nanofiltration: improvements of water quality in a large distribution system," *Water Science and Technology: Water Supply*, vol. 3, no. 1-2, pp. 193–200, 2003.

[438] G. L. Jadav and P. S. Singh, "Synthesis of novel silica-polyamide nanocomposite membrane with enhanced properties," *Journal of Membrane Science*, vol. 328, no. 1-2, pp. 257–267, 2009.

[439] M. F. Ottaviani, P. Favuzza, M. Bigazzi, N. J. Turro, S. Jockusch, and D. A. Tomalia, "A TEM and EPR investigation of the competitive binding of uranyl ions to starburst dendrimers and liposomes: potential use of dendrimers as uranyl ion sponges," *Langmuir*, vol. 16, no. 19, pp. 7368–7372, 2000.

[440] E. R. Birnbaum, K. C. Rau, and N. N. Sauer, "Selective anion binding from water using soluble polymers," *Separation Science and Technology*, vol. 38, no. 2, pp. 389–404, 2003.

[441] A. Bottino, G. Capannelli, V. D'Asti, and P. Piaggio, "Preparation and properties of novel organic-inorganic porous membranes," *Separation and Purification Technology*, vol. 22-23, pp. 269–275, 2001.

[442] K. Ebert, D. Fritsch, J. Koll, and C. Tjahjawiguna, "Influence of inorganic fillers on the compaction behaviour of porous polymer based membranes," *Journal of Membrane Science*, vol. 233, no. 1-2, pp. 71–78, 2004.

[443] T.-H. Bae and T.-M. Tak, "Effect of TiO_2 nanoparticles on fouling mitigation of ultrafiltration membranes for activated sludge filtration," *Journal of Membrane Science*, vol. 249, no. 1-2, pp. 1–8, 2005.

[444] N. Maximous, G. Nakhla, K. Wong, and W. Wan, "Optimization of Al_2O_3/PES membranes for wastewater filtration," *Separation and Purification Technology*, vol. 73, no. 2, pp. 294–301, 2010.

[445] M. T. M. Pendergast, J. M. Nygaard, A. K. Ghosh, and E. M. V. Hoek, "Using nanocomposite materials technology to understand and control reverse osmosis membrane compaction," *Desalination*, vol. 261, no. 3, pp. 255–263, 2010.

Hindawi Publishing Corporation
Advances in Materials Science and Engineering
Volume 2014, Article ID 102695, 6 pages
http://dx.doi.org/10.1155/2014/102695

Research Article

Thermomechanical Behavior of High Performance Epoxy/Organoclay Nanocomposites

Artur Soares Cavalcanti Leal,[1] Carlos Jose de Araújo,[2] Antônio Gilson de Barbosa Lima,[3] and Suédina Maria Lima Silva[3]

[1] *Post-Graduate Program in Process Engineering, Federal University of Campina Grande, Avenue Aprígio Veloso 882, 58429-900 Campina Grande, PB, Brazil*
[2] *Mecanichal Engineering Department, Federal University of Campina Grande, Avenue Aprígio Veloso 882, 58429-900 Campina Grande, PB, Brazil*
[3] *Materials Engineering Department, Federal University of Campina Grande, Avenue Aprígio Veloso 882, 58429-900 Campina Grande, PB, Brazil*

Correspondence should be addressed to Artur Soares Cavalcanti Leal; arturcleal@yahoo.com.br

Received 28 February 2014; Accepted 11 May 2014; Published 5 June 2014

Academic Editor: J. M. P. Q. Delgado

Nanocomposites of epoxy resin containing bentonite clay were fabricated to evaluate the thermomechanical behavior during heating. The epoxy resin system studied was prepared using bifunctional diglycidyl ether of bisphenol A (DGEBA), crosslinking agent diaminodiphenylsulfone (DDS), and diethylenetriamine (DETA). The purified bentonite organoclay (APOC) was used in all experiments. The formation of nanocomposite was confirmed by X-ray diffraction analysis. Specimens of the fabricated nanocomposites were characterized by dynamic mechanical analysis (DMA). According to the DMA results a significant increase in glass transition temperature and storage modulus was evidenced when 1 phr of clay is added to epoxy resin.

1. Introduction

Polymeric nanocomposites are hybrid materials where the dispersed phase has nanodimensions not exceeding 10 nm [1]. Similar to traditional composites, the continuous phase is an organic matrix (polymer) in which inorganic particles are dispersed in nanodimensions. By presenting significant gains in thermal, mechanical, and thermomechanical properties, barrier to gases and liquids, and flame retardance, nanocomposites of polymer/clay have attracted considerable attention in recent years [2].

The thermal behavior of epoxy systems depends on a number of factors such as type and concentration of the used components, mixing conditions, curing conditions, and postcure treatment. An increase in glass transition temperature (T_g) of epoxy/clay nanocomposites was observed by Lan et al. [3], while Massam and Pinnavaia [4] observed a reduction in T_g of the material. The increase in T_g was attributed to the slowing of molecular motion due to the interaction of nanoparticles, while the decrease can be explained by disruption of the reticulated structure, or residual monomers polymerization.

Like most epoxy nanocomposites actually presenting an intercalated structure, it is not surprising that most studies have shown that there was a reduction in T_g. However, different concentrations of curing agent and various methods for obtaining these nanocomposites, as well as the type of clay used, directly influence the results. Based on this description it is evident that the preparation of polymeric nanocomposites does not always contribute to an increase in thermal stability of epoxy systems. Santos [5] in his work on the cure kinetics and thermal stability of epoxy systems showed that variations in the structure of the nanocomposite can produce contradictory results on the thermal stability. The author found that although he had a considerable gain in the mechanical properties of epoxy/clay nanocomposite,

thermal properties were not improved. The thermal stability and glass transition temperature of these materials were lower than the epoxy system without nanoparticles dispersed.

An interesting characteristic that enables epoxy/clay nanocomposite to be used as a matrix for receiving a Ni-Ti shape memory alloy (SMA) is the thermal stability, which is directly influenced by the structure of nanocomposites. Exfoliated structures have better thermal stability in the range of transformation of SMA compared to nanocomposites with intercalated structures [6–10], and these results were observed in the results of dynamic mechanical analysis (DMA), for proportions of clay below 5% in mass.

The results, sometimes divergent of the thermomechanical properties of nanocomposites, are due to the fact that these properties are affected not only by the structure of nanocomposite, but also for many other factors, such as the crosslinking density, charge-matrix adhesion, reaction kinetics, and the method of determination of the thermal proprieties [11].

An effective method to study the thermal properties of nanocomposites is the dynamic mechanical analysis (DMA). In this work, the thermal behavior of a polymer matrix composed of one bifunctional crosslinking monomer diglycidyl ether of bisphenol A (DGEBA) and two different types of crosslinking agent, aliphatic amines diethylenetriamine (DETA) and aromatic amine diaminodiphenylsulfone (DDS), was evaluated in order to select it as polymeric matrix of better thermal stability.

In this context, this paper aims to apply the general technique of dynamic mechanical analysis (DMA) to evaluate the effect of curing agent and of the treatment of postcuring in the thermal properties of different systems. In order to select an adequate epoxy polymer matrix to be used in nanocomposites, the incorporation of Ni-Ti alloy wire with shape memory effect is studied.

2. Experimental Procedure

2.1. Materials. Sodium bentonite purified (APOC), with cation exchange capacity (CEC) value of about 100 meq/100 g, was purchased from Bentonit União Nordeste, Campina Grande, Paraíba State, Brazil. The preparation of organobentonite by ion exchange was carried out according to previously reported methods [12]; the organobentonite was modified with cetyl trimethyl ammonium bromide ($C_{16}H_{33}(CH_3)_3NBr$). The used epoxy resin was the diglycidyl ether of bisphenol A (DGEBA) supplied by Silaex Química Ltda., São Paulo, São Paulo State, Brazil. The epoxide equivalent weight of epoxy resin was 182–192 g eq^{-1}. Aliphatic amines, diaminodiphenylsulfone (DDS) and diethylenetriamine (DETA), were used as curing agents for epoxy resin. The chemical structures of DDS and DETA epoxy resins are shown in Figure 1.

For the isothermal cure experiment, the epoxy resin and the curing agent are mixed in the stoichiometric ratio of 44 parts per hundred resin (phr) to curing agent DDS and to 36 phr to curing agent (DETA). The mixture was then mixed with 1% organobentonite powder.

Table 1: Specification of the polymer matrix studied.

Component	Curing	Postcure	Coding
DGEBA/DETA	7 hours/110°C	160°C/2 hours	DGEBA_DETApc
DGEBA/DETA	7 hours/110°C	—	DGEBA_DETA
DGEBA/DDS	5 hours/160°C	200°C/2 hours	DGEBA_DDSpc
DGEBA/DDS	5 hours/160°C	—	DGEBA_DDS

2.2. Synthesis of the Epoxy Resin. For the synthesis of epoxy resin using DGEBA/DDS (resin/hardener), a specific quantity (40 g) of DGEBA was placed in a Becker glass and heated in an oven at 110°C for 15 minutes and an amount equivalent to 44 phr (parts per hundred resin) of DETA hardener was added. The mixture DGEBA/DDS was mixed mechanically at low rotation speed (~200 rpm) at temperature 90°C for 15 minutes before being inserted into the cast in a metallic mold, previously manufactured with rectangular cavities 125 × 12.7 × 3.2 mm, corresponding to the shape of a flexion test specimens according to ASTM D790. The samples were kept at 160°C for a period of 5 hours. After this period, the epoxy resin was postcured at 200°C for 2 hours to obtain the maximum conversion.

The procedure used for the synthesis of DGEBA/DETA resin was similar to that used for DGEBA/DDS. However, in this case 36 phr of crosslinking agent was used (DETA). The resin was cured at 110°C for 7 hours and postcured at 135°C for 2 hours. The curing and postcure conditions as well as the codification of the epoxy systems studied are presented in Table 1.

2.3. Synthesis of the Nanocomposite. The epoxy resin DGEBA (40 g) was mixed with the desired amount of organophilic clay. The organoclay (325 mesh) was dispersed uniformly in epoxy monomer at 50°C and 200 rpm for 1 h. Then, the curing agent (DDS) was added into the epoxy/clay hybrid system and mixed thoroughly by stirring. The mixtures were cast into a mold. The samples were cured with DDS for 5 h and 160°C and postcured for 2 h at 200°C. The procedure used in the synthesis of DGEBA/DETA was similar to that used for DGEBA/DDS. However, in this case the mixture DGEBA/DETA poured into the mold cavity was placed in an oven at 110°C, maintained for a period of 7 hours, and postcured at 160°C for 2 hours. Conditions for healing and posttreatment, including the codes of the systems studied, are shown in Table 1.

2.4. Experimental Tests. In order to study the phase morphology, all samples were examined by DMA analysis, a powerful technique to study the relaxation and miscibility behavior of polymers and blends. The tangent to the peak of temperature, that is, T_g, can be used to evaluate miscibility and immiscibility of polymer blends [13]. Dynamic mechanical properties of nanocomposites and composites were measured with a TA Q800 dynamical mechanical analyzer (DMA) in fixed frequency mode at 1 Hz with 15 μm oscillation amplitude, and temperature ranges from 30 to 250°C with variation of 5°C/min loaded under single cantilever mode. The sample

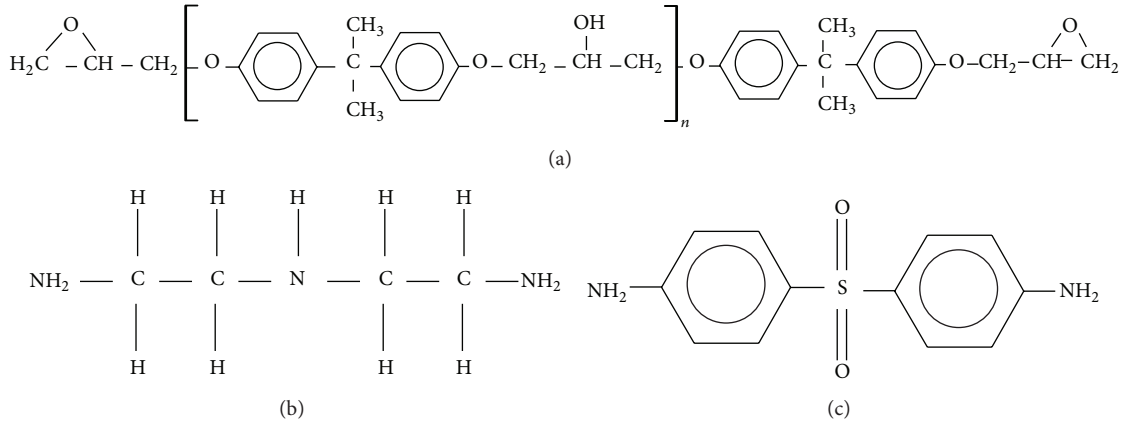

Figure 1: Chemical structures of epoxy resins. (a) DGEBA, (b) DETA, and (c) DDS.

size was 12.7 × 3.47 × 2 mm. The glass transition temperature (T_g) was determined from the peak of the tan δ curve. X-ray diffraction (XRD) analysis was performed on a Shimadzu XRD-6000 diffractometer with Cu Kα radiation (λ = 0.154 nm, 40 kV, 30 mA) at room temperature. Diffraction was performed from 1.5° to 12° at a scan rate of 2°/min with a step size of 0.02°.

3. Results and Discussion

3.1. Thermomechanical Properties of the Epoxy Resin. The dynamic mechanical analysis (DMA) was performed to investigate the influence of the APOC concentration and postcuring treatment on the storage modulus and on the transition (tan δ) of the nanocomposites. Figures 2(a) and 2(b) show the curves of damping (tan δ) and storage modulus E' as a function of the temperature for epoxy systems cured with hardener DETA (EPX_DETA) and with hardener DDS (EPX_DDS), after having undergone postcuring treatment at different conditions (EPX_DETApc and EPX_DDSpc). A postcuring treatment in the systems evaluated at a temperature slightly above the T_g of the material was perfomed, in order to obtain the maximum convection system.

It was evident (Figure 2 and Table 2) that the thermal behaviors of epoxy resin diglycidyl ether of bisphenol A (DGEBA) are affected by the type of curing agent (hardener) and postcure treatment. The epoxy resin cured with DDS hardeners (EPX_DDS system) showed higher values of T_g (determined by the value of the peak of tan δ) than that cured with hardener DETA (EPX_DETA). When these systems were subjected to the treatment of postcure, EPX_DETApc and EPX_DDSpc, the increase in the value of T_g was even more significant. According to Jones [14], the T_g changes with the structure of cured resin and thermal history of the sample. These authors showed that even after the complete reaction of epoxy groups, that is, degree of conversion (X_e) of approximately 99%, an increase in T_g was observed. For long times of postcuring, the T_g is still increasing, although all epoxy groups have reacted. The reason for this behavior is due to variations in the chemical structure of the lattice that occur after essentially all epoxy groups have reacted; moreover, there are considerable variations in density and variations in T_g for times of healing or postcure when the extent of reaction is kept essentially constant, that is, $X_e \sim 0.99$. These reactions allowed restricting the molecular mobility in the region of glass transition and, therefore, considerable increases in the values of T_g are observed [15].

Table 2: Cure and postcure temperature peak factor and the glass transition temperature T_g for different epoxy systems.

Epoxy system	Cure and postcure temperature	Peak factor (Γ)	T_g (°C)
EPX_DETA	110°C/7 h	0.1706	126.5
EPX_DDS	160°C/5 h	0.2878	175.1
EPX_DETApc	130°C/7 h/2 h	0.7590	140.5
EPX_DDSpc	200°C/5 h/2 h	0.1690	212.2

As shown in Figure 2(a) the amplitude and the width of the peak tan δ were modified when the epoxy systems were undergoing postcure treatment, especially for the system cured with DDS. According to literature [13], the peak factor (Γ) (Table 1), defined as the full width at half maximum of the tan δ divided by its height, can be qualitatively used to evaluate the homogeneity of epoxy network. A higher peak factor for nanocomposite indicates a lower cross-link density and greater heterogeneity, which suggest intercalation of the epoxy network into the layers. Then, probably the homogeneity of the reticulation system for the epoxy cured with DDS was higher than for the system cured with DETA.

3.2. X-Ray Diffraction Analysis. Figure 3 shows X-ray diffraction patterns of the clay APOC and systems cured with epoxy curing agents DETA and DDS containing 1 parts per hundred resin (phr) of organoclay APOC (EPX_DETA.APOC and EPX_DDS.APOC) postcured. The clay showed the peak (001) at 2θ = 4.75° corresponding to a basal spacing of 1.85 nm, which corresponds to an interlayer spacing of the clay. The absence of peak (001) for EPX_DETA.APOC and EPX_DDS.APOC systems indicates the penetration of resin in the galleries of the clay and the formation of predominantly

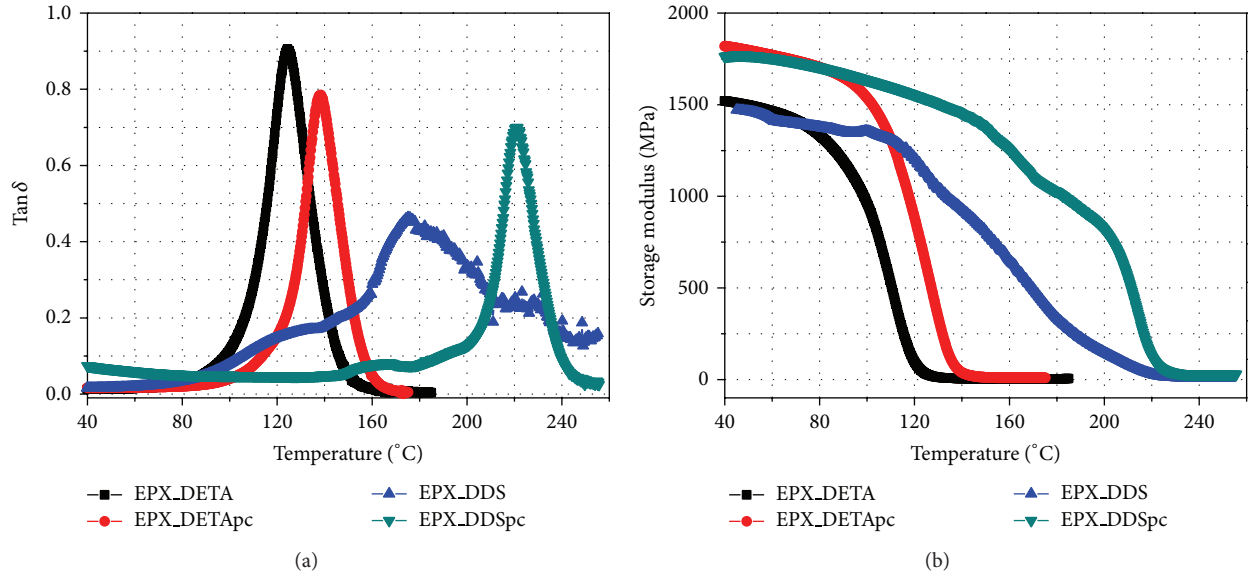

FIGURE 2: (a) Tan δ and storage modulus; (b) Tan δ as a function of the temperature for DGEBA/DDS and DGEBA/DETA epoxy system.

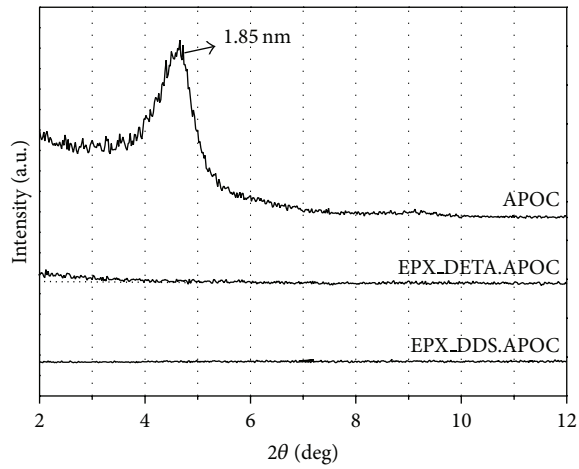

FIGURE 3: X-ray diffraction patterns of organoclay (APOC) and the nanocomposite containing 1 parts per hundred of organoclay (EPX_DDS.APOC) and (EPX_DETA.APOC) resins.

exfoliated nanocomposite EPX_DDS.APOC for the system (as the absence of the peak in the diffractogram) and is indicative of exfoliation for the EPX_DETA.APOC system (as slight inclination of 2θ around 2°). These results are similar to those reported in the literature, where the authors have shown that there is a direct correlation between the X-ray diffraction data and transmission electron microscopy (TEM); that is, absence of peak (001) in the diffractogram corresponds to a nanocomposite with exfoliated structure [8, 9, 16].

3.3. Thermal Mechanical Properties of the Nanocomposites. The incorporation of only 1 phr of organoclay in the postcured epoxy systems (EPX_DETA.APOC and EPX_DDS.APOC) resulted in an increase of the glass transition temperature (T_g) and of the thermal stability of these systems (Figure 4(a) and Table 2). The increase in T_g was approximately of 9°C when the APOC organoclay was incorporated. These results can be attributed to high aspect ratio of clay dispersion in polymer matrix that can act as physical crosslinker, whereas the epoxy resin was intercalated in the galleries of the clay, forming a predominantly exfoliated structure, as XRD data shown in Figure 3. It is also observed that the T_g of the system EPX_DDS.APOC was considerably higher (72°C) than the system EPX_DETA.APOC probably due to greater exfoliation of clay layers in polymer matrix.

Note that the nanocomposites are more thermally stable than the pure epoxy systems, especially the nanocomposite EPX_DDS.APOC, as indicated by higher plateau modulus vitreous and a lower percentage of loss modulus with temperature (Figure 4 and Table 3). These results can be attributed to restricted mobility of polymer chains due to high aspect ratio and high stiffness of the silicate layers dispersed in the polymer matrix. A significant improvement in storage modulus between 40 and 90°C was also portrayed in other works [16, 17].

According to Figure 4(b) the increases in storage modulus E' of exfoliated nanocomposites were more pronounced in the glassy region ($T < T_g$), indicating that the organoclay nanolayers were well exfoliated and dispersed homogeneously in the polymer matrix, especially for system cured with DDS [11]. This may have contributed to the formation of strong interaction forces between the epoxy resin and organoclay as the epoxy polymer chains are trapped in the clay surface through hydrogen bonds, due to the interactions between the hydroxyl groups of the organoclay and groups of ether epoxy resin, as shown in Figure 5 [16].

In summary, the thermomechanical properties observed in the epoxy cured with DDS hardener proved to be useful when used as matrix and Ni-Ti shape memory alloy (SMA) which are embedded in the nanocomposite, since it has both

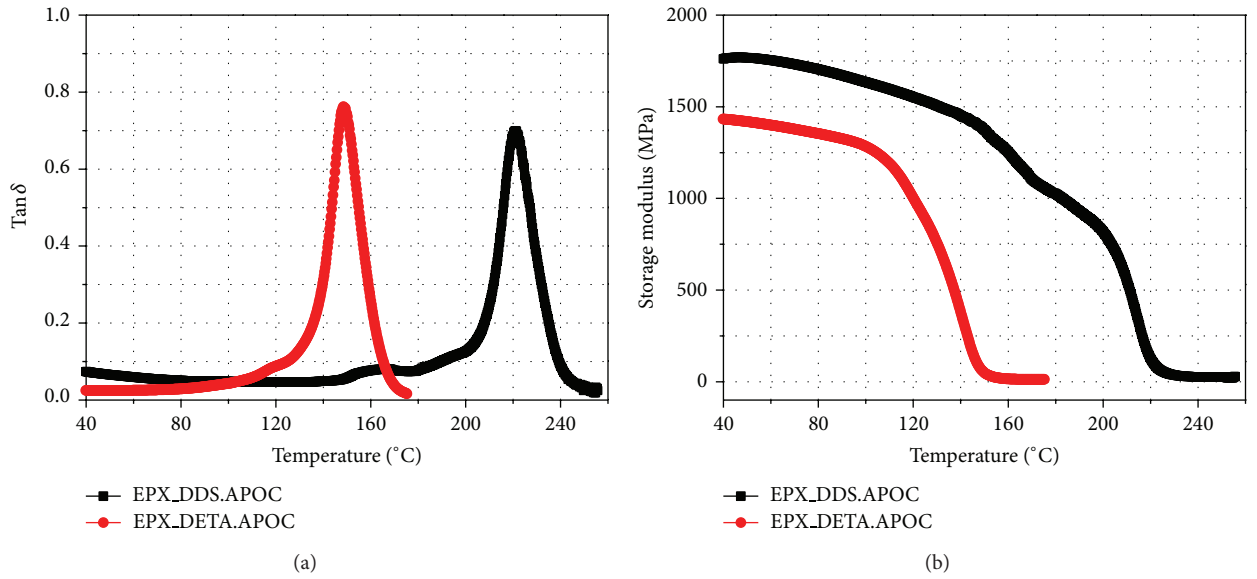

Figure 4: (a) Tan δ and storage modulus; (b) Tan δ as a function of the temperature for DGEBA/DDS and DGEBA/DETA epoxy system.

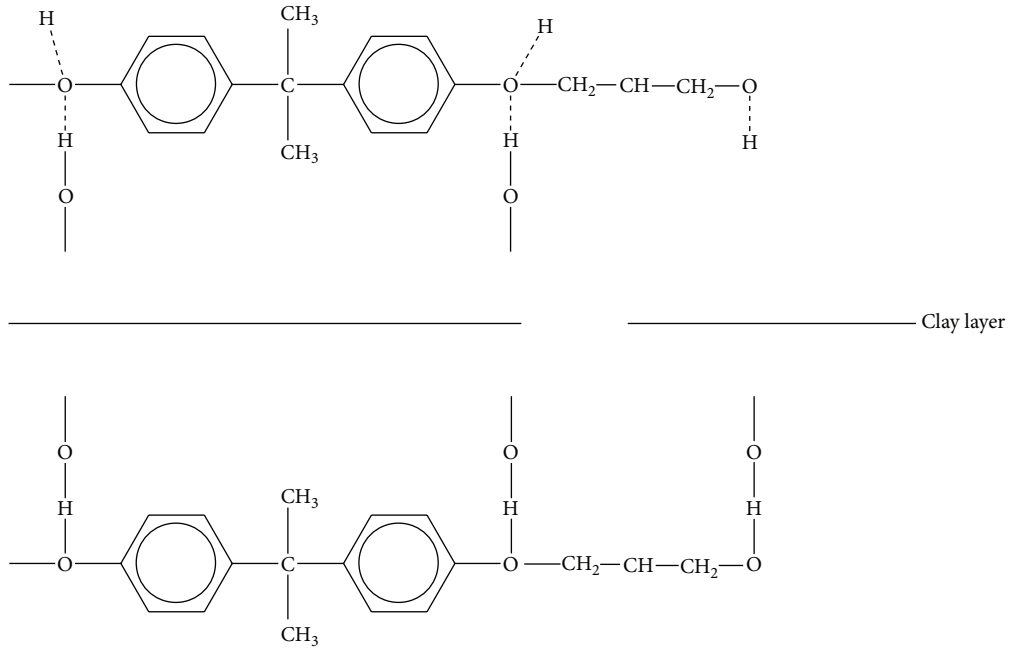

Figure 5: Interactions of hydrogen bonds between DGEBA and epoxy clay layer.

Table 3: Storage modulus (E') and T_g (tan δ peak) for different epoxy systems.

Epoxy system	E' (GPa)						% lost of E'	T_g (°C)
	40°C	50°C	60°C	70°C	80°C	90°C		
EPX_DETApc	1.82	1.79	1.77	1.74	1.70	1.64	9.89	140.52
EPX_DDSpc	1.33	1.30	1.29	1.25	1.23	1.21	9.02	212.23
EPX_DETA.APOC	1.43	1.41	1.40	1.37	1.35	1.32	7.69	149.08
EPX_DDS.APOC	1.76	1.76	1.75	1.73	1.70	1.67	5.11	221.11

T_g and thermal stability high enough to withstand repeated heating of SMA wires in the range of transformation phase, and the transformation temperatures of this type of material are found in regions near the temperature where the matrix is thermally stable.

4. Conclusions

The thermal behavior of the epoxy systems investigated was affected by thermal treatment of postcuring, especially when bentonite purification is used. XRD analysis showed exfoliation in the organoclay nanolayers for nanocomposite EPX_DDS.APOC and was indicative of exfoliation for the system EPX_DETA.APOC. Thermomechanical tests (DMA) indicated that EPX_DDS.APOC nanocomposites present higher T_g and thermal stability, compared with pure EPX_DETA, EPX_DDS, and EPX_DETA.APOC. Thus, the system EPX_DDS.APOC can be used in future work or preparation of nanocomposites activated with shape memory alloys (SMA) since the transformation temperature of SMA occurs approximately at the temperature where the matrix is thermally stable, that is, between 40 and 80°C.

Conflict of Interests

The authors declare that there is no conflict of interests regarding the publication of this paper.

Acknowledgments

The authors thank CNPQ, CAPES, and FINEP by financial support and to the researchers cited in the text that helped in the improvement of this work.

References

[1] L. A. Utracki, *Clay-Containing Polymeric Nanocomposites*, vol. 1-2, Rapra Technology Limited, London, UK, 2004.

[2] S. Sinha Ray and M. Okamoto, "Polymer/layered silicate nanocomposites: a review from preparation to processing," *Progress in Polymer Science*, vol. 28, no. 11, pp. 1539–1641, 2003.

[3] T. Lan, P. D. Kaviratna, and T. J. Pinnavaia, "Mechanism of clay tactoid exfoliation in epoxy-clay nanocomposites," *Chemistry of Materials*, vol. 7, no. 11, pp. 2144–2150, 1995.

[4] J. Massam and T. J. Pinnavaia, *MRS Symposia Proceedings*, Materials Research Society, Pittsburgh, Pa, USA, 1998.

[5] R. G. S. Santos, *Study of effect on chemorheology of nanostructured organophilic clay epoxy resin composite due to filler-matrix interaction [M.S. thesis]*, Escola de Engenharia de Lorena, Universidade de São Paulo, Lorena, Brazil, 2009.

[6] J. Lee, T. Takekoshi, and E. Giannelis, "Fire retardant polyetherimide nanocomposites," in *Nanophase and Nanocomposite Materials II*, S. Komarneni, J. C. Parker, and H. J. Wollenberger, Eds., vol. 457 of *MRS Proceedings*, pp. 513–518, Materials Research Society, Pittsburgh, Pa, USA, 1998.

[7] D. Ratna, N. R. Manoj, R. Varley, R. K. Singh Raman, and G. P. Simon, "Clay-reinforced epoxy nanocomposites," *Polymer International*, vol. 52, no. 9, pp. 1403–1407, 2003.

[8] A. Yasmin, J. L. Abot, and I. M. Daniel, "Processing of clay/epoxy nanocomposites by shear mixing," *Scripta Materialia*, vol. 49, no. 1, pp. 81–86, 2003.

[9] K. Wang, L. Chen, M. Kotaki, and C. He, "Preparation, microstructure and thermal mechanical properties of epoxy/crude clay nanocomposites," *Composites Part A: Applied Science and Manufacturing*, vol. 38, no. 1, pp. 192–197, 2007.

[10] A. Asif, R. V. Lakshmana, V. Saseendran, and K. N. Ninan, "Thermoplastic toughened layered silicate epoxy ternary nanocomposites-preparation, morphology, and thermomechanical properties," *Polymer Engineering and Science*, vol. 10, pp. 1002–1017, 2009.

[11] R. Kotsilkova, V. Petkova, and J. Pelovski, *Thermoset Nanocomposites for Engineering Applications*, Smithers Rapra Technology Limited, 2007.

[12] I. F. Leite, A. P. S. Soares, L. H. Carvalho, C. M. O. Raposo, O. M. L. Malta, and S. M. L. Silva, "Characterization of pristine and purified organobentonites," *Journal of Thermal Analysis and Calorimetry*, vol. 100, no. 2, pp. 563–569, 2010.

[13] Y. Zhou, F. Pervin, M. A. Biswas, V. K. Rangari, and S. Jeelani, "Fabrication and characterization of montmorillonite clay-filled SC-15 epoxy," *Materials Letters*, vol. 60, no. 7, pp. 869–873, 2006.

[14] F. R. Jones, "Composite materials," in *Chemistry and Technology of Epoxy Resins*, B. Ellis, Ed., pp. 256–302, Chapman & Hall, London, UK, 1993.

[15] R. Velmurugan and T. P. Mohan, "Room temperature processing of epoxy-clay nanocomposites," *Journal of Materials Science*, vol. 39, no. 24, pp. 7333–7339, 2004.

[16] X. Kornmann, H. Lindberg, and L. A. Berglund, "Synthesis of epoxy-clay nanocomposites. Influence of the nature of the curing agent on structure," *Polymer*, vol. 42, no. 10, pp. 4493–4499, 2001.

[17] W.-B. Xu, S.-P. Bao, and P.-S. He, "Intercalation and exfoliation behavior of epoxy resin/curing agent/montmorillonite nanocomposite," *Journal of Applied Polymer Science*, vol. 84, no. 4, pp. 842–849, 2002.

Hindawi Publishing Corporation
Advances in Materials Science and Engineering
Volume 2014, Article ID 659148, 5 pages
http://dx.doi.org/10.1155/2014/659148

Research Article

Influence of Processing Type in the Morphology of Membranes Obtained from PA6/MMT Nanocomposites

Rodholfo da Silva Barbosa Ferreira, Caio Henrique do Ó Pereira, Rene Anisio da Paz, Amanda Melissa Damião Leite, Edcleide Maria Araújo, and Hélio de Lucena Lira

Federal University of Campina Grande, Avenida Aprígio Veloso, 882 Bodocongó, 58429-140 Campina Grande, PB, Brazil

Correspondence should be addressed to Rodholfo da Silva Barbosa Ferreira; rodholfoferreira@gmail.com

Received 30 November 2013; Revised 25 February 2014; Accepted 25 February 2014; Published 16 April 2014

Academic Editor: A. G. Barbosa de Lima

The nanocomposites have an extensive use in the current process of membrane preparation, taking into account their unique features as membranes. Thus, the study of nanocomposite processing to obtain membranes is highly important. In this work, Brazilian clay was used (Brasgel PA) for the preparation of polyamide/clay nanocomposite. The nanocomposites were produced in a high rotation homogenizer and in a twin screw extruder. From the nanocomposites and pure polymers processed in the two equipments, membranes were prepared by the immersion-precipitation method, using formic acid as solvent. By X-ray diffraction (XRD), the formation of exfoliated and/or partially exfoliated structures with changes in the crystalline phases of the polyamide was observed. From scanning electron microscopy images, it was observed that the processing clearly influenced the membrane morphology.

1. Introduction

Recently, the membrane technology is applied in several industrial processes presenting numerous advantages, such as continuous processing with low energy consumption and easy combination with other separation processes [1]. In the early 1970s, besides the development of classical separation techniques, new synthetic membranes, which can be used as a selective barrier, were developed. The synthetic membranes were designed to improve the characteristics of selectivity and permeability of natural membranes. The addition of inorganic nanoparticles (clay) greatly improves the filtration properties of the membrane. Several studies indicate that the addition of inorganic nanoparticles in the polymer solution, used to prepare membrane by phase inversion, can control the formation and growth of macropores, increase the number of small pores, and improve the hydrophilicity, porosity, and permeability and mechanical and antifouling properties [2, 3].

The membranes can be considered polymeric or inorganic films that work as a semipermeable barrier to filtration in a molecular scale, separating two phases and restricting, totally or partially, the transport of one or several chemical species (solutes) present in a solution [4, 5].

Most membranes used worldwide and so-called second generation are produced from synthetic polymers, such as polyamide, polysulfone, polyacrylonitrile, polycarbonate, and poly(vinylidene fluoride), among others. They show resistance to the action of strong acids and bases (pH from 2 to 12) and support temperatures close to or even superior to 100°C. These membranes can also be used with nonaqueous solvents and have long lifetime [6].

Most of polymer membranes used commercially are prepared by phase inversion technique, which consists of three main steps: preparation of polymer solution, spreading the solution on a surface forming a film with controlled thickness, and, finally, precipitating nonsolvent for formation of the polymeric structure of the membranes by using a phase separation system [7, 8].

Many materials may be used to prepare polymer membranes, among them is the polyamide. This polymer presents high performance and excellent mechanical and thermal properties [9]. In addition, the polyamides being used as nanocomposites matrices where have presented attractive

properties, for instance, barrier properties to gas permeation. The hybrids organic/inorganic films obtained from clay present a waterproofing due to the lamellas of montmorillonite that act as a barrier with less loads than the conventional composite films [10].

The polymer nanocomposites are hybrid materials where particles with nanometric size are dispersed in a polymeric matrix. They can be considered a new class of polymer composed of inorganic phases with ultrafine dimensions that interact with the polymer, thus offering a better combination of properties such as toughness and resistance, difficult to be achieved with pure polymer. Reinforced polymers with low content of clay (1 to 5% in mass) have raised interest in academic and industrial environments, due to the considerable improvement in the physical and mechanical properties, as well as permitting the processing from conventional techniques such as extrusion and/or injection [11–13].

The aim of this work is to analyze the structure and morphology of polymeric membranes using X-ray diffraction (XRD) and scanning electron microscopy (SEM), respectively. The membranes were prepared by the phase inversion method from PA6/MMT nanocomposites.

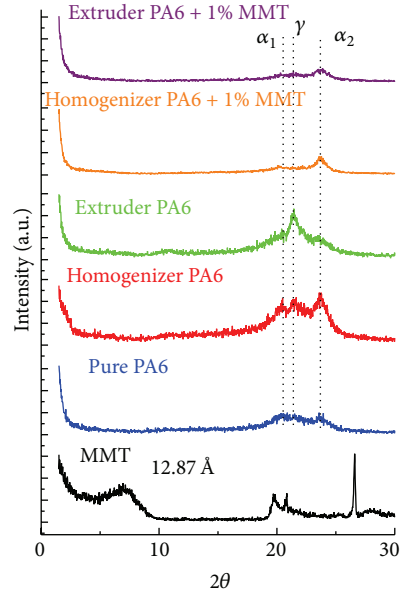

Figure 1: X-ray diffraction curves of clay, pure polyamide, and nanocomposites.

2. Materials and Methods

2.1. Materials. A sample of Brasgel PA clay was used, supplied by Bentonit União do Nordeste (BUN), from Campina Grande, Paraiba, Brazil), with cation exchange capacity (CEC) of 90 meq/100 g, and passed in a sieve ABNT 200 mesh. Polyamide 6 from Polyform B300, with average viscosity IV = 140–160 mL/g, in the form of granules in white was used. Formic acid PA from Vetec, with 98% of purity, was used as solvent to dissolve the polymer and nanocomposites to prepare the membranes.

2.2. Methods

2.2.1. Preparation of Nanocomposites. For the nanocomposites preparation, 1% was used in mass of clay to the polymer and two processing equipment: a high rotation homogenizer, MH-50H model, and a corotational twin screw extruder from Coperion. In the first, the clay was dispersed directly in the equipment. In the second, a concentrated (50 : 50% in mass) in the homogenizer was obtained and then incorporated in a polymer matrix in the proportion of 1% in mass of clay, using the extruder. Processing conditions were as follows: mixed in the homogenizer for 30 to 40 seconds until PA6 melting. The processing in the extruder is done in a temperature of 260°C for 7 existing zones and a screw rotation of 250 rpm. For each processing step, all materials with polyamide 6 were dried in a circulating air oven at 80°C for 2 h and in a vacuum oven at 80°C for 24 hours.

2.2.2. Preparation of Membranes. For the membrane preparation, the phase inversion method was used through the immersion-precipitation technique. The polyamide and its nanocomposites were dissolved in formic acid in a proportion of 20% in mass of polymer under constant stirring for 24 hours, for total polymer dissolution. The solution was spread in a glass plate, previously washed and dried. The spreading was done manually with a spacer and the polymer film was quickly immersed in a precipitation bath with distilled water. Then, the membranes were removed, washed with distilled water to remove the residual solvent, and dried at room temperature. This procedure is according to Leite [14]. The nomenclature used is the following: Pure PA6 (polyamide without processing), Extruder PA6, Homogenizer PA6, PA6 + 1%MMT, Extruder PA6 + 1%MMT, and Homogenizer PA6 + 1%MMT.

2.2.3. Materials Characterization. The nanocomposites were characterized by X-ray diffraction (XRD), using a Shimadzu XRD-6000 equipment, with CuKα radiation (λ = 1.5418 Å), 40 kV, 30 mA, and scanning 2θ from 1.5° to 30° at a scanning rate of 2°/min.

The membranes were characterized by scanning electron microscopy, using a SSX 550 Superscan from Shimadzu, operating at 15 kV. Both top and cross section surfaces of the membranes were evaluated. For the cross section analysis, the samples were fractured in liquid nitrogen to avoid plastic deformation. The surfaces were coated with gold.

3. Results and Discussion

3.1. X-Ray Diffraction (XRD). The analysis of X-ray diffraction of the bentonite clay (MMT) without treatment (Figure 1) revealed the presence of characteristic peaks of bentonite and other minerals such as quartz (Q). A peak was observed in the interplanar distance of 12.77 Å, characteristic

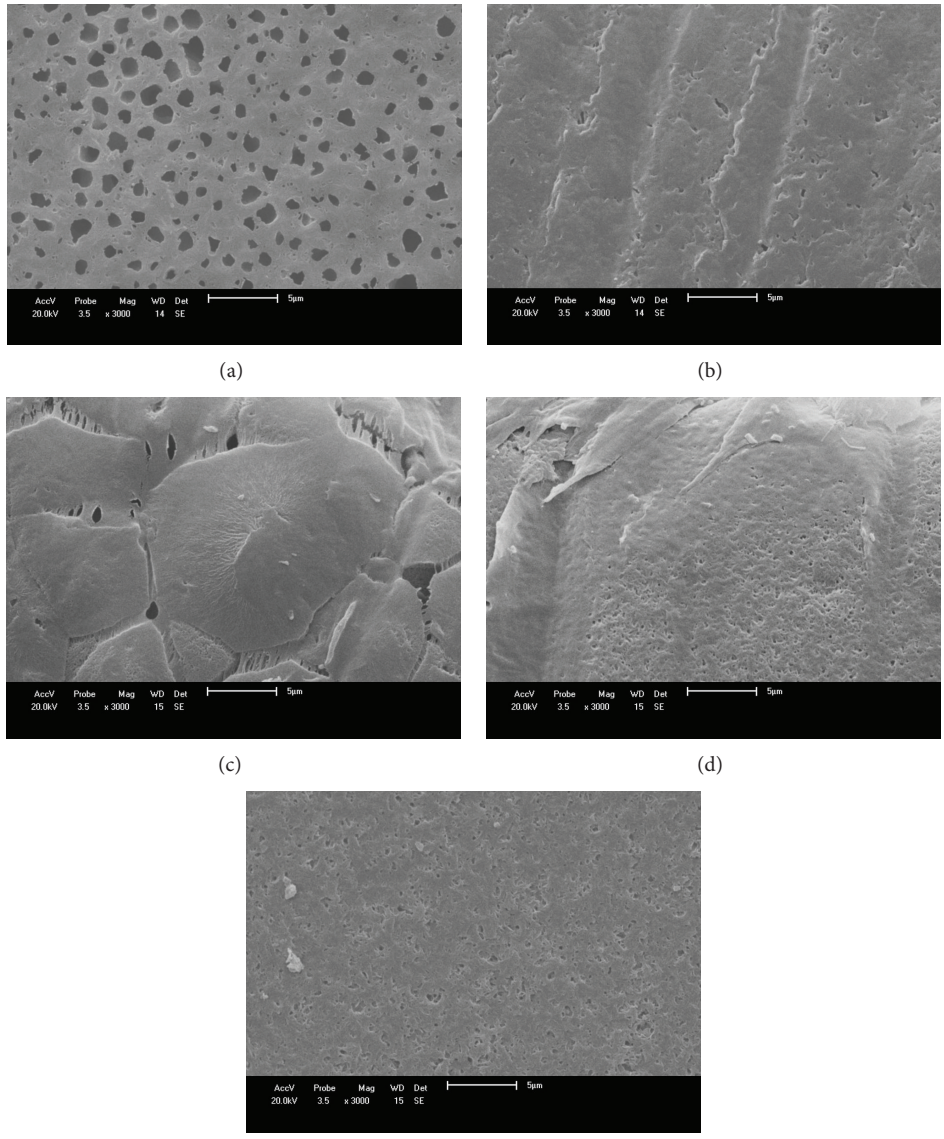

Figure 2: SEM images of the top surface of the membranes: (a) Pure PA6, (b) Homogenizer PA6, Extruder PA6, (c) Extruder PA6, (d) Homogenizer PA6 + 1%MMT, and (e) Extruder PA6 + 1%MMT.

of sodium montmorillonite with small hydration [15] (Santos, 1989).

Through the X-ray results, the presence of two peaks in the range from 20° to 23° can be observed, related to the crystalline planes (200) and (002) of the α phase of polyamide 6. These results are in agreement with the literature [14, 16–18]. A crystalline plane (001) that corresponds to the γ phase of the polymer was also identified. This reflection occurred for all samples, with higher incidence for extruded polyamide 6 (close to 21°). In this case, it is possible to observe that the predominant crystalline phase of polyamide is α. The polyamide 6 is a semicrystalline polymer and the enlargement of the peaks indicates the existence of amorphous regions. As can be seen, the incorporation of clay can change the shape of these peaks, modifying probably the crystallinity for PA6. According to Khanna and Kuhn [19], the polyamide 6 can assume two crystallographic forms (α monoclinic and γ monoclinic and/or pseudohexagonal).

From Figure 1, the disappearance of the characteristic peak of the clay can be seen, indicating a possible exfoliation and/or partial exfoliation of nanocomposites formed by polyamide 6 + 1% of clay. Similar behavior was observed by Ray and Okamoto and Fornes et al., for the polyamide 6/clay systems [20, 21].

However, for the sample PA6 extruded, a small contribution of the α crystalline phase and, more pronounced, the formation of γ phase, which does not occur for the sample processed in the high rotation homogenizer, should be noted. This behavior indicates that the processing has influenced the formation of crystalline arrangement.

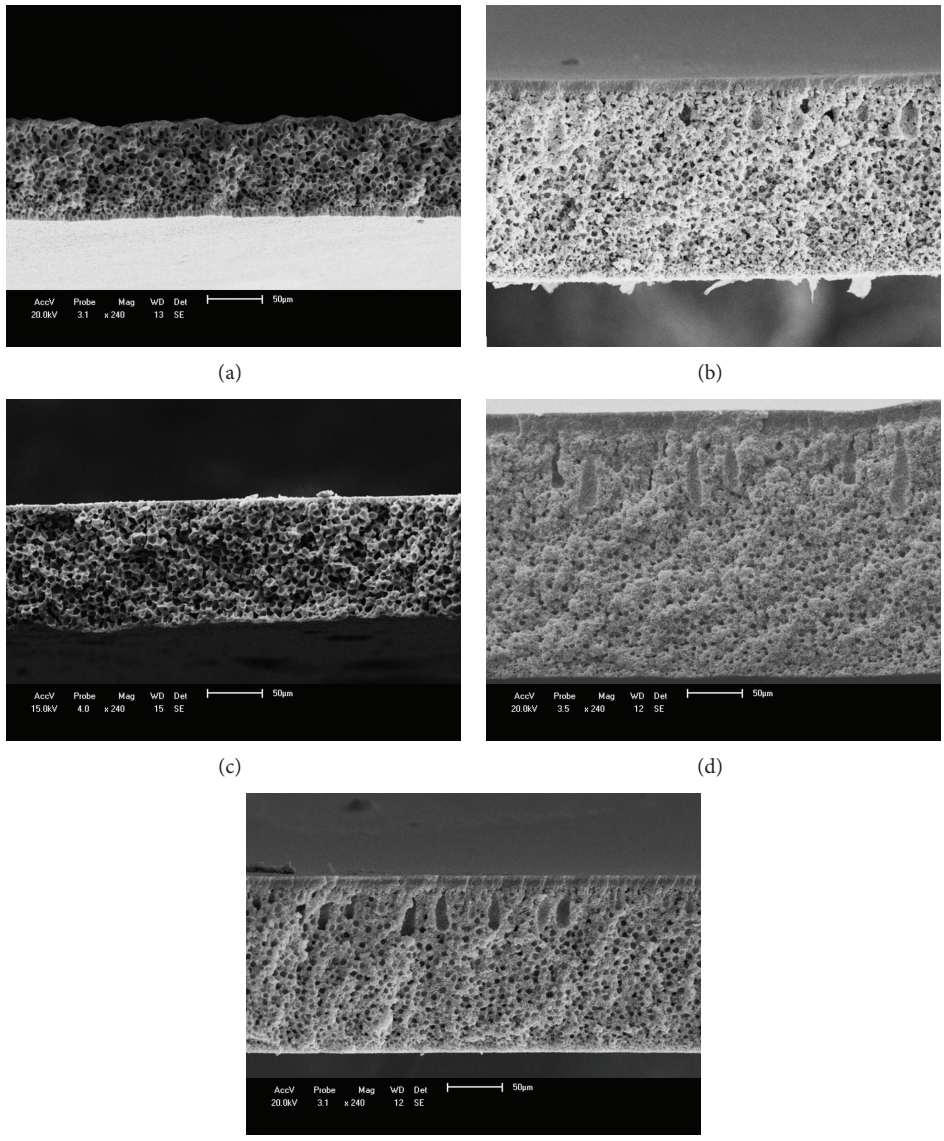

Figure 3: SEM images of the cross section of the membranes: (a) Pure PA6, (b) Homogenizer PA6, (c) Extruder PA6, (d) Homogenizer PA6+1%MMT, and (e) Extruder PA6+1%MMT.

3.2. Scanning Electron Microscopy (SEM)

3.2.1. Top Surface. Figure 2 presents the SEM images of the following membrane surfaces: Pure PA6, Homogenizer PA6, Extruder PA6, and their nanocomposites with 1% of clay.

From Figure 2(a), it can be verified that Pure PA6 presents pores with uniform distribution. It is possible to see that there are less pores for both Homogenizer PA6 (Figure 2(b)) and Extruder PA6 (Figure 2(c)), when compared to the morphology presented by Pure PA6. Possibly, this change could be due processing of material.

It was observed that the presence of clay (1%) for the nanocomposites prepared in the homogenizer and in the extruder changed considerably the quantity and uniformity of pores in the membrane, compared to the pure PA6 membrane. The membranes prepared with nanocomposites with 1% of clay presented a greater number of pores due to the presence of clay in the polymer matrix.

3.2.2. Cross Section. Figure 3 presents the SEM images with an overview of the cross sections for the membranes: Pure PA6, Homogenizer PA6, Extruder PA6, and their nanocomposites with 1% of clay.

According to the SEM images, it can observed that PA6 (Figure 3(a)) presented a well-defined surface with micropores, allowing for a greater selectivity. The cross section indicates a thickness of approximately 92.5 μm, with uniform distribution of pores in the whole membrane. The Homogenizer PA6 membrane (Figure 3(b)) showed a wide selective layer, when compared with Pure PA6 membrane, with a thickness of approximately 183 μm and good pore size

distribution with presence of "fingers." The Extruder PA6 membrane (Figure 3(c)) presents a very thin selective layer when compared with pure PA6 and Homogenizer PA6, with a thickness of approximately 109 μm, with small, uniform, and interconnected pores. This behavior can be explained by the processing performed in the homogenizer and extruder. Membranes with 1% of clay show "finger" shaped pores with no connections, which block fluid flows through the membrane. The Homogenizer PA6 + 1%MMT presented a thickness of approximately 242 μm. For the Extruder PA6 + 1%MMT, a thickness of approximately 161 μm was observed.

4. Conclusions

Membranes were prepared from PA6/MMT nanocomposites. From X-ray diffraction results, it was observed that the nanocomposites presented exfoliated and/or partially exfoliated structure. From SEM images, it was observed that the Pure PA6 membrane presented uniform pores. Membrane PA6, prepared with nanocomposites processed in the homogenizer and extruder, presented small amount of pores, showing that the processing has influence in the morphology of the membranes. Membranes prepared from nanocomposites with 1% of clay presented more pores than PA6 membrane, showing that the presence of clay has considerably influenced the morphology. From the images showing the cross section of the membranes, it was observed that the processing influenced the thickness of the selective layer of the membranes. Membranes with clay had not interconnected pores and a thicker selective layer, which probably blocked flow membrane.

Conflict of Interests

The authors declare that there is no conflict of interests regarding the publication of this paper.

Acknowledgments

The authors are grateful to Bentonit União Nordeste (BUN), DEMa/UFCG, MCT/CNPq, CAPES, Petrobras, and PRH-25/ANP for financial support.

References

[1] P. Poletto, J. Durate, M. S. Lunkes et al., "Avaliação das características de transporte em membranas de poliamida 66 preparadas com diferentes solventes," *Polímeros*, vol. 22, no. 3, pp. 273–277, 2012.

[2] A. C. Habert, C. P. Borges, and R. Nobrega, *Processo de Separação com Membranas*, E-papers Serviços Editoriais Ltda, Rio de Janeiro, Brazil, 1 edition, 2006.

[3] Y. N. Yang, W. Jun, Z. Qing-zhu, C. Xue-si, and Z. Hui-xuan, "The research of rheology and thermodynamics of organic-inorganic hybrid membrane during the membrane formation," *Journal of Membrane Science*, vol. 311, no. 1-2, pp. 200–207, 2008.

[4] A. Hamza, V. A. Pham, T. Matsuura, and J. P. Santerre, "Development of membranes with low surface energy to reduce the fouling in ultrafiltration applications," *Journal of Membrane Science*, vol. 131, no. 1-2, pp. 217–227, 1997.

[5] J. Han, W. Lee, J. M. Choi, R. Patel, and B.-R. Min, "Characterization of polyethersulfone/polyimide blend membranes prepared by a dry/wet phase inversion: Precipitation kinetics, morphology and gas separation," *Journal of Membrane Science*, vol. 351, no. 1-2, pp. 141–148, 2010.

[6] J. F. Bassetti, *Preparação, Caracterização e Aplicação de Membranas Poliméricas Microporosas Assimétricas [Tese]*, Universidade Estadual de Campinas—UNICAMP, Campinas, Brazil, 2002.

[7] S. A. Altinkaya, H. Yenal, and B. Ozbas, "Membrane formation by dry-cast process: Model validation through morphological studies," *Journal of Membrane Science*, vol. 249, no. 1-2, pp. 163–172, 2005.

[8] J. L. Thomas, M. Olzog, C. Drake, C. H. Shih, and C. C. Gryte, "Polyamide membrane precipitation studied by confocal backscattering microscopy," *Polymer*, vol. 43, no. 15, pp. 4153–4157, 2002.

[9] E. M. ARAÚJO, *Tenacificação da Poliamida 6 com ABS por meio da Técnica de Compatibilização in situ com o uso de Copolímeros Acrílicos Reativos [Tese]*, Universidade Federal de São Carlos, São Carlos, Brazil, 2001.

[10] A. Ranade, N. A. D'Souza, B. Gnade, and A. Dharia, "Nylon-6 and montmorillonite-layered silicate (MLS) nanocomposites," *Journal of Plastic Film and Sheeting*, vol. 19, no. 4, pp. 271–285, 2003.

[11] H. J. Sue, K. T. Gam, N. Bestaoui, A. Clearfield, M. Miyamoto, and N. Miyatake, "Fracture behavior of α-zirconium phosphate-based epoxy nanocomposites," *Acta Materialia*, vol. 52, no. 8, pp. 2239–2250, 2004.

[12] I. F. Leite, *Preparação de nanocompósitos de poli(tereftalato de etileno)/bentonita [Dissertação]*, Universidade Federal de Campina Grande—UFCG, Campina Grande, Brazil, 2005.

[13] R. Pfaendner, "Nanocomposites: Industrial opportunity or challenge?" *Polymer Degradation and Stability*, vol. 95, no. 3, pp. 369–373, 2010.

[14] A. M. D. Leite, *Desenvolvimento de Membranas Assimétricas de Nanocompósitos de Poliamida 6/Argila por Inversão de Fases [Tese]*, Universidade Federal de Campina Grande—UFCG, Campina Grande, Brazil, 2011.

[15] P. S. SANTOS, *Ciência E TEcnologia dE Argilas*, vol. 1, Edgar Blucher, São Paulo, Brazil, 2nd edition, 1989.

[16] T. D. Fornes and D. R. Paul, "Crystallization behavior of nylon 6 nanocomposites," *Polymer*, vol. 44, no. 14, pp. 3945–3961, 2003.

[17] X. Hu and X. Zhao, "Effects of annealing (solid and melt) on the time evolution of polymorphic structure of PA6/silicate nanocomposites," *Polymer*, vol. 45, no. 11, pp. 3819–3825, 2004.

[18] Z. Zhao, W. Yu, Y. Liu, J. Zhang, and Z. Shao, "Isothermal crystallization behaviors of nylon-6 and nylon-6/ montmorillonite nanocomposite," *Materials Letters*, vol. 58, no. 5, pp. 802–806, 2004.

[19] Y. P. Khanna and W. P. Kuhn, "Measurement of crystalline index in nylons by DSC: complexities and recommendations," *Journal of Polymer Science B: Polymer Physics*, vol. 35, no. 14, pp. 2219–2231, 1997.

[20] S. S. Ray and M. Okamoto, "Polymer/layered silicate nanocomposites: a review from preparation to processing," *Progress in Polymer Science*, vol. 28, no. 11, pp. 1539–1641, 2003.

[21] T. D. Fornes, P. J. Yoon, H. Keskkula, and D. R. Paul, "Nylon 6 nanocomposites: the effect of matrix molecular weight," *Polymer*, vol. 42, no. 25, pp. 9929–9940, 2001.

Hindawi Publishing Corporation
Advances in Materials Science and Engineering
Volume 2014, Article ID 582536, 12 pages
http://dx.doi.org/10.1155/2014/582536

Research Article

Numerical Analysis of the Energy Improvement of Plastering Mortars with Phase Change Materials

A. Váz Sá,[1] R. M. S. F. Almeida,[2,3] H. Sousa,[1] and J. M. P. Q. Delgado[3]

[1] *Construction Technology, Quality and Management (GEQUALTEC), Faculdade de Engenharia da Universidade do Porto, Rua Dr. Roberto Frias s/n, 4200-465 Porto, Portugal*
[2] *Polytechnic Institute of Viseu-School of Technology & Management, Campus Politécnico de Repeses, 3504-510 Viseu, Portugal*
[3] *Laboratory of Building Physics (LFC), Civil Engineering Department, Faculdade de Engenharia da Universidade do Porto, Rua Dr. Roberto Frias s/n, 4200-465 Porto, Portugal*

Correspondence should be addressed to J. M. P. Q. Delgado; jdelgado@fe.up.pt

Received 28 February 2014; Accepted 13 March 2014; Published 10 April 2014

Academic Editor: A. G. Barbosa de Lima

Building components with incorporated phase change materials (PCMs) meant to increase heat storage capacity and enable stabilization of interior buildings surface temperatures, whereby influencing the thermal comfort sensation and the stabilization of the interior ambient temperatures. The potential of advanced simulation tools to evaluate and optimize the usage of PCM in the control of indoor temperature, allowing for an improvement in the comfort conditions and/or in the cooling energy demand, was explored. This paper presents a numerical and sensitivity analysis of the enthalpy and melting temperature effect on the inside building comfort sensation potential of the plastering PCM.

1. Introduction

Nanotechnology and nanoproducts offer interesting new opportunities in many civil engineering areas and architecture including design and construction processes, such as the development of novel insulation materials. These novel materials with very good insulation values are already available on the market, enable a thermal rehabilitation of buildings in which conventional insulation is not possible, and can help to improve energy efficiency. On the construction industry not all products that feature the term "nano" actually contain nanomaterials. Often, the term "nano" merely refers to structures in the nanosize range. Nanotechnology in the construction industry is currently concentrated in the following sectors:

(i) cement-bound construction materials,

(ii) noise reduction and thermal insulation or temperature regulation,

(iii) surface coatings to improve the functionality of various materials,

(iv) fire protection.

This paper presents the application of nanotechnology, in the construction process, to improve the building energy efficiency. One of the greatest challenges in the construction sector is the thermal renovation of existing buildings; and applying new insulation materials based on nanotechnology could make an important contribution. In the past, energy consumption has increased steadily. However, the energy efficiency of buildings is today a prime objective for energy policy at regional, national, and international levels [1]. Innovations attributable to nanotechnology also enable thermally insulating buildings in which a conventional insulation is not possible (e.g., in older buildings with structured facade) and thereby achieve very good insulation values, for example, aerogels, phase change materials (PCMs), and vacuum insulation panels.

A PCM is a substance that changes from one state of matter to another at a certain temperature and represents a technology that may reduce peak loads and HVAC energy consumption in buildings. Building materials with incorporated PCM are meant to increase heat storage capacity and enable stabilization of building interior surface temperature, whereby influencing the thermal comfort sensation and the stabilization of the interior ambient temperatures [2].

Thermal energy storage based on the latent heat of phase change material has attracted attention of researchers and engineers in different fields, and a considerable number of numerical researches on PCMs have attempted to estimate potential energy savings through building energy simulation. To analyse energy and peak load benefits from PCMs a significant number of commercial building energy simulation programs such as CoDyBa, EnergyPlus, ESP-r, and TRNSYS were used.

EnergyPlus PCM algorithm uses a one-dimensional conduction finite difference solution algorithm (CondFD). This algorithm was tested and validated against multiple tests suites [3, 4]. However, when simulating complex models over extended periods this procedure becomes very time consuming and computationally demanding. In the problem under study the objective is to evaluate and minimize the annual heating load while guaranteeing a good thermal comfort performance.

As far as the organization of this paper is concerned, Sections 2 and 3 deal with the manufacturing methods used for the achievement of the PCM-based plastering mortar, as well as with the characterization of the developed material. Section 4 is dedicated to the numerical analysis of the plastering mortars energy improvement with phase change materials, with the BESTest (Building Energy Simulation Test) of EnergyPlus. Section 5 closes the paper with the main conclusions and prospects of the research work.

2. Phase Change Materials (PCMs)

2.1. Properties, Groups, and Categories. Thermal comfort of interior building spaces can be achieved using sensible heat form, related to conventional building materials, or via latent heat form, associated with PCMs. PCMs used for latent heat storage in buildings are characterized by an endothermic behaviour (with energy accumulation) during solid-liquid transition and exothermal process (with energy liberation) during liquid-solid phase shift. The solid-liquid PCM group comprises three categories: organic PCMs (paraffins and fatty acids); inorganic PCMs (salt hydrates and metallics); and eutectic mixtures (organic-organic, organic-inorganic, and inorganic-inorganic).

Thermal properties, like melting temperature and phase change enthalpy, are crucial to the process of selecting a suitable PCM for thermal energy storage. The scheme shown in Figure 1 makes a distribution of the existing PCMs trough those two essential thermal properties.

Salt hydrates and eutectic mixtures present the highest phase change enthalpy for the operative temperatures required inside building spaces. However, the set of characteristics presented by paraffins makes of these the most

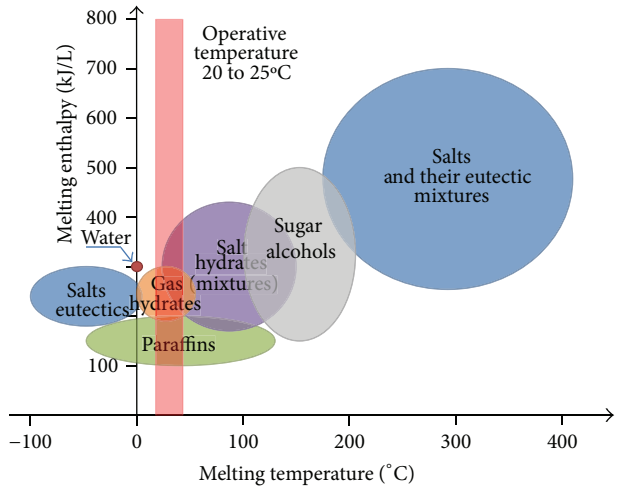

Figure 1: Melting temperatures and phase change enthalpy for existing PCMs (adapted from [7]).

desirable materials to be used in latent heat storage systems. Organic materials, such as paraffins, are chemically stable, offer no supercooling, and are available in a large temperature range with low cost.

2.2. PCM in Building Materials: Incorporation Methods. Phase change materials can be incorporated into conventional construction materials mainly by three different technics: direct incorporation, immersion, and encapsulation [8]. Direct incorporation is the simplest method in which liquid or powdered PCMs are directly added to building materials such as gypsum, concrete, or plaster during production. Immersion technic of PCM is used in porous construction materials such as concrete or bricks. Those materials are dipped into melted PCM that is absorbed by capillarity. With direct incorporation or immersion methods construction materials are imposed to be in contact with PCM. No extra equipment is needed in both methods but leakage and incompatibility with construction materials may be the biggest problems [9].

To avoid incompatibility problems, due to the direct contact between conventional construction materials and PCMs, encapsulation method arises. Encapsulation eases the process of handling and incorporating of PCM into building materials, the leakage problem can be avoided, and the function of the construction structure can be less affected.

Macroencapsulation for PCM can present many different shapes, tubes, spheres, or panels, and can be obtained from several materials like aluminium or polymers. Macroencapsulated PCMs can be easily placed in ceilings [10] or underfloor systems [11]. It has the disadvantages of poor thermal conductivity and tendency of solidification at the edges (crystallization) [12]. Microencapsulation can be described as the technology in which PCM particles are enclosed in a thin, sealed, and high molecular weight polymeric film. Microcapsules, with diameters that can vary from 1 to 1000 μm, prevent PCM from leakage during the phase change process. Microencapsulated PCMs are easy to incorporate and do

Table 1: Required tests for hardened mortars of general purpose (GP) and of lightweight (LW).

Test parameter	Test methods	Requirements	
		GP	LW
Dry bulk density [kg/m^3]	EN 1015-10	Declared range of values	Declared range of values: $\rho \leq 1300$ kg/m^3
Compressive strength [N/mm^2]	EN 1015-11	CS I to CS IV	CS I to CS III
Adhesion [N/mm^2] and fracture pattern FP (A, B, or C)	EN 1015-12	≥declared value and FP	
Capillary water absorption	EN 1015-18	W0 to W2	
Water vapour permeability coefficient (μ)	EN 1015-19 a b	≤declared value	
Thermal conductivity [W/(m·°C)]	Tabulated mean value	EN 1745:2002, Table A.12	

not request for a modification in known construction manufacturing processes. Plasterboard with microencapsulated PCMs is one of the most widespread solutions of PCM incorporation into building materials [13–16].

3. PCM Plastering Mortar

3.1. Test Methods and Requirements. The main goal of this section is to evaluate the feasibility of a new composite material, with inclusion of microencapsulated paraffin in cement based mortars, to be used in interior coatings for buildings. In order to be marketed within the European Union (EU) plastering mortars should respond to European Norm EN 998-1 [5]. Therefore, the development of a plastering mortar should comply with characteristics presented in Table 1 where test parameters and target properties for mortars are identified. In the scope of this work, apart from performing tests on the properties mentioned in Table 1 while developing a PCM-based mortar, complementary properties like enthalpy and specific heat were also evaluated.

3.2. Components and Formulation. The achieved mixture (used later on for further characterization) resulted from a set of preliminary analyses performed with the goal of evaluating the technical viability of the incorporation of microencapsulated PCM (industrially manufactured) into cement/lime based plastering mortar. Due to initial problems associated with the high cracking proneness of mortars containing PCM, the mixture composition was adjusted by an iterative process of trial and error, until the samples of the hardened mortar presented no visible cracking after the first hours of drying in controlled environment (with a temperature of 22 ± 2°C and a relative humidity of $50\% \pm 5\%$). The trial samples, with 10 cm × 10 cm × 1 cm, resulted from spreading of the fresh mortar over a brick surface. Besides all conventional components used in common plastering mortars,cement, lime, sand, and/or industrial fillers, and different kinds of additions (resins, fibers, cellulose deviants, and others) the trial mortars involved the use of PCM. The following text provides further information on the several constituents mentioned above, encompassing their main characteristics. The cement used is a type I class 42,5R according to NP-EN 197-1 [6]. The industrial aggregate used was calcium carbonate with 0.5–1.5 mm granulometric distribution. Resins (polymer ethyl-vinyl acetate, VAE) were applied in some of the trial formulations, with the primary function of improving adherence to the substrate (brick or concrete substrate) on low cement concentrations. However, they are known to reduce the blend's elasticity. The added fibers—polyacrylonitrile (PAN) 6 mm fibers—and aluminium powder are meant to compensate and redistribute the internal tension in the mortar, thus turning the shrinkage crack formation invisible. Cellulose deviants (cellulose ether) are used for high consistency development, as they impart good workability and enhance water retention considerably [17]. A microencapsulated paraffin powder (based on polymethyl methacrylate, highly cross-linked paraffin mixture), with commercial designation of "Micronal DS5008x," is used as PCM, with 23°C of melting point, an enthalpy of 100–110 kJ/kg, and 300 kg/m^3 density, approximately [18].

After a trial-and-error procedure that consisted in casting several test specimens (formulations A to L shown in Table 2, together with the corresponding compositions), adequate behaviour (i.e., absence of drying cracks) was obtained with formulations J, K, and L. The formulation of a reference mortar, named as REFM, is also shown in Table 2, to better illustrate the similitude between formulation L and the formulation of a common plastering, which is commercially available for interior coating.

3.3. Characterization and Classification: Thermal Properties. The characterization of the developed plastering mortar had two main goals: the compliance with normative required values and consequent classification of the PCM mortar and the identification of the thermal complementary properties given by the presence of the PCM (like enthalpy and specific heat). The hardened mortars of the selected formulation L, now renamed as PCMM (PCM mortar), were submitted to a set of characterization tests required by European Norm EN 998-1 [5]. The measured properties for PCMM are summarized in Table 3, where the corresponding test method/normalization is shown (the normalizations required for the developed tests are EN 1015 [19] and EN 1745 [20]). In regard to the properties shown in Table 3, it should be remarked that the water vapor permeability coefficient and the specific heat were estimated from the values presented in Table A.12 of EN 1745:2002 [20], as a function of the measured density of the composite mortar (1170 kg/m^3).

A heat flow meter apparatus was used to determine thermal conductivity of the new composite material according to ISO8301:1991 [21]. The thermal conductivity measured

Table 2: Mix proportions of formulations A to L and REFM and surface appearance of samples A to L.

Sample	Formulation [%]		Surface appearance	Comments
A	Cement	40.00		Appearance: fissuring/cracking without evident direction (aprox. ⊥). Causes: high cement dosage induces low ductility. A narrow particle sizes distribution with high percentage of fines due to the presence of PCM.
	PCM	50.00		
	Sand (filler)	10.00		
B	Cement	40.00	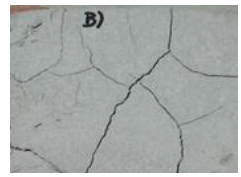	Appearance: fissuring/cracking without evident direction (aprox. ⊥). Causes: high cement dosage induces low ductility. A narrow particle sizes distribution with high percentage of fines.
	PCM	50.00		
	Sand (filler)	9.90		
	Cellulose ether	0.10		
C	Cement	25.00	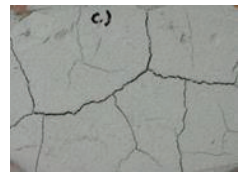	Appearance: fissuring/cracking without evident direction (aprox. ⊥). Causes: a narrow particle sizes distribution with high percentage of fines.
	PCM	50.00		
	Sand (filler)	24.92		
	Cellulose ether	0.08		
D	Cement	25.00	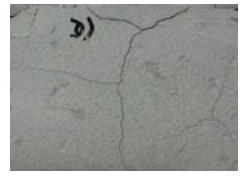	Appearance: better appearance with less fissuring. Causes: better particle size distribution. Reduction on fines content.
	PCM	25.00		
	Sand (filler)	49.92		
	Cellulose ether	0.08		
E	Cement	25.00	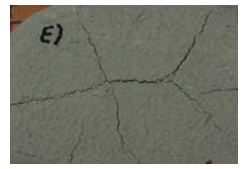	Appearance: better appearance with less fissuring. Causes: use of industrial filler. Better particle size distribution. Reduction on fines content.
	PCM	25.00		
	Sand (filler)	29.92		
	Industrial filler	20.00		
	Cellulose ether	0.08		
F	Cement	25.00		Appearance: fissuring/cracking without evident direction (aprox. ⊥). Causes: the addition of a water repellent could have affected relaxation and shrinkage.
	PCM	25.00		
	Industrial filler	49.87		
	Cellulose ether	0.05		
	Calcium stearate	0.08		

Table 2: Continued.

Sample	Formulation [%]		Surface appearance	Comments
G	Cement	25.00		Appearance: fissuring/cracking without evident direction. Causes: the addition of a water repellent could have affected relaxation and shrinkage.
	PCM	25.00		
	Industrial filler	49.85		
	Cellulose ether	0.05		
	Calcium stearate	0.08		
	Resins (VAE)	0.02		
H	Cement	10.00	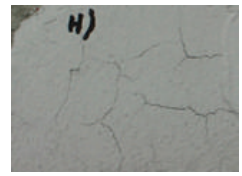	Appearance: better appearance with less fissuring. Causes: higher ductility mainly due to the addition of lime. The use of dispersed fibers and resins that improves cracking susceptibility.
	Lime	20.00		
	PCM	25.00		
	Industrial filler	42.80		
	Resins (VAE)	2.00		
	Fibres (PAN)	0.20		
I	Cement	10.00	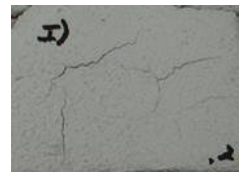	Appearance: better performance concerning cracking. Causes: higher ductility mainly due to the addition of lime. The use of dispersed fibers and resins that improves cracking susceptibility.
	Lime	20.00		
	PCM	25.00		
	Industrial filler	42.70		
	Resins (VAE)	2.00		
	Fibres (PAN)	0.20		
	Aluminium powder	0.10		
J	Cement	10.00	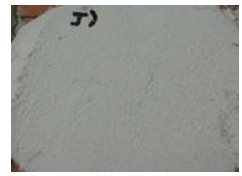	Appearance: adequate behavior (i.e., absence of drying cracks). Results: very low tensile resistance: $R_t \ll 1500$ MPa. Causes: higher ductility mainly due to the addition of lime.
	Lime	10.00		
	PCM	25.00		
	Industrial filler	52.80		
	Resins (VAE)	2.00		
	Fibres (PAN)	0.20		

Table 2: Continued.

Sample	Formulation [%]		Surface appearance	Comments
K	Cement	10.00	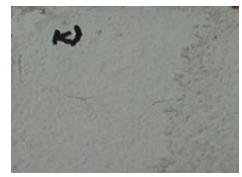	Appearance: adequate behavior (i.e., absence of drying cracks). Results: very low tensile resistance: $R_t \ll 1500$ MPa. Causes: higher ductility mainly due to the addition of lime.
	Lime	10.00		
	PCM	25.00		
	Industrial filler	52.65		
	Resins (VAE)	2.00		
	Fibres (PAN)	0.20		
	Aluminium powder	0.10		
	Cellulose ether	0.05		
L	Cement	10.00	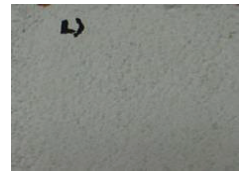	Appearance: adequate behavior (i.e., absence of drying cracks). Results: satisfactory (Table 3).
	Lime	5.00		
	PCM	25.00		
	Industrial filler	57.65		
	Resins (VAE)	2.00		
	Fibres (PAN)	0.20		
	Aluminium powder	0.10		
	Cellulose ether	0.05		
REFM	Cement	12.00	—	Table 3.
	Lime	2.48		
	Sand	65.00		
	Industrial filler	20.00		
	Fibres (PAN)	0.05		
	Aluminium powder	0.09		
	Cellulose ether	0.09		
	Calcium stearate	0.29		

EN 998-1 [5].

Table 3: Results of the test performed to the composite mortar with formulation L (PCMM) and comparison to reference mortars (REFM).

Test parameter	Results		Classification of PCMM/comments
	PCMM (LW)	REFM (GP)	
Dry bulk density [kg/m^3]	1170	1400	LW/declared range of values: $\rho \leq 1300$ kg/m^3.
Compressive strength [N/mm^2]	2.40	2.25	CS I/similar behaviour.
Adhesion [N/mm^2] and fracture pattern FP (A, B, or C)	0.35 FP: B	0.30 FP: B	Similar behaviour.
Capillary water absorption (intended use in external elements)	4.89	≤4.0	W0/similar behaviour.
Water vapour permeability coefficient (μ) (intended use in external elements)	5–10	<15	EN 1745 [6], Table A.12.
Thermal conductivity [W/(m·°C)]	0.29	0.61	Similar behaviour when compared to LW mortars.
Latent heat [kJ/kg]	≈25	—	—
Melting temperature [°C]	≈23	—	—
Melting temperature range [°C] (90%)	23–25	—	—
Specific heat (solid) [kJ/(kg·°C)]	1.0	1.0	EN 1745 [6], Table A.12.

with this experimental technique was 0.295 W/m K. Also, the melting temperature and the fusion enthalpy were experimentally determined through differential scanning calorimetry (DSC) tests with recourse to a Diamond DSC from Perkin Elmer. A sample of the supplied PCM mortar (powder) of approximately 7.7 mg was tested and an enthalpy of 22.6 kJ/kg was registered. This result came close to what would be expected (25 kJ/kg), assuming that the enthalpy is linearly proportional to the fraction of paraffin amount in the sample (25%), bearing in mind that the PCM is the only material in the mixture to experiment phase transition (from solid to liquid) in the range of studied temperatures (5–50°C). From these results it may be concluded that the PCM keeps its characteristics when integrated into hardened cement based mortars. Therefore, from now on, it will be considered that the composite mortar containing 25% of PCM has a melting point of 23°C and a melting enthalpy of 25 kJ/kg in a 2°C temperature range.

The comparison of characteristics between PCMM and REFM is presented in Table 3. These results confirm the expected similarity in behaviour for the developed plastering mortar in view of the PCM chemically inert characteristics, which was introduced in the mix by replacing aggregates.

4. Numerical Simulation

4.1. Field Equations: PCM Model with EnergyPlus. Traditionally EnergyPlus uses conduction transfer functions (CTF) to simulate surface constructions. These are linear equations, relatively simple, which allow the calculation of the conduction heat transfer through a completed layered building surface. However, with this method, it is impossible to include temperature dependent thermal properties, and thus modelling behaviours such as phase change enthalpy become unmanageable [22].

The inclusion of a new solution algorithm that utilizes an implicit finite difference procedure (CondFD) upgraded EnergyPlus to simulate the effect of PCM. This new model was tested and validated against multiple test suites [3, 4]. The CondFD algorithm in EnergyPlus uses an implicit finite difference scheme coupled with an enthalpy-temperature function. This function is the users' input to accurately account for energy transfer during phase change. EnergyPlus includes two different options for the specific scheme or formulation used for the finite difference model. Before version 7, EnergyPlus used Crank-Nicholson solution scheme and then a new algorithm was added and is referred to as fully implicit. Both algorithms are based on an Adams-Moulton solution approach but the fully implicit one is considered of first order in time (Crank-Nicholson solution scheme is considered of second order). The model equation for the fully implicit scheme is described in [23]

$$C_p \cdot \rho \cdot \Delta x \cdot \frac{T_i^{j+1} - T_i^j}{\Delta t} = \left(k_w \cdot \frac{T_{i+1}^{j+1} - T_i^{j+1}}{\Delta x} + k_E \cdot \frac{T_{i-1}^{j+1} - T_i^{j+1}}{\Delta x} \right), \quad (1)$$

where T is the node temperature; i is the node being modelled; $i+1$ is the adjacent node to interior of construction; $i-1$ is the adjacent node to exterior of construction; $j+1$ is the new time step; j is the previous time step; Δt is the calculation time step; Δx is the finite difference layer thickness (always less than construction layer thickness); C_p is the specific heat of material; k_w is the thermal conductivity for interface between i node and $i+1$ node; k_E is the thermal conductivity for interface between i node and $i-1$ node; and ρ is the density of material.

This equation is complemented by (2) that relates enthalpy and temperature and is used to develop an equivalent specific heat at each time step:

$$h_i = \mathrm{HTF}\left(T_i\right), \quad (2)$$

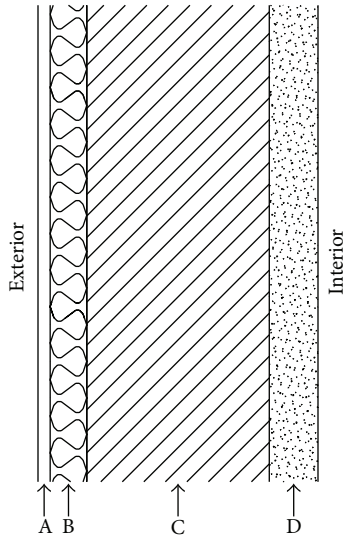

Figure 2: Wall configuration.

where HTF is an enthalpy-temperature function that uses data from user input.

The algorithm also permits including a temperature dependent thermal conductivity:

$$k = k_0 + k_1 \left(T_i - 20\right), \tag{3}$$

where k_0 is the 20°C thermal conductivity value and k_1 is the change in conductivity per degree temperature difference from 20°C.

4.2. Geometry Model and Parameters. In this research the effect of introducing PCM in a plastering mortar on the external walls of a simple office cell located in Portugal is explored. A sensitivity analysis was performed, which included the study of the influence of material properties variation, such as melting temperature ranges and enthalpy, and the study of the influence of installing the office cell in different climatic regions. Discomfort due to overheating and cooling energy demand were the outputs used in the analysis.

The geometry adopted was an office cell like the one of ASHRAE Standard 140—Bestest Case 900 [24] as well as the internal gains and ventilation. The introduction of PCM on a plastering mortar in the building envelope (PCMM) and the use of a reference mortar (REFM) were compared. Figure 2 shows the main configuration used to model the walls and Table 4 provides the thermal conductivity, density, specific heat, and thickness of each layer.

Simulations were performed in two cities of Portugal, Lisbon and Porto, which represent different climatic regions. Both cities are located near the coast but, especially during summer, Lisbon is warmer than Porto. Figure 3 presents the monthly mean air temperature (T_{air}), the sol-air temperature ($T_{\text{sol-air}}$), and the total solar radiation (direct and diffuse) of Lisbon and Porto [23].

All the simulations were performed with software EnergyPlus, for the cooling season, between 01/04 and 30/09, on an hourly basis and considering 60 time steps per hour.

Table 4: Material properties.

Element ID	Conductivity [W/(m·K)]	Density [kg/m^3]	Specific heat [kJ/(kg·K)]	Thickness [m]
(a) Render	1.00	1800	1000	0.005
(b) Insulation	0.04	10	1400	0.04
(c) Block	0.51	1400	1000	0.10
(d) Mortar	0.30	1400	1000	0.03

Table 5: "Free-floating" scenario.

Case ID	L [kJ/kg]	T_1 [°C]	T_2 [°C]
PCM23/25_25	25	23	25
PCM23/25_100	100	23	25
PCM23/25_200	200	23	25
PCM24/26_25	25	24	26
PCM24/26_100	100	24	26
PCM24/26_200	200	24	26
PCM25/27_25	25	25	27
PCM25/27_100	100	25	27
PCM25/27_200	200	25	27
PCM26/28_25	25	26	28
PCM26/28_100	100	26	28
PCM26/28_200	200	26	28
REFM	—	—	—

4.2.1. Discomfort Analysis due to Overheating. The first performed analysis was the evaluation of the discomfort due to overheating, assuming a "free-floating" scenario (without cooling system). The discomfort was assessed by computing the degree-hours. The degree-hours (DH_{25}) can be defined as the sum of the differences between air temperature and a reference value as follows:

$$\text{DH}_{25} = \sum_{i=1}^{n} \left(T_i - 25\right) \wedge T_i > 25, \tag{4}$$

where T_i is the interior temperature.

It performed a sensitivity analysis that aimed to understand if overheating minimization can be achieved by the increasing of enthalpy amount in the mortar or by changing the PCM melting temperature range. A numerical simulation was carried out, which included 13 cases resulting from the combination of different phase change ranges (melting temperatures from 23/25°C to 26/28°C) with varied enthalpy values of 25, 100, and 200 kJ/kg, as well as the reference case without PCM, as can be observed in Figure 4 and Table 5.

4.2.2. Analysis of the Effect of Introducing an HVAC System. In the second analysis, the effect of introducing an HVAC system in the office cell was evaluated by computing the energy demand for cooling assuming a temperature set point of 25°C. For this sensitivity analysis only two melting temperature ranges were considered, resulting in 7 cases (Table 6).

4.3. Simulation Results. The comfort sensation is guaranteed by temperature level and stabilization inside a building space

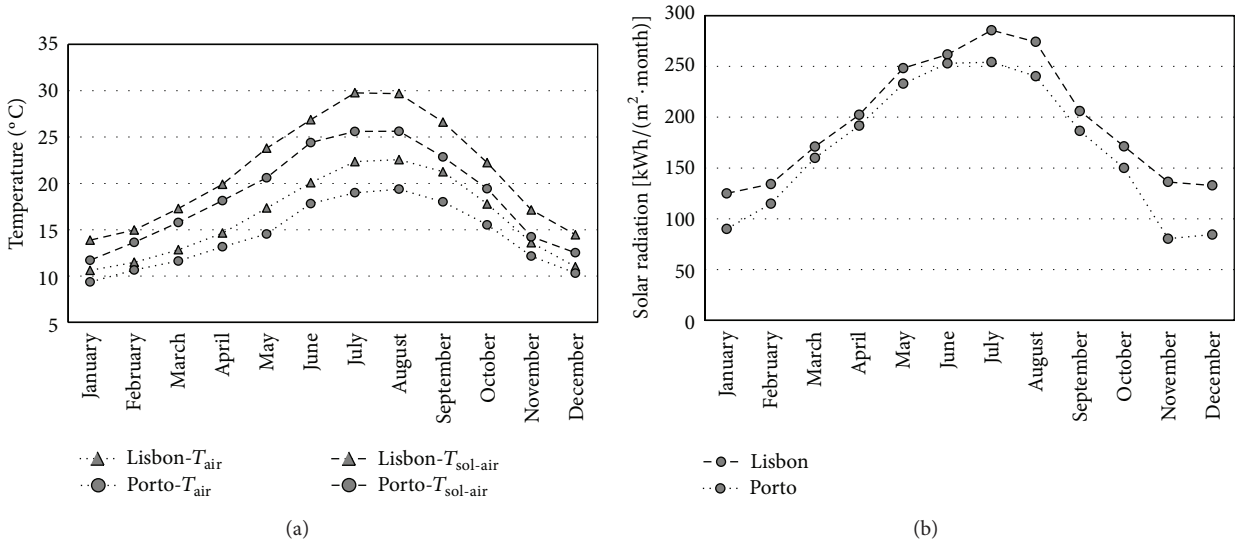

Figure 3: Monthly mean temperature.

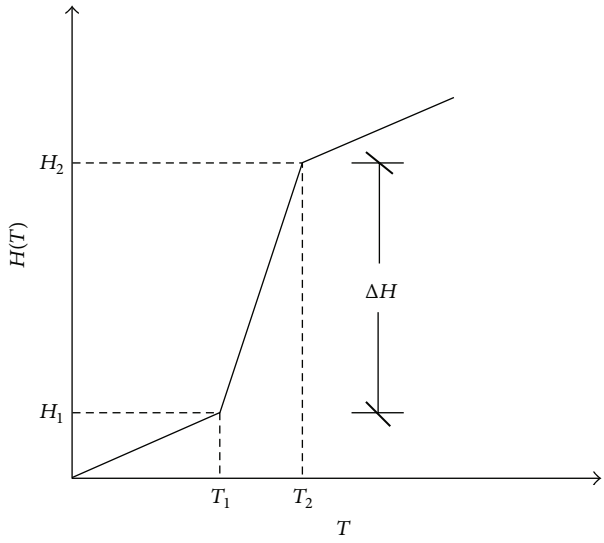

Figure 4: Enthalpy versus temperature.

Table 6: HVAC scenario.

Case ID	L [kJ/kg]	T_1 [°C]	T_2 [°C]
PCM23/25_25	25	23	25
PCM23/25_100	100	23	25
PCM23/25_200	200	23	25
PCM24/26_25	25	24	26
PCM24/26_100	100	24	26
PCM24/26_200	200	24	26
REFM	—	—	—

[25]. PCM contributes to interior temperature stabilization being an interesting solution to improve comfort conditions and to minimize energy consumption [1, 12, 26].

4.3.1. Results for the Discomfort Analysis due to Overheating. The first approach of the sensitivity analysis was for the "free-floating" situation. Degree-hours for 25°C basis were used as the evaluation parameter to assess the discomfort due to overheating. As an example, Figure 5 shows the simulation result of a daily temperature profile in Lisbon for different scenarios: the effect of enthalpy variation is exposed in Figure 5(a), where the same melting temperature, of 24–26°C, for three different enthalpies, was calculated, and in Figure 5(b), where the same enthalpy, of 200 kJ/kg, for four different melting temperature ranges, was studied.

Attending to the results shown in Figure 5(a) the peak temperature for the reference case REFM was 30.4°C, dropping to 28.7°C when considering a PCMM with 24–26°C and an enthalpy of 200 kJ/kg (PCM24/26_200). With this plastering mortar, PCM24/26_200, the interior temperature of the office cell varied between 24.5 and 28.7°C, reaching a temperature interval of $\Delta T_{PCM24/26\_200} = 3.3$°C inside the building. On the other hand, with the REFM (without PCM), an interval of $\Delta T_{REFM} = 5.3$°C, between 25.1 and 30.4°C, was achieved. The presence of the PCM was observed lowering the interior temperature peak, reducing the temperature variation within the building, and increasing the period of time during which the temperature is maintained within the melting range near 25°C (i.e., comfort temperatures).

Regarding Figure 5(b) the most interesting performance was obtained with PCM25/27_200 and PCM24/26_200 with a temperature variation between 24.7 and 28.4°C, with $\Delta T_{PCM25/27\_200} = 3.7$°C, and 24.5 and 28.7°C, with $\Delta T_{PCM24/26\_200} = 4.2$°C, respectively. However, it is important to underline that all the simulated scenarios correspond to an improvement when compared to the reference case without PCM (REFM). It is clear that PCM incorporated in plastering mortars changed the interior temperature profile, helping to stabilize them and dropping temperature peaks.

The "overheating improvement" was evaluated by a percentage resulting from the difference of degree-hours DH_{25}

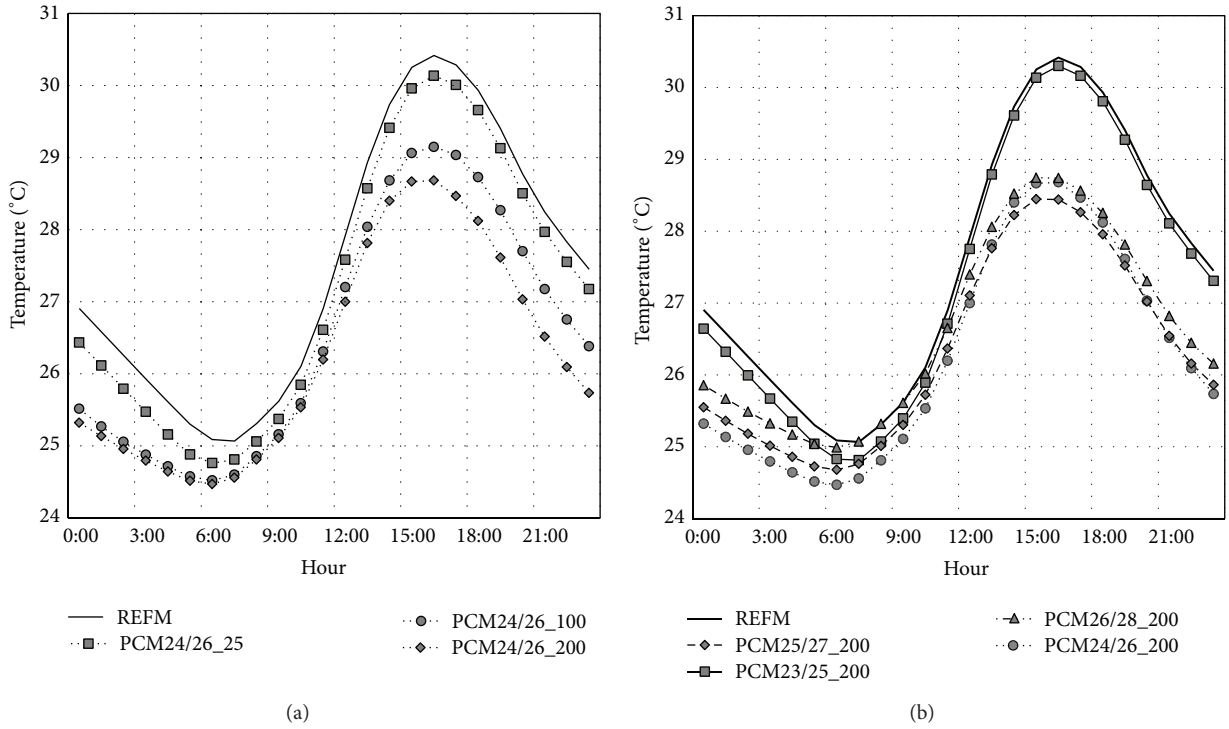

Figure 5: Assessed interior temperatures for the office cell located in Lisbon: (a) enthalpy effect, (b) melting temperature effect.

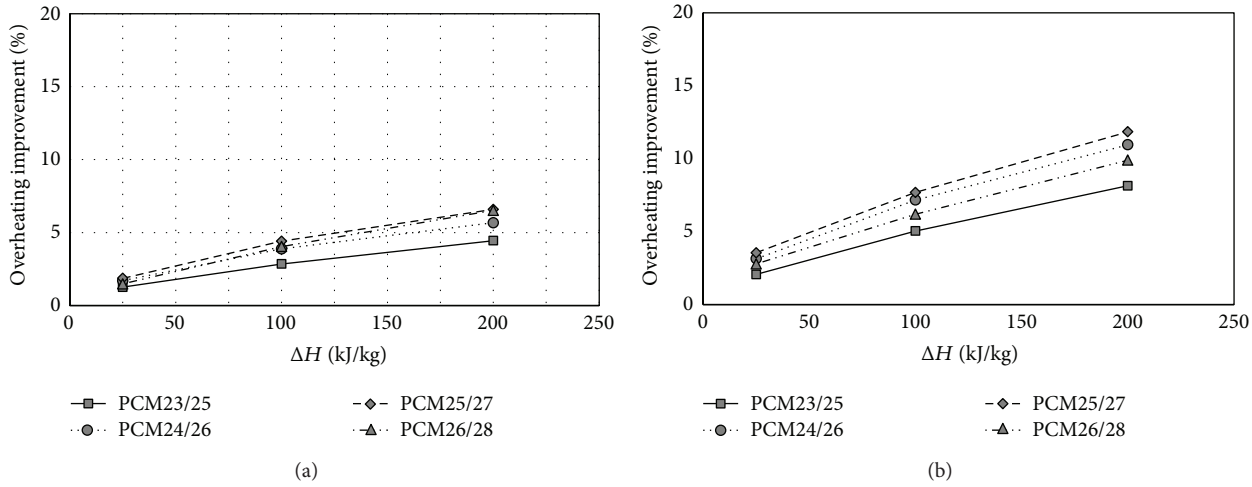

Figure 6: Discomfort analysis due to overheating inside an office cell placed in (a) Lisbon and (b) Porto.

between the use of REFM as plastering in the office cell and the use of different PCMM. Attending to the analysis for "free-floating" situation, with a 25°C basis for DH to assess the discomfort due to overheating, with results plotted in Figure 6, maximum overheating improvement was 12%, obtained for the office cell placed in Porto with PCM25/27_200. The lowest value was registered for the office cell placed in Lisbon for PCM23/25_25 (a PCM with an enthalpy of 25 kJ/kg and a fusion temperature range between 23 and 25°C). Still, the overheating improvement was 2%.

These results are in line with other authors [1, 12, 26, 27]. Some additional improvement would be expected if some changes were made in the building envelope and ventilation. Indeed, the model used in this analysis is very exposed to overheating problems, due to a combination of large solar heat gains (no adequate solar shading device is used), lack of insulation in the roof, and poor ventilation rates especially during the night (no night ventilation procedure is established). This situation leads to very high interior temperatures (situations with interior temperatures over 30°C were regularly observed) and, therefore, there is a large untapped potential in the PCM. The lower overheating improvements obtained in Lisbon are also explained by this situation since the exterior climate conditions are more aggressive than in

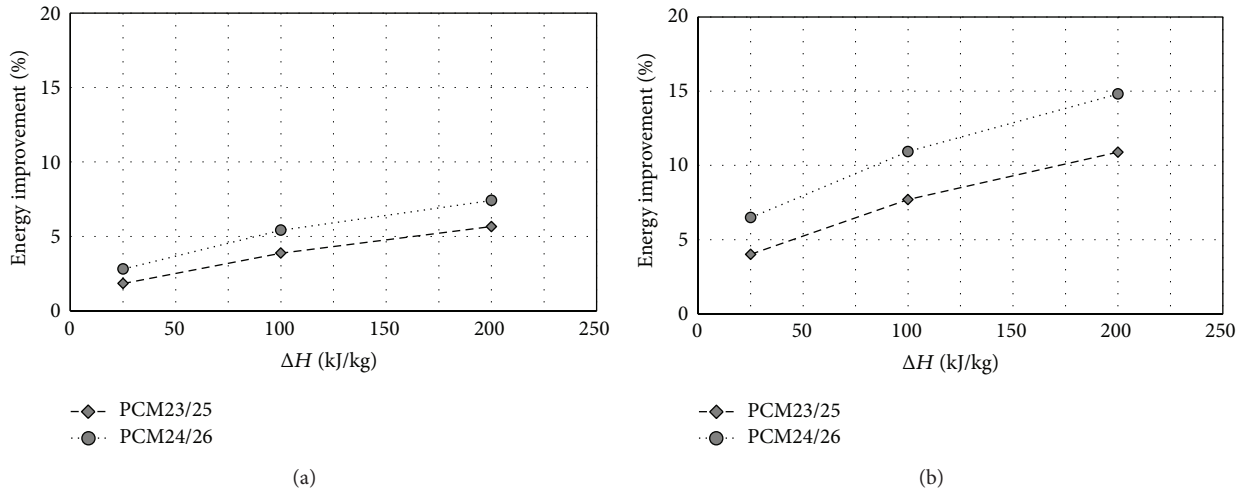

Figure 7: Energy savings analysis of the inside of an office cell placed in (a) Lisbon and (b) Porto.

Porto (higher temperatures and more intense solar radiation).

4.3.2. Results for the Effect Analysis of Introducing an HVAC System. A similar analysis can be made for the improvement in the cooling energy demand when using PCM in the office cell with an HVAC system. The "energy savings" are evaluated by a percentage resulting from the difference in the annual cooling energy demand between the use of REFM as plastering in the office cell and the use of different PCMM. Attending to the results, shown in Figure 7, plastering mortar PCM24/26_200 used in an office cell placed at Porto can reduce cooling energy demand by 15%. The same solution for the climatic conditions set for Lisbon resulted in 8% of energy savings.

On the analysis of the effect of introducing an HVAC system, the PCM presence was observed lowering the cooling energy demand necessary to maintain the temperatures inside the office cell close to the comfort temperature, 25°C.

Both sensitivity analyses produced very encouraging results that sustain future works on this research in order to optimize the use of PCM, adapting enthalpy and melting temperature ranges to climatic conditions and building's envelope.

5. Conclusions and Future Works

The main conclusions of this study are as follows.

(i) PCM can be incorporated into mortars without compromising the properties that are desirable for their application as plastering materials.

(ii) The potential of advanced simulation tools to evaluate and optimize the usage of PCM materials in the indoor temperature control, allowing for an improvement in the comfort conditions and/or in the cooling energy demand, was explored in this paper.

(iii) A sensitivity analysis regarding the enthalpy and melting temperature effect was performed and the temperature stabilization potential of the plastering PCM has been demonstrated. It was found that changes in the enthalpy value can produce a higher impact than varying the melting temperature of the PCM.

(iv) Considering a "free-floating" space, the inclusion of a plastering mortar containing PCM with an enthalpy of 200 kJ/kg and a fusion temperature range between 25 and 27°C can improve the comfort conditions by 12%. For the office with an HVAC system, the inclusion of a plastering mortar containing PCM with an enthalpy of 200 kJ/kg and a fusion temperature range between 24 and 26°C can improve the cooling energy demand by 15%.

Conflict of Interests

The authors declare that there is no conflict of interests regarding the publication of this paper.

References

[1] P. Ahadi, "Applications of nanomaterials in construction with an approach to energy issue," *Advanced Materials Research*, vol. 261–263, pp. 509–514, 2011.

[2] A. V. Sá, M. Azenha, H. de Sousa, and A. Samagaio, "Thermal enhancement of plastering mortars with Phase Change Materials: experimental and numerical approach," *Energy and Buildings*, vol. 49, pp. 16–27, 2012.

[3] P. C. Tabares-Velasco and B. Griffith, "Diagnostic test cases for verifying surface heat transfer algorithms and boundary conditions in building energy simulation programs," *Journal of Building Performance Simulation*, vol. 5, pp. 329–346, 2011.

[4] P. C. Tabares-Velasco, C. Christensen, and M. Bianchi, "Verification and validation of EnergyPlus phase change material model for opaque wall assemblies," *Building and Environment*, vol. 54, pp. 186–196, 2012.

[5] CEN, "EN 998-1: specification for mortar masonry. Part 1: rendering and plastering mortar," CEN, (European Commitee for Stardardization), Brussels, Belgium, 2013.

[6] CEN, "EN 197-1: cement. Part 1: composition, specifications and conformity criteria for common cements," CEN, (European Commitee for Stardardization), Brussels, Belgium, 2001.

[7] J. Dieckmann, "Latent heat storage in concrete," 2008, http://www.eurosolar.org/new/pdfs_neu/Thermal/IRES2006_Dieckmann.pdf.

[8] D. W. Hawes, D. Feldman, and D. Banu, "Latent heat storage in building materials," *Energy and Buildings*, vol. 20, no. 1, pp. 77–86, 1993.

[9] D. Zhou, C. Y. Zhao, and Y. Tian, "Review on thermal energy storage with phase change materials (PCMs) in building applications," *Applied Energy*, vol. 92, pp. 593–605, 2012.

[10] M. Koschenz and B. Lehmann, "Development of a thermally activated ceiling panel with PCM for application in lightweight and retrofitted buildings," *Energy and Buildings*, vol. 36, no. 6, pp. 567–578, 2004.

[11] K. Lin, Y. Zhang, X. Xu, H. Di, R. Yang, and P. Qin, "Experimental study of under-floor electric heating system with shape-stabilized PCM plates," *Energy and Buildings*, vol. 37, no. 3, pp. 215–220, 2005.

[12] L. F. Cabeza, C. Castellón, M. Nogués, M. Medrano, R. Leppers, and O. Zubillaga, "Use of microencapsulated PCM in concrete walls for energy savings," *Energy and Buildings*, vol. 39, no. 2, pp. 113–119, 2007.

[13] D. Feldman, D. Banu, and D. W. Hawes, "Development and application of organic phase change mixtures in thermal storage gypsum wallboard," *Solar Energy Materials and Solar Cells*, vol. 36, no. 2, pp. 147–157, 1995.

[14] F. Kuznik, J. Virgone, and J.-J. Roux, "Energetic efficiency of room wall containing PCM wallboard: a full-scale experimental investigation," *Energy and Buildings*, vol. 40, no. 2, pp. 148–156, 2008.

[15] C.-M. Lai, R. H. Chen, and C.-Y. Lin, "Heat transfer and thermal storage behaviour of gypsum boards incorporating microencapsulated PCM," *Energy and Buildings*, vol. 42, no. 8, pp. 1259–1266, 2010.

[16] C. Hasse, M. Grenet, A. Bontemps, R. Dendievel, and H. Sallée, "Realization, test and modelling of honeycomb wallboards containing a Phase Change Material," *Energy and Buildings*, vol. 43, no. 1, pp. 232–238, 2011.

[17] A. K. Athienitis, C. Liu, D. Hawes, D. Banu, and D. Feldman, "Investigation of the thermal performance of a passive solar test-room with wall latent heat storage," *Building and Environment*, vol. 32, no. 5, pp. 405–410, 1997.

[18] BASF, BASF The Chemical Company, GmbH. Phase Change Material. Micronal PCM, 2010, http://www.micronal.de/portal/basf/ien/dt.jsp?setCursor=1_290798.

[19] CEN, "EN, 1015: methods of test for mortar for masonry," vol. EN1015, CEN, (European Commitee for Stardardization), Brussels, Belgium, 2006.

[20] CEN, "EN, 1745: masonry and masonry products. Methods for determining design thermal values," CEN, (European Commitee for Stardardization), Brussels, Belgium, 2002.

[21] ISO, "ISO, 8301: thermal insulation: determination of steady-state thermal resistance and related properties. Heat flow meter apparatus," ISO, (International Organization for Standardization), Geneve, Switzerland, 1991.

[22] C. O. Pedersen, "Advanced zone simulation in EnergyPlus: incorporation of variable properties and phase change material (PCM) capability," Building Simulation 2007, Beijing, China, 2007.

[23] EnergyPlus, EnergyPlus Engineering Reference: The Reference to EnergyPlus Calculations: Ernest Orlando Lawrence Berkeley National Laboratory, 2012.

[24] ASHRAE, "ASHRAE Standard 140-2007: Standard Method of Test for the Evaluation of Building Energy Analysis Computer Programs," Atlanta, Ga, USA, 2007.

[25] ISO, "ISO, 7730: ergonomics of the thermal environment. Analytical determination and interpretationof thermal comfort using calculation of the PMV and PPD indices and local thermal comfort criteria," ISO, (International Organization for Standardization), Geneve, Switzerland, 2005.

[26] A. Castell, I. Martorell, M. Medrano, G. Pérez, and L. F. Cabeza, "Experimental study of using PCM in brick constructive solutions for passive cooling," *Energy and Buildings*, vol. 42, no. 4, pp. 534–540, 2010.

[27] N. Soares, J. J. Costa, A. R. Gaspar, and P. Santos, "Review of passive PCM latent heat thermal energy storage systems towards buildings'energy efficiency," *Energy and Buildings*, vol. 59, pp. 82–103, 2013.

Hindawi Publishing Corporation
Advances in Materials Science and Engineering
Volume 2014, Article ID 549275, 6 pages
http://dx.doi.org/10.1155/2014/549275

Research Article

Tunable Nanodielectric Composites

Daniel Qi Tan,[1] Yang Cao,[1,2] Xiaomei Fang,[1] and Patricia C. Irwin[1]

[1] *GE Global Research Center, Niskayuna, NY 12309, USA*
[2] *Department of Electrical and Computer Engineering, University of Connecticut, Storrs, CT 06269, USA*

Correspondence should be addressed to Daniel Qi Tan; tan@ge.com

Received 12 November 2013; Revised 22 January 2014; Accepted 12 February 2014; Published 25 March 2014

Academic Editor: A. G. Barbosa de Lima

This paper presents a progress update with the development of nanodielectric composites with electric field tunability for various high energy, high power electrical applications. It is demonstrated that nonlinear electrical/dielectric properties can be achieved via the nanostructure and interface engineering. A high level summary was given on the progress achieved as well as challenges remaining in nanodielectric engineering towards high energy density capacitors for energy storage and conversion, nonlinear dielectrics for tunable device, and high voltage varistor for surge suppression.

1. Introduction

The rapid expansion of renewable energy applications demands higher efficiency and higher density energy storage and energy conversion systems [1, 2]. Various DC-AC, AC-AC conversions are needed for solar and wind farms, while primary and secondary electrochemical devices are in need for transportation and telecommunication applications. Advanced devices and components are critical enablers for these emerging applications. As an example, in a typical electrical converter/inverter, state-of-art DC-link capacitors take up about 30% total volume and weight. In addition, the wide usage of renewable energy resources such as wind and solar posts challenges in grid stability. Advanced passive and active devices will be needed for future grid for harmonic filtration, static/dynamic volt-ampere reactive (VAR) compensation, transient suppression, and so forth [3, 4].

All these advanced apparatus and future electric power infrastructure rely on the breakthroughs of material engineering and better understanding of the device physics [1]. For instance, the development of high dielectric constant materials and the understanding of the behavior of dielectric materials under extremely high electric fields are critical for energy storage applications [5]. In addition, better understanding and control of charge transport cross interfaces are crucial for nonlinear devices. The advance in nanotechnology offers a unique opportunity to engineer materials with controlled microstructures so that desirable electrical properties can be greatly enhanced [1, 6]. On the other hand, dielectric response of materials can be utilized to facilitate the formation of nanostructures [7]. In this paper, progress updates are given as exemplary cases on the development of nanoenabled composite materials for high energy density capacitors for energy storage and conversion, field tunable nonlinear dielectrics, and miniaturized varistors for high voltage/high current transient suppression.

2. Experimental

In this investigation, polyetherimide (PEI), silicone, cyanoethyl cellulose, polyimide, and poly(vinylidene difluoride) were used as the polymer matrices in the investigation. Nanoparticles of interest include oxides of silicon, niobium, aluminum, zinc, bismuth, antimony, cobalt, titanium, and barium titanate and lead zirconates, with the particle size in the range of 10 to 100 nm. Polymer nanocomposites were prepared by first dissolving a polymer resin in a solvent at room temperature with a magnetic stirrer and then mixing with nanoparticles of 2–50 vol% in a high-energy sonicator (Sonics & Materials, Inc. Newtown, CT). The films were solvent cast onto a glass slide and dried at 100°C for two hours followed by a vacuum dry at 120°C to 150°C overnight. Ceramic composites were formulated with at least 85 mol%

ZnO and other oxide additives. A conventional mixed oxide process was used for powder processing. Green compacts of 1″ diameter were pressed using a uniaxial hydraulic press and then sintered at temperatures of 850–1000°C.

DC breakdown test was conducted following ASTM D149 (method A) using a ball-plane electrode configuration. The sample was immersed into insulation oil and DC voltage was applied at a ramp rate of 500 V/s until the sample failed. Dielectric responses were measured using a broadband dielectric spectrometer from Novacontrol GmbH. Scanning electron microscopy (SEM) imaging was done using a Zeiss Supra 55VP (Carl Zeiss AG, Oberkochen, Germany). Transmission electron microscopy (TEM) imaging was taken using a FEI Tecnai F20 transmission electron microscope.

3. Results and Discussions

High energy density capacitor dielectrics, field tunable composite dielectrics, and metal oxide varistors (MOVs) are taken as examples in this section to demonstrate the achievable electrical/dielectric properties via the nanodielectric and interface engineering to fulfill the aforementioned development needs.

3.1. Nanofilled Polymer Film for Capacitors. Capacitors represent a big family of non-Faradic energy storage components used in applications ranging from decoupling in circuit board to series capacitive compensation banks at power transmission class. The state-of-art polymeric film capacitors are based primarily on low permittivity polymers such as polypropylene or polyester. One natural approach for higher energy density capacitor is the synthesis of higher permittivity composites with higher dielectric strength by incorporating ceramic fillers into polymer matrix. This is because the energy density of a film capacitor takes the simple form of $1/2\varepsilon_o KE^2$, where K is the dielectric constant and E is the dielectric strength of the polymer film.

Although the dielectric constant can be increased to some extent at higher particle loading level, increasing the dielectric strength remains a great challenge. Instead, the addition of particles exceeding 10 wt% usually results in the considerable loss of dielectric strength of the polymer. Figure 1 is a graphical comparison of the DC breakdown strength for various nanofilled PEI films. With more conductive fillers, lower breakdown strength is not surprising. However, the insulating ceramic fillers of higher breakdown strength do not improve the electrical field endurance of the nanocomposites.

With decreasing particle size, interfacial fraction increases and the particle-polymer interface adhesion also becomes critical. Poor particle dispersion and interaction with polymer matrix is shown in Figures 2(a) and 2(b). It can be seen that both dry alumina and silica particles are agglomerated and remain to be in poor dispersion even after mixing using a high energy ultrasonic vibration. The high surface energy and new chemistry on the nanoparticle surface tend to bond the particles together tightly.

In order to minimize the particle surface effect, colloidal particles that were already well dispersed in a solvent were procured and mixed with a polymer resin in the wet state. Figure 2(c) shows the image of precursor SiO_2 particles. After performing in situ polymerization of the polyamic acid, a polymer nanocomposite containing 5 vol% SiO_2 nanoparticles was synthesized. Great particle dispersion was achieved as shown in Figure 2(d). In order to achieve high energy density in a nanodielectric composite, a compromise between increase in dielectric constant and decrease of dielectric strength when doing nanodielectric engineering appears to be the direction.

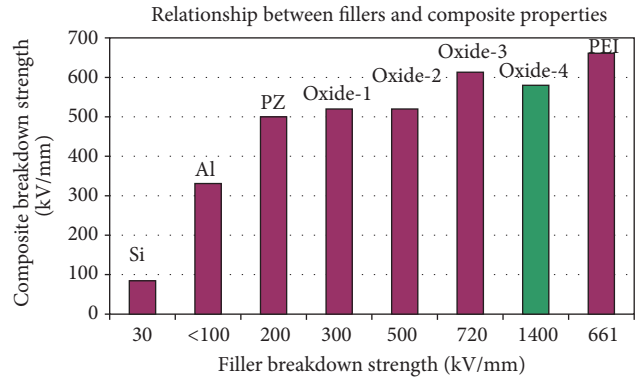

Figure 1: The breakdown strength of PEI nanocomposites with various fillers of about 5 wt% loading. PZ stands for lead zirconate. All polymer films were processed using a solvent cast.

3.2. Field Tunable Nonlinear Composites. The success of nanodielectric engineering depends on several factors, including (1) higher dielectric constant polymer matrix, (2) high permittivity ceramic fillers with low (hysteresis) loss, (3) proper dispersion, and (4) good interfacing between filler and polymer matrix [8, 9]. This becomes even more critical when the particle polarity is increased resulting in higher dielectric constant. Among the polar ceramic materials are ferroelectric (FE) and antiferroelectric (AFE) particles, whose impact on dielectric properties and dispersion are still not well understood [9]. Figure 3 shows the increase of the effective dielectric constant of nanocomposites from addition of particles. Typically, the dielectric constant contrast between high-k ceramic filler and polymer matrix is so high that the electric field concentration in polymer phase will reduce the breakdown strength of the nanocomposites. In addition, high dielectric constant contrast also leads to low electric field penetration into the particles and thus the reduced overall energy storage density in the composites.

In order to enable the nonlinear tunability of polymer, we leveraged ferroelectric $BaTiO_3$ and antiferroelectric lead zirconate nanoparticles (nPZ). The electric filed tunable behavior of the composites was further studied under high electric fields. The nonlinear dependence of the dielectric constant of the polymer composites was fully exhibited as the electric field is increased exceeding the coercive field of lead zirconate (nPZ) as shown in Figure 4. The higher the electric field and loading fraction of particles, the higher the dielectric constant was reached. The field tunable behavior of composites enabled by the polar particles can be applicable for

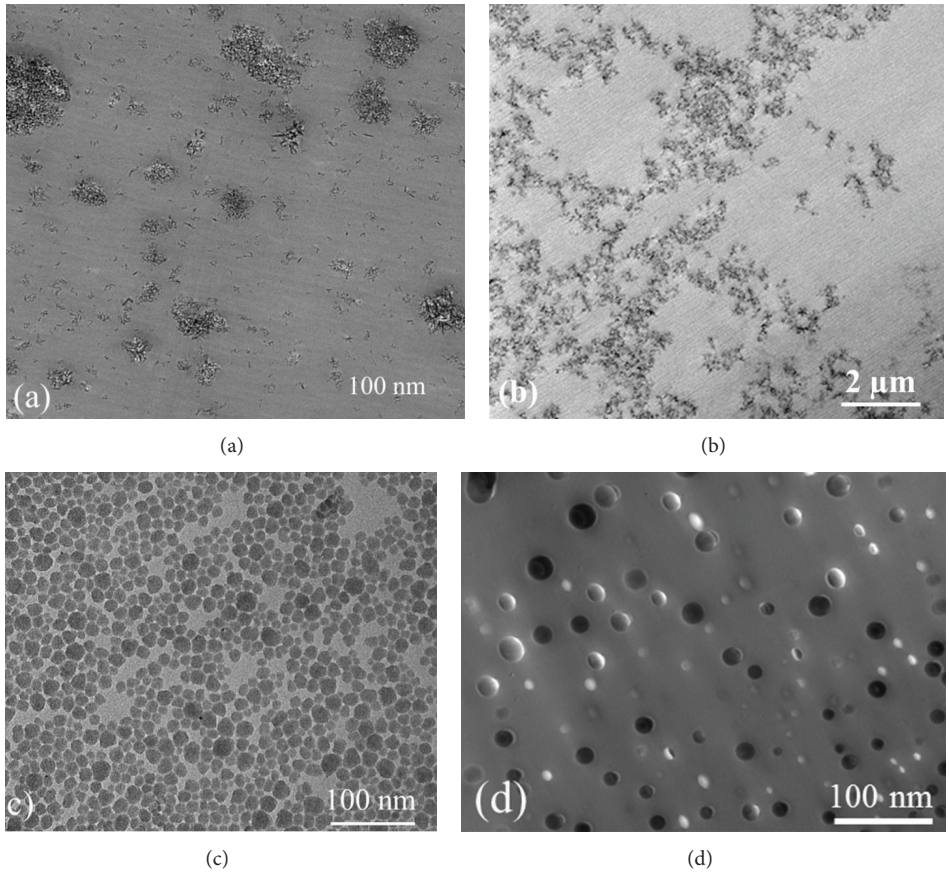

Figure 2: TEM image of 5 vol% nanoparticles dispersing in polymer films. (a) Dry Al_2O_3, (b) dry silica, (c) colloidal SiO_2, and (d) colloidal SiO_2 in a polyimide.

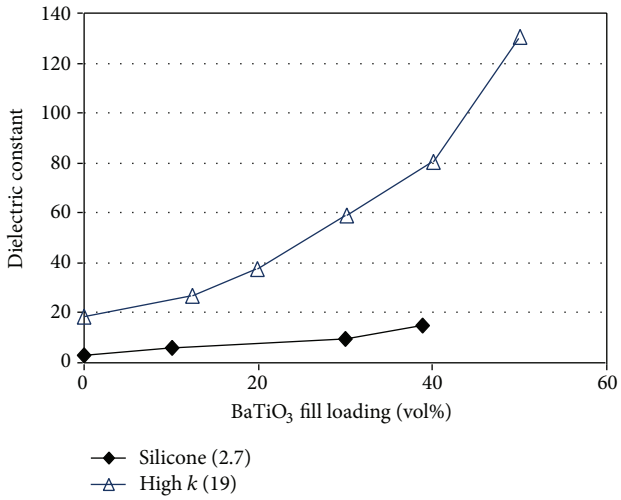

Figure 3: The dielectric constant of nanocomposites as a function of volume pertentage loading of $BaTiO_3$ nanoparticle in silicone and cyanoethyl cellulose with dielectric constant of 2.7 and 19, respectively.

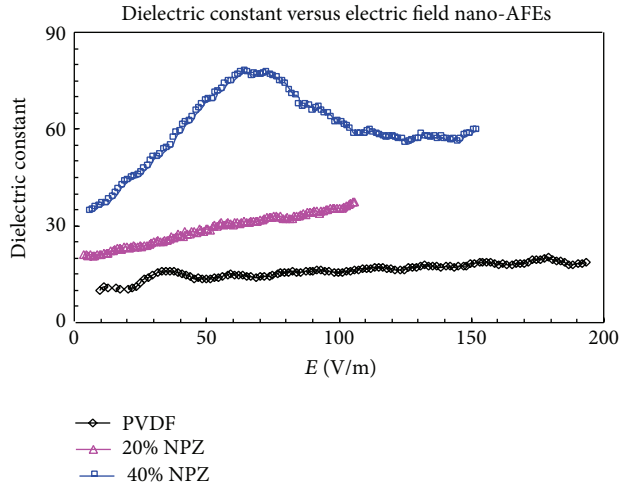

Figure 4: Room temperature dielectric constant under an increased electric field. Values were obtained from the hysteresis loop measurements of a PVDF polymer containing nPZ particles (10 Hz).

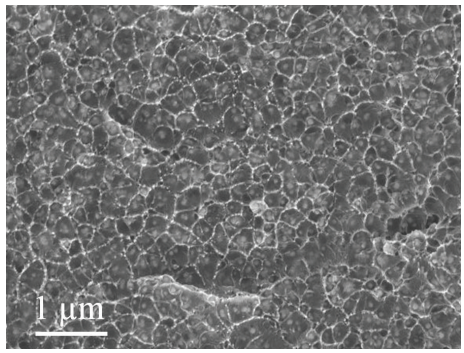

Figure 5: TEM image of polyimide containing 15 vol% 40 nm $BaTiO_3$ nanoparticles through in situ polymerization of 2,2-bis[4-(3,4-dicarboxyphenoxy) phenyl]propane dianhydride (BPADA) with 4,4′-oxydianiline (ODA). Film was solution cast and dried and completely imidized at elevated temperatures.

various devices such as antenna and phase shifters requiring frequency tunability. A breakdown strength of >300 kV/mm was also achieved in the polar nanodielectric composites, rendering an energy density of up to 15 J/cm^3.

TEM imaging shows the great dispersion and particle distribution in the polymer achieved using properly processed particles and mixing method (Figure 5). The fractured cross-section image of the film reveals only cohesive fracture within polymer rather than adhesive failure at interface indicating a strong polymer-particle bonding.

3.3. Nanoenabled Nonlinear Resistor (Varistors). High capacity, high density power system may be subject to high voltage transients and surge protection devices are widely used. Compared with other protection devices such as TVS, metal oxide varistor (MOV) as an example of ceramic-based nonlinear dielectric material at low voltage provides a good combination of high voltage scalability, peak current carrying capability, and fast response speed [10]. Nanoenabled dielectric composites were also studied in both metal oxide varistors and polymer based varistors. MOV is made of bulk ceramic containing predominate grain-boundary barrier junctions. However, the underlying oxide processing requires high sintering temperatures (1000–1300°C) for densification. As a result, compositional and microstructural heterogeneity and large average grain sizes (typically from a few microns to tens of microns, as shown in Figure 6(a)) as well as high porosity caused by exaggerated grain growth during high-temperature sintering limit the performance of existing MOVs. Also shown in Figure 6, fine microstructures can be obtained for nanoenabled MOVs which can be sintered at reduced temperatures (<1000°C). More varistor junctions in a unit MOV device can be provided so that higher voltage can be applied or smaller device can be fabricated for an equivalent voltage requirement.

Higher breakdown voltage (>1 kV/mm) and excellent electrical performance were achieved using the nanopowder precursors, new composition, and sintering profile. The electric field dependence of current for the MOV processed under different sintering conditions is shown in Figure 7. Not only the resistance of the ceramic composites decreases in a nonlinear way with an increase in the electric field, but also the transition field for the nonlinearity is pushed up by 10 times. This will enable miniaturization of MOVs and

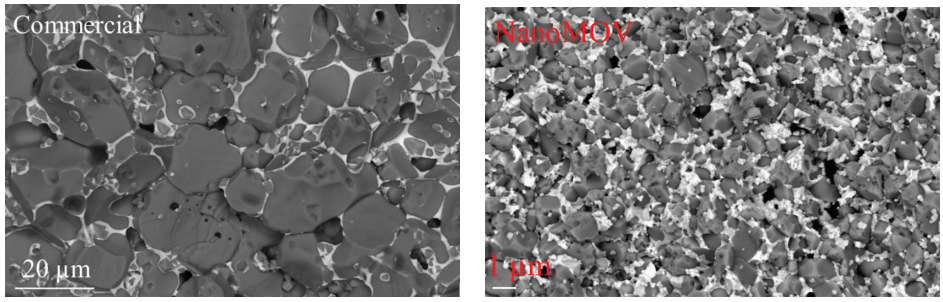

(a) (b)

Figure 6: SEM images of microstructures of a commercial metal oxide varistor (a) and nanoenabled MOV sintered at 850°C (b).

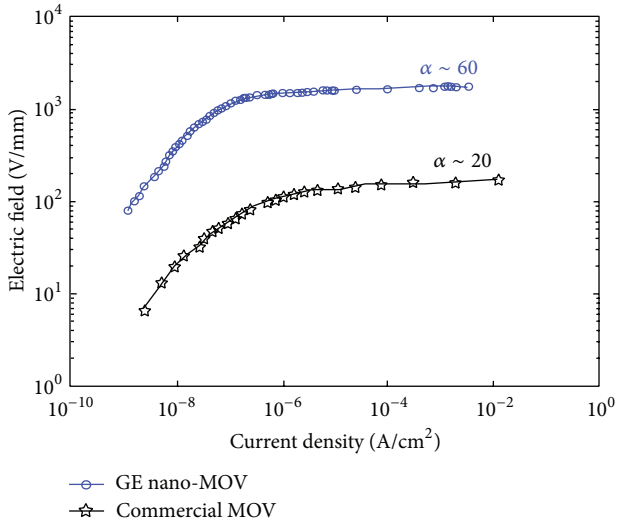

Figure 7: Nanoenabled MOVs with higher breakdown voltage after sintering at lower temperatures. The commercial MOVs made of coarse powder precursors were tested for comparison.

high voltage surge suppression. Besides, when the nano-sized metal oxide precursors were mixed with polymers to form composites, the similar *I-V* characteristics can be observed. The field tuning behavior of the resistance can be fulfilled in the nanodielectric composites.

4. Conclusions

It is demonstrated that novel electrical/dielectric properties can be achieved via the nanodielectric engineering and interface engineering.

(1) Nanodielectric composites can be processed to host variety of ceramic particles and great particle dispersion and bonding with the host polymers can be fulfilled. The loading fraction and particle morphology, however, need to be controlled not to dramatically lower the dielectric strength.

(2) Electrically tunable composites were processed and a nonlinearly dependent dielectric constant was demonstrated by mixing polar nanoparticles with either low-K polyimide polymer or high-K PVDF polymers. The challenges are making the composite tunable at very low electric fields.

(3) High energy density (15 J/cm^3) can be achieved in nanodielectric composites containing nonlinear ferroelectric particles, with proper particle morphology, dispersion, and particle-polymer adhesion.

(4) 10x increase of voltage withstanding capability with low leakage current and higher nonlinearity can be realized in nanoenabled varistors. Refined and uniform submicron structures can be further explored in polymer based tunable resistors.

Further optimization of the performance of these electric device/component based such principles is undertaken.

Conflict of Interests

The authors declare that they have no conflict of interests regarding the publication of this paper.

Acknowledgment

Part of the work was sponsored by US Department of Defense under Contract of FA9451-08-C-0166.

References

[1] A. S. Aricò, P. Bruce, B. Scrosati, J.-M. Tarascon, and W. Van Schalkwijk, "Nanostructured materials for advanced energy conversion and storage devices," *Nature Materials*, vol. 4, no. 5, pp. 366–377, 2005.

[2] A. Nourai, B. P. Martin, and D. R. Fitchett, "For new electricity storage technologies, the proof is in AEP's own tests," *IEEE Power & Energy Magzine*, pp. 41–46, 2005.

[3] B. P. Roberts, "Growing use of large-scale power quality protection systems," in *Proceedings of the Conference on Electrical Supply Industry*, Shanghai, China, 2004.

[4] R. Baldick, "Reactive issues: reactive power in restructured markets," *IEEE Power and Energy Magazine*, vol. 2, no. 6, pp. 14–17, 2004.

[5] Q. Tan, P. Irwin, and Y. Cao, "Advanced dielectrics for capacitors," *IEEJ Transactions on Fundamentals and Materials*, vol. 126, no. 11, pp. 1153–1159, 2006.

[6] Y. Cao, P. C. Irwin, and K. Younsi, "The future of nanodielectrics in the electrical power industry," *IEEE Transactions on Dielectrics and Electrical Insulation*, vol. 11, no. 5, pp. 797–807, 2004.

[7] Y. Cao, S. Zhang, P. Irwin et al., GE TISCAT report 2010GRC431.

[8] D. Q. Tan, Q. Chen, Y. Cao, P. Irwin, and S. Heidger, "Polymer based nanodielectric composites," Presentation at EMA, Orlando, Fla, USA, 2010.

[9] Q. Tan, Y. Cao, and P. Irwin, "DC breakdown in polyetherimide composites and implication for structural engineering," in *Proceedings of the International Conference on Solid Dielectrics (ICSD '07)*, pp. 411–414, Winchester, UK, July 2007.

[10] D. Q. Tan, K. Younsi, Y. Zhou, P. Irwin, and Y. Cao, "Nano-enabled metal oxide varistors," *IEEE Transactions on Dielectrics and Electrical Insulation*, vol. 16, no. 4, pp. 934–939, 2009.

Hindawi Publishing Corporation
Advances in Materials Science and Engineering
Volume 2014, Article ID 107352, 4 pages
http://dx.doi.org/10.1155/2014/107352

Research Article

Enhanced Performance of Dye-Sensitized Solar Cells with Nanostructure Graphene Electron Transfer Layer

Chih-Hung Hsu, Jia-Ren Wu, Lung-Chien Chen, Po-Shun Chan, and Cheng-Chiang Chen

Department of Electro-Optical Engineering, National Taipei University of Technology, No. 1, Section 3, Chung-Hsiao E. Road, Taipei 106, Taiwan

Correspondence should be addressed to Lung-Chien Chen; ocean@ntut.edu.tw

Received 8 November 2013; Revised 3 February 2014; Accepted 3 February 2014; Published 5 March 2014

Academic Editor: J.M.P.Q. Delgado

The utilization of nanostructure graphene thin films as electron transfer layer in dye-sensitized solar cells (DSSCs) was demonstrated. The effect of a nanostructure graphene thin film in DSSC structure was examined. The nanostructure graphene thin films provides a great electron transfer channel for the photogenerated electrons from TiO_2 to indium tin oxide (ITO) glass. Obvious improvements in short-circuit current density of the DSSCs were observed by using the graphene electron transport layer modified photoelectrode. The graphene electron transport layer reduces effectively the back reaction in the interface between the ITO transparent conductive film and the electrolyte in the DSSC.

1. Introduction

Dye-sensitized solar cells (DSSCs), also known as Grätzel's cell, are of particular interest in the field of solar energy owing to their low cost and simplicity of fabrication [1–5]. The DSSCs have a basic structure that comprises two conductive substrates, an absorbing layer of semiconductor materials with wide band gap, dye molecules, and a redox electrolyte.

The basic principle of operation of DSSCs is that electrons are injected from the photoexcited dye into the conductive band of the semiconductor under illumination; meanwhile, the electrolyte reduces the oxidized dye and transports the positive charges to the counter electrode. However, one of the major issues hindering the rapid commercialization of DSSCs is their lower conversion efficiency compared to conventional p-n junction solar cells [6]. That may be attributed to poor charge separation in DSSC structure. Therefore, charge transfer structure, such as Au nanoparticles and quantum dots, has been employed in a DSSC to improve the device performance through charge separation in the photoelectrodes [7–10]. Graphene is a potential material for many applications due to their high electron mobility, outstanding optical properties, and thermal, chemical, and mechanical stability [11–15]. Therefore, this study investigates the effect on the graphene layer as electron transport layer in the DSSC structure deposited by the magnetron sputtering method; in particular, it examines the performance of the DSSCs with the graphene electron transport layer.

2. Experimental

A 60 nm thick graphene layer was sputtered on indium tin oxide (ITO) conductive glass substrate by radio-frequency magnetron sputtering using a graphite target as an electron transport layer to improve the electron transfer in the DSSC structure. Next, the solution consisting of 1 g TiO_2 nanocrystalline powder with diameter ~25 nm, 1 mL of triton X-100, acetic acid, and deionized water were mixture as colloidal solution, and the colloidal solutions were daubed uniformly onto the graphene electron transfer layer to form a thick film. The films were annealed at 450°C for 10 min. Thereafter, the photoelectrode with the graphene layer was immersed in a 3×10^{-4} M solution of N719 dye adsorption ($(Bu_4N)_2$-$[Ru(dcbpyH)_2(NCS)_2]$ complex) in ethanol for 24 hr, before being sintered at 450°C for 30 min, to increase its anatase content. The electrolyte was composed of 0.05 M iodide and 0.5 M lithium iodide with and without 0.5 M 4-tert-butylpyridine (TBP) in propylene carbonate. Then, a 100 nm thick layer of platinum was sputtered onto ITO substrate as a counter electrode. Cells were fabricated by placing sealing

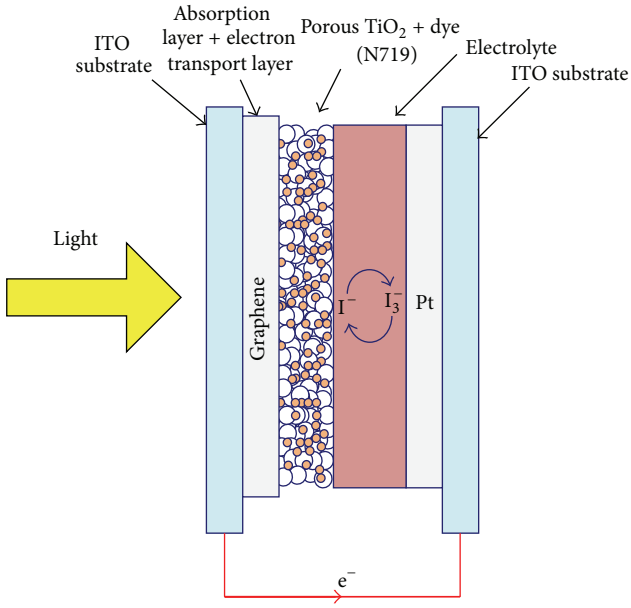

Figure 1: Schematic cross-section of the completed structure.

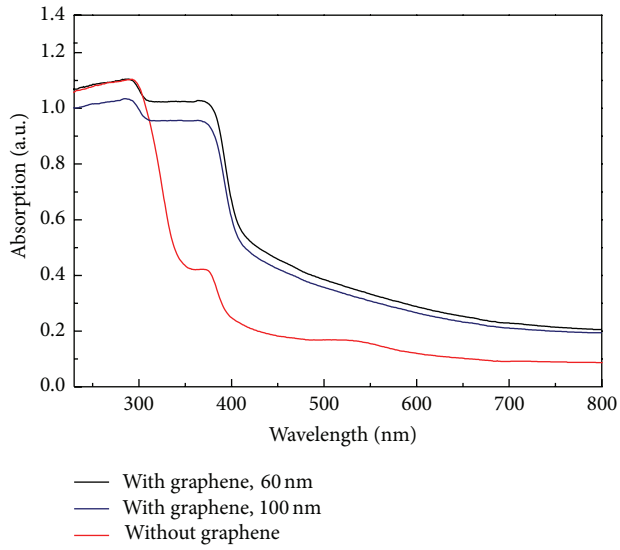

Figure 2: Absorbance spectra of the DSSCs with and without the graphene electron transfer layer.

films (SX1170-60, SOLARONIX) between the two electrodes and leaving just two via-holes for injection electrolyte. The sealing process was carried out on a hot plate at 100°C for 3 min. Then, the electrolyte was injected into the space between the two electrodes through the via-holes. Finally, the via-holes were sealed using the epoxy with low vapor transmission rate. Figure 1 schematically depicts the complete structure. Figure 1 shows the cross-section of the completed structure. The current density-voltage (J-V) characteristics were measured using a Keithley 2420 programmable source meter under irradiation by a 1000 W xenon lamp. Finally, the irradiation power density on the surface of the sample was calibrated at 100 mW/cm^2.

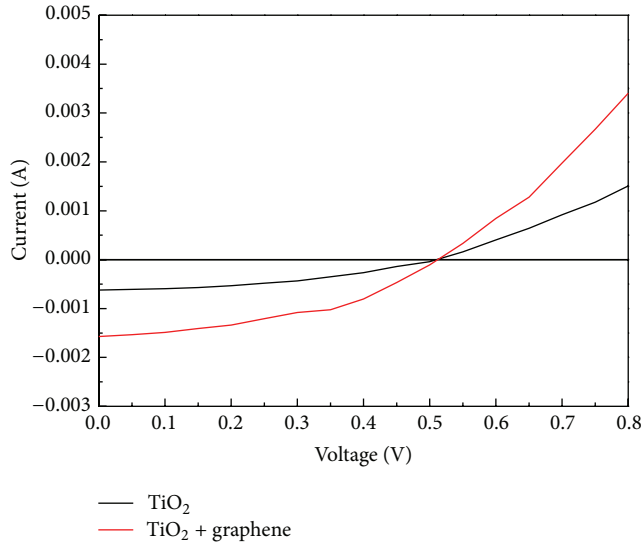

Figure 3: J-V curves of the DSSCs with and without the graphene electron transfer layer under illumination.

3. Results and Discussion

Figure 2 shows the absorption of TiO_2 DSSCs with and without the graphene electron transfer layer. Absorption of the DSSC with the 60 nm thick graphene electron transport layer has obviously higher absorption intensity than the DSSC with the 100 nm thick graphene electron transport layer and without the graphene electron transport layer in visible range, especially in the range of 310–400 nm. That means the graphene electron transport layer has an increased absorption coefficient. Therefore, the graphene electron transport layer is also as an absorption layer to improve the absorption of the solar cells.

Figure 3 shows the I-V characteristics of the DSSCs. The cell performance was measured under AM 1.5 illumination with a solar intensity of 100 mW/cm^2 at 25°C. The cell has an active area of 3 × 3 mm^2 and no antireflective coating. The measured cell parameters, open-circuit voltage (V_{oc}), short-circuit current (J_{sc}), fill factor (FF), and energy conversion efficiency (E_{ff}) are shown in Table 1. As shown in Figure 3, TiO_2 DSSCs with graphene electron transfer layer exhibited the following static parameters: V_{oc} of 0.5 V and J_{sc} of 17.5 mA/cm^2. The fill factor (FF) can be estimated by [16]

$$\mathrm{FF} = \frac{J_m V_m}{J_{sc} V_{oc}}, \tag{1}$$

where J_m is the maximum output current density and V_m is the maximum output voltage. Therefore, the value of FF results is equal to 0.456. Similarly, the energy conversion efficiency (E_{ff}) can be calculated by [16]

$$E_{ff} = \frac{J_m V_m}{P_{inc}} \tag{2}$$

with P_{inc} as the incident power and E_{ff} results to be 3.98%, respectively. The improvement may be attributed to

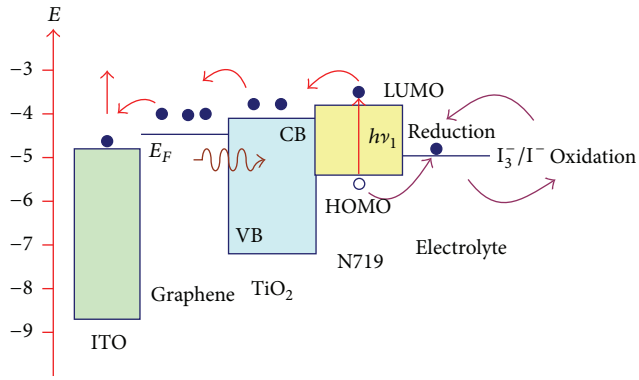

Figure 4: Energy level diagram and mechanism of photocurrent generation in the DSSCs with the graphene electron transfer layer.

Table 1: The parameters for TiO_2 DSSCs with and without graphene electron transport layer.

	TiO_2	Graphene + TiO_2
J_{sc} (mA/cm^2)	6.9	17.5
V_{oc} (V)	0.5	0.5
FF	0.419	0.456
η (%)	1.45	3.98

the incorporation of the graphene electron transport layer. Figure 4 shows the energy level diagram and mechanism of photocurrent generation in TiO_2 DSSCs with the graphene layer. The work function of the graphene layer is around 4.5 eV [17, 18]. Graphene has a work function similar to that of the ITO (4.8 eV) electrode. The graphene layer does not prevent the flow of injected electrons down to the ITO electrode because its work function exceeds that of the ITO electrode [19–21]. The CB and VB are the conduction band and valence band, respectively. The LUMO and HOMO are the lowest unoccupied molecular orbit and highest occupied molecular orbit, respectively. Therefore, the brief operating process is as follows. Dye N719 was excited by incident light, and electrons transit from HOMO to LUMO. Electrons are injected into the graphene electron transport layer via the TiO_2 photoelectrode. The electrons transferred to the graphene electron transport layer were collected at the back contact to generate a photocurrent. Therefore, the inserted graphene layer collects electrons and acts as a transporter in the effective separation of charge and rapid transport of the photogenerated electrons. According to Figures 2 and 3, the enhanced performance of DSSCs with a graphene was attributed to the increase in electron transport efficiency and light absorption in visible range.

4. Conclusions

DSSCs with a graphene electron transport layer were prepared on an indium tin oxide glass substrate by radiofrequency magnetron sputtering. This work discusses the improvement associated with the introduction of a graphene layer in DSSCs. The enhanced performance of DSSCs with a graphene may be attributed to the increase in electron transport efficiency and light absorption in visible range, especially in the range of 310–400 nm. Therefore, the short-circuit current density and efficiency of conversion of solar energy to electricity were increased from 6.9 mA/cm^2 and 1.45% to 17.5 mA/cm^2 and 3.98%, respectively, under simulated full sun illumination. By incorporation of the graphene electron transport layer, the device efficiency can be increased by over 170%.

Conflict of Interests

The authors declare that there is no conflict of interests regarding the publication of this paper.

Acknowledgment

The financial support of this paper was provided by the National Science Council of the Republic of China under Contract no. NSC 102-2622-E-027-021-CC3.

References

[1] B. O'Regan and M. Gratzel, "A low-cost, high-efficiency solar cell based on dye-sensitized colloidal TiO_2 films," *Nature*, vol. 353, no. 6346, pp. 737–740, 1991.

[2] B. O'Regan, J. Moser, M. A. Anderson, and M. Gratzel, "Vectorial electron injection into transparent semiconductor membranes and electric field effects on the dynamics of light-induced charge separation," *The Journal of Physical Chemistry*, vol. 94, no. 24, pp. 8720–8726, 1990.

[3] N. G. Park, J. van de Lagemaat, and A. J. Frank, "Comparison of dye-sensitized rutile- and anatase-based TiO_2 solar cells," *The Journal of Physical Chemistry B*, vol. 104, no. 38, pp. 8989–8994, 2000.

[4] M. Y. Song, D. K. Kim, K. J. Ihn, S. M. Jo, and D. Y. Kim, "Electrospun TiO_2 electrodes for dye-sensitized solar cells," *Nanotechnology*, vol. 15, no. 12, pp. 1861–1865, 2004.

[5] J. Bisquert, D. Cahen, G. Hodes, S. Rühle, and A. Zaban, "Physical chemical principles of photovoltaic conversion with nanoparticulate, mesoporous dye-sensitized solar cells," *The Journal of Physical Chemistry B*, vol. 108, no. 24, pp. 8106–8118, 2004.

[6] T. Bora, H. H. Kyaw, S. Sarkar, S. K. Pal, and J. Dutta, "Highly efficient ZnO/Au Schottky barrier dye-sensitized solar cells: role of gold nanoparticles on the charge-transfer process," *Beilstein Journal of Nanotechnology*, vol. 2, no. 1, pp. 681–690, 2011.

[7] C. Hagglund, M. Zach, and B. Kasemo, "Enhanced charge carrier generation in dye sensitized solar cells by nanoparticle plasmons," *Applied Physics Letters*, vol. 92, no. 1, Article ID 013113, 2008.

[8] S. Barazzouk and S. Hotchandani, "Enhanced charge separation in chlorophyll a solar cell by gold nanoparticles," *The Journal of Applied Physics*, vol. 96, no. 12, pp. 7744–7746, 2004.

[9] S. W. Tong, C. F. Zhang, C. Y. Jiang et al., "Improvement in the hole collection of polymer solar cells by utilizing gold nanoparticle buffer layer," *Chemical Physics Letters*, vol. 453, no. 1–3, pp. 73–76, 2008.

[10] L. C. Chen, C. C. Wang, and B. S. Tseng, "Enhancement in nanocrystalline TiO_2 solar cells sensitized with ZnPc by nanoparticles," *Journal of Optoelectronic and Biomedical Materials*, vol. 1, no. 3, pp. 249–254, 2009.

[11] X. Du, I. Skachko, A. Barker, and E. Y. Andrei, "Approaching ballistic transport in suspended grapheme," *Nature Nanotechnology*, vol. 3, no. 8, pp. 491–495, 2008.

[12] R. R. Nair, P. Blake, A. N. Grigorenko et al., "Fine structure constant defines visual transparency of graphene," *Science*, vol. 320, no. 5881, p. 1308, 2008.

[13] X. Wang, L. Zhi, N. Tsao, Z. Tomovic, J. Li, and K. M. Müllen, "Transparent carbon films as electrodes in organic solar cells," *Angewandte Chemie International Edition*, vol. 47, no. 16, pp. 2990–2992, 2008.

[14] X. Wang, L. Zhi, and K. Müllen, "Transparent, conductive graphene electrodes for dye-sensitized solar cells," *Nano Letters*, vol. 8, no. 1, pp. 323–327, 2008.

[15] S. Bae, H. Kim, Y. Lee et al., "Roll-to-roll production of 30-inch graphene films for transparent electrodes," *Nature Nanotechnology*, vol. 5, no. 8, pp. 574–578, 2010.

[16] S. M. Sze, *Physics of Semiconductor Devices*, John Wiley & Sons, New York, NY, USA, 2nd edition, 1981.

[17] M. Koshino and T. Ando, "Electronic structures and optical absorption of multilayer graphenes," *Solid State Communications*, vol. 149, no. 27-28, pp. 1123–1127, 2009.

[18] G. Giovannetti, P. A. Khomyakov, G. Brocks, V. M. Karpan, J. van den Brink, and P. J. Kelly, "Doping graphene with metal contacts," *Physical Review Letters*, vol. 101, no. 2, Article ID 026803, 2008.

[19] R. Czerw, B. Foley, D. Tekleab, A. Rubio, P. M. Ajayan, and D. L. Carroll, "Substrate-interface interactions between carbon nanotubes and the supporting substrate," *Physical Review B*, vol. 66, Article ID 033408, 2002.

[20] A. Kongkanand, R. Martinez-Dominguez, and P. V. Kamat, "Single wall carbon nanotube scaffolds for photoelectrochemical solar cells. Capture and transport of photogenerated electrons," *Nano Letters*, vol. 7, no. 3, pp. 676–680, 2007.

[21] F. Xu, J. Chen, X. Wu et al., "Graphene scaffolds enhanced photogenerated electron transport in ZnO photoanodes for high-efficiency dye-sensitized solar cells," *The Journal of Physical Chemistry C*, vol. 117, pp. 8619–8627, 2013.

Hindawi Publishing Corporation
Advances in Materials Science and Engineering
Volume 2014, Article ID 602495, 12 pages
http://dx.doi.org/10.1155/2014/602495

Research Article

TiO_2 Photocatalyst Nanoparticle Separation: Flocculation in Different Matrices and Use of Powdered Activated Carbon as a Precoat in Low-Cost Fabric Filtration

Carlos F. Liriano-Jorge, Ugur Sohmen, Altan Özkan, Holger Gulyas, and Ralf Otterpohl

Institute of Wastewater Management and Water Protection, Hamburg University of Technology, Eissendorfer Straße 42, 21073 Hamburg, Germany

Correspondence should be addressed to Holger Gulyas; holli@tuhh.de

Received 5 December 2013; Accepted 15 January 2014; Published 23 February 2014

Academic Editor: J. M. P. Q. Delgado

Separation of photocatalyst nanoparticles is a problem impeding widespread application of photocatalytic oxidation. As sedimentation of photocatalyst particles is facilitated by their flocculation, the influence of common constituents of biologically pretreated wastewaters (NaCl, $NaHCO_3$, and their combination with humic acid sodium salt) on flocculation was tested by the pipet method. Results showed that the impact of these substances on TiO_2 nanoparticle flocculation is rather complex and strongly affected by pH. When humic acid was present, TiO_2 particles did not show efficient flocculation in the neutral and slightly basic pH range. As an alternative to photocatalyst separation by sedimentation, precoat vacuum filtration with powdered activated carbon (PAC) over low-cost spunbond polypropylene fabrics was tested in the presence of two PAC types in aqueous NaCl and $NaHCO_3$ solutions as well as in biologically treated greywater and in secondary municipal effluent. PAC concentrations of $\geq$ 2 g/L were required in order to achieve a retention of nearly 95% of the TiO_2 nanoparticles on the fabric filter when TiO_2 concentration was 1 g/L. Composition of the aqueous matrix and PAC type had a slight impact on precoat filtration. PAC precoat filtration represents a potential pretreatment for photocatalyst removal by micro- or ultrafiltration.

1. Introduction

Biological treatment of municipal wastewater does not remove all trace organics. For example, some pharmaceuticals such as carbamazepine are not susceptible to biodegradation. Therefore, ozonation is widely discussed as an oxidative tertiary treatment in municipal wastewater treatment [1]. Besides ozonation which is highly energy-consuming (6–10 kW h are required for the production of 1 kg O_3 in large-scale ozone generators), advanced oxidation processes (AOPs) are increasingly focused for this purpose [2]. An AOP which can be powered by the sun is heterogeneous photocatalytic oxidation (PCO). TiO_2 nanoparticles were most frequently investigated, because they represent absolutely stable photocatalysts. As an industrial bulk product, TiO_2 is easily available.

Although TiO_2 is looked at as nontoxic, a concentration of TiO_2 nanoparticles (diameter $\approx$ 100 nm) as small as 2 mg/L has recently been shown to inhibit the second molting of age-synchronized *Daphnia magna* neonates by about 90%, while the first molting was not affected [3]. At the end of a 96 h incubation period, around 70% of the organisms were immobilized due to TiO_2 nanoparticles. TiO_2 particles with diameters around 100 nm were significantly more toxic toward *D. magna* than 200 nm particles. These findings emphasize the need of a safe barrier for TiO_2 photocatalyst nanoparticles within the PCO process in order to prevent them from spreading into the aqueous environment.

Investigations with a laboratory-scale wastewater treatment plant resulted in considerable escape of nanoparticles with the effluent [4]. Sedimentation for separation of the photocatalyst subsequent to the accomplished PCO process

is usually insufficient. Even when the photocatalyst flocculates, there is often a residue of suspended photocatalyst as observed by the authors in settled samples from laboratory-scale PCO experiments with biologically pretreated greywater. Sometimes, turbidity was visible even after centrifugation of the sedimentation supernatants. Photocatalyst flocculation depends on the wastewater matrix [5] and is hardly predictable.

One option making photocatalyst separation unnecessary is photocatalyst immobilisation. However, data on long-term stability of immobilized photocatalysts is very scarce. Another drawback of photocatalyst immobilization on surfaces of larger particles such as powdered activated carbon (PAC), silica, or zeolite (which are more rapidly settling than nanoparticles) is that these composites have to be especially produced requiring special know-how and additional financial resources.

Alternatives to sedimentation and to photocatalyst immobilization on surfaces are sand filtration, hydrocyclones, or membrane filtration. Sand filtration is not a safe method for recovering TiO_2 nanoparticles, because only under conditions leading to TiO_2 agglomeration (pH 7), retention of photocatalyst particles in a sand filter was observed, while at pH 5 flocculation and also retention of particles were low [6]. In contrast, TiO_2 immobilized by sol-gel method on 20 to 200 μm diameter glass spheres could be removed by sand filtration subsequent to PCO [7].

There exists little experience with hydrocyclones for photocatalyst removal. However, as hydrocyclones are based on centrifugal forces, they might be similarly inefficient as laboratory centrifuges with several 1000 times gravitational acceleration, g, as frequently observed by the authors during particle removal from samples taken from PCO experiments utilizing TiO_2 "P25." Bickley et al. [8] have tested large particle size (1–100 μm) photocatalysts which were proven to be separated by means of hydrocyclones. However, such large photocatalyst particles exhibit low specific surfaces. The consequence is poor adsorption of organics and thus low reaction rates [9]. Additionally, microparticles do not show any "quantum size effect." This makes them also less efficient PCO catalysts than nanoparticles [10].

Membrane filtration processes are more successful in photocatalyst removal. Sopajaree et al. [11] found separation of nanosized photocatalyst TiO_2 "P25" to be complete with ultrafiltration membranes, but concentration polarisation increased with increasing photocatalyst concentration. Additionally, there is little to no experience with working life of organic membranes when the feed/retentate contains abrasive TiO_2 particles. Doll and Frimmel [12] gathered positive lab-scale experience combining heterogeneous PCO with a ceramic single channel microfiltration membrane made of α-aluminium oxide. Flocculation of nanoparticles is beneficial for their retention by microfiltration. Another disadvantage of membrane filtration is that it adds to power consumption of a PCO reactor (which is also the case for hydrocyclones due to the strong pumps necessary for their operation).

A more economically feasible solution for photocatalyst separation would be fabric filtration using cheap fabrics such as the raw material for disposable laboratory coats (Wendland, personal communication) made from spunbond polypropylene. However, fabrics like this are not expected to be able to retain nanoparticles. Therefore, precoat filtration using powdered activated carbon (PAC) might be useful in combination with fabric filters. As the combination of particular PAC types with PCO was shown to be advantageous for removal of phenol [13–16] and also other compounds, the precoat filtration of TiO_2 with PAC suggests itself.

For evaluating the feasibility of precoat filtration for nanoparticle separation, TiO_2 "P25" suspensions (1 g/L) were mixed with different amounts of two PAC types. A TiO_2 concentration of 1 g/L was chosen because it is very common in PCO studies. These mixtures were subjected to vacuum filtration over small pieces of spunbond polypropylene fabrics and the filtrates were analyzed for total solids. Another aim of the study was to investigate TiO_2 "P25" nanoparticle flocculation in model wastewaters containing different amounts of NaCl, $NaHCO_3$, and humic acid sodium salt by means of the pipet method.

2. Materials and Methods

2.1. Flocculation Experiments. Flocculation of photocatalyst in different model wastewaters was investigated by the "pipet method" as described elsewhere [5] by allowing 1 g/L TiO_2 (Aeroxide P25, Evonik Industries AG, Hanau-Wolfgang, Germany) suspensions in aqueous solutions containing different NaCl or $NaHCO_3$ concentrations (0–1000 mg/L) and different concentrations (0–50 mg/L) of humic acid sodium salt (HANa, Carl Roth GmbH, Karlsruhe, Germany) to settle for 1 hour prior to taking a 50 mL sample with a pipet the tip of which was fixed exactly 10 cm below the liquid surface. These samples were subsequently membrane-filtered (0.45 μm pore width) and the TiO_2 mass retained on the filter was gravimetrically determined after drying at 105°C.

2.2. Precoat Fabric Filtration of TiO_2. Circular pieces of 5 cm diameter were cut from 100 g/m^2 spunbond polypropylene fabrics used for disposable laboratory coats manufacture (Figure 1).

The fabric pieces were fixed in a vacuum filtration apparatus using a water-jet vacuum pump for creating the vacuum. For filtration over the fabrics, the following suspensions were prepared: 1 g/L TiO_2 "P25" suspension either in NaCl or $NaHCO_3$ solutions of different concentrations (0, 0.1, 0.5 or 1 g/L) in deionized water, in a matrix of biologically pretreated greywater (effluent of a constructed wetland for greywater treatment described in more detail elsewhere [17]) or in secondary municipal effluent. 100 mL of these suspensions were added to different amounts of two types of PAC (Merck article no. 102186 or Lurgi Hydraffin WG; for properties of both PAC types, see Table 1) resulting in activated carbon concentrations in the range from 0 to 5000 mg/L.

Volumes of 50 mL of the stirred suspensions were pipetted on to the filter pieces and vacuum-filtered. The filtrates were collected in 100 mL beakers with exactly recorded tare weights. The beakers with the filtrate were heated in a furnace at 80°C until all the water was evaporated and dried at 105°C

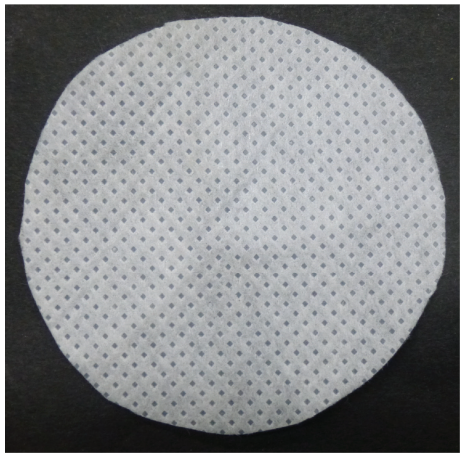

Figure 1: Circular piece of spunbond polypropylene fabric (5 cm diameter) used as filter medium for TiO_2 nanoparticles precoat filtration with PAC.

Table 1: Providers' information about properties of the investigated activated carbons.

	Merck 102186	Hydraffin WG
Ash content	<1	About 5
pH (in deionised water)	4–7	3–5
Particle size	About 60 μm[a], 50% ≤30 μm, 90% ≤100 μm	85% ≤40 μm
BET surface (m^2/g)	775[a]	1100
Iodine uptake (mg/g)	888	1050

[a][16].

until weight constancy, cooled in a desiccator and weighed again for total solids (TS) determination. TS concentrations of the matrices (without TiO_2 and PAC) were recorded in the same way by drying 50 mL of each solution. These values representing total solids of the matrix (TS_{matrix}) were subtracted from the TS concentrations of the filtrates.

3. Results and Discussion

3.1. Aqueous Matrix Impact on TiO_2 Flocculation. In Figure 2, the influence of NaCl concentration on TiO_2 flocculation at different HANa concentrations is shown. When no humic acid was present, TiO_2 flocculation was increasing with increasing NaCl concentration (Figure 2(a)). At an NaCl concentration of 1 g/L, about 90% of TiO_2 settled from the top 10 cm of the suspension after 1 h indicating a high extent of flocculation, while in deionized water the concentration of suspended TiO_2 was only diminished by 10%. Enhanced flocculation with increasing NaCl concentration can be attributed to compression of the electric double layer around the photocatalyst particle. When 10 mg/L of humic acid sodium salt was present (Figure 2(b)), flocculation was very pronounced nearly irrespective of NaCl concentration. This can be referred to the influence of HANa on pH of the suspensions which was about 5.8 at this humic acid sodium salt concentration (Figure 2(b)). It can be assumed that this pH is close to the point of zero charge (PZC) of TiO_2 "P25" in the given matrix. At PZC, maximum flocculation is achieved. This PZC was also found in another TiO_2 flocculation study in aqueous matrices containing the nondissociable organic tetraethyleneglycol dimethylether and different inorganic salts [5].

With 20 mg/L HANa (Figure 2(c)), flocculation increased with increasing NaCl concentration similar to experiments without humic acid, but not as pronounced. At this HANa concentration, the pH of the suspensions was 6.3 instead of 4.5 to 5 as determined in the absence of HANa. An HANa concentration of 50 mg/L (Figure 2(d)) led only to slight flocculation. This can be interpreted by efficient adsorption of humic acid anions to the photocatalyst surface [18] with the consequence of more negative surface charges leading to increased repulsion of particles.

It has to be noted that artifacts caused by the applied methodology for evaluating nanosized photocatalyst flocculation cannot be excluded. Nonflocculated nanoparticles might not have been retained by microfiltration. In this case, flocculation would have been overestimated. However, the study of Armanious et al. [5] clearly showed full retention of nonflocculated TiO_2 nanoparticles in a deionized water matrix by microfiltration.

The inorganic salt $NaHCO_3$ showed an influence on flocculation (Figure 3) different from that of NaCl. Concentrations of $NaHCO_3$ of 100 mg/L and more resulted in a pH above 8, irrespective of HANa concentration. The graphs in Figures 3(b), 3(c), and 3(d)) clearly show that TiO_2 flocculation was increased in matrices containing humic acid when $NaHCO_3$ concentration was augmented from 100 to 200 mg/L. Further enhancement of bicarbonate concentration did not result in markedly intensified flocculation, probably due to efficient adsorption of humic acid anions which are predominantly negatively charged at pH > 8 (pK_a of humic acids is reported to be in the range of 3.5–5 [19]) leading to particle repulsion. When no humic acid sodium salt was present (Figure 3(a)), flocculation was much more pronounced. There was a sharp increase in flocculation for small $NaHCO_3$ concentrations of 10 and 20 mg/L obviously due to pH adjustment by these $NaHCO_3$ concentrations to PZC which may be around pH 7 when no humic acid anions were present. Compression of the electric double layer can be assumed to play an additional role at $NaHCO_3$ concentrations above 500 mg/L in the absence of humic acid (Figure 3(a)).

PZC in the presence of HANa can be assumed to be around 5-6 because the lowest TiO_2 concentration after 1 h sedimentation time in HANa-containing suspensions was recorded in this pH range (Figure 2(b)). When pH was elevated to around 7 by $NaHCO_3$ and further HANa addition, humic acids adsorbed to the photocatalyst surface were predominantly negatively charged leading to repulsion of photocatalyst particles (compare Figure 3(b) to Figure 2(b)). Elevating pH to more than 7.5 by adding $NaHCO_3$ (compare Figure 3(d) to Figure 2(d)) may lead to more negatively charged TiO_2 surfaces which may cause reduced adsorption of humic acid anions on the photocatalyst. A lower repulsion between photocatalyst particles because of less negative

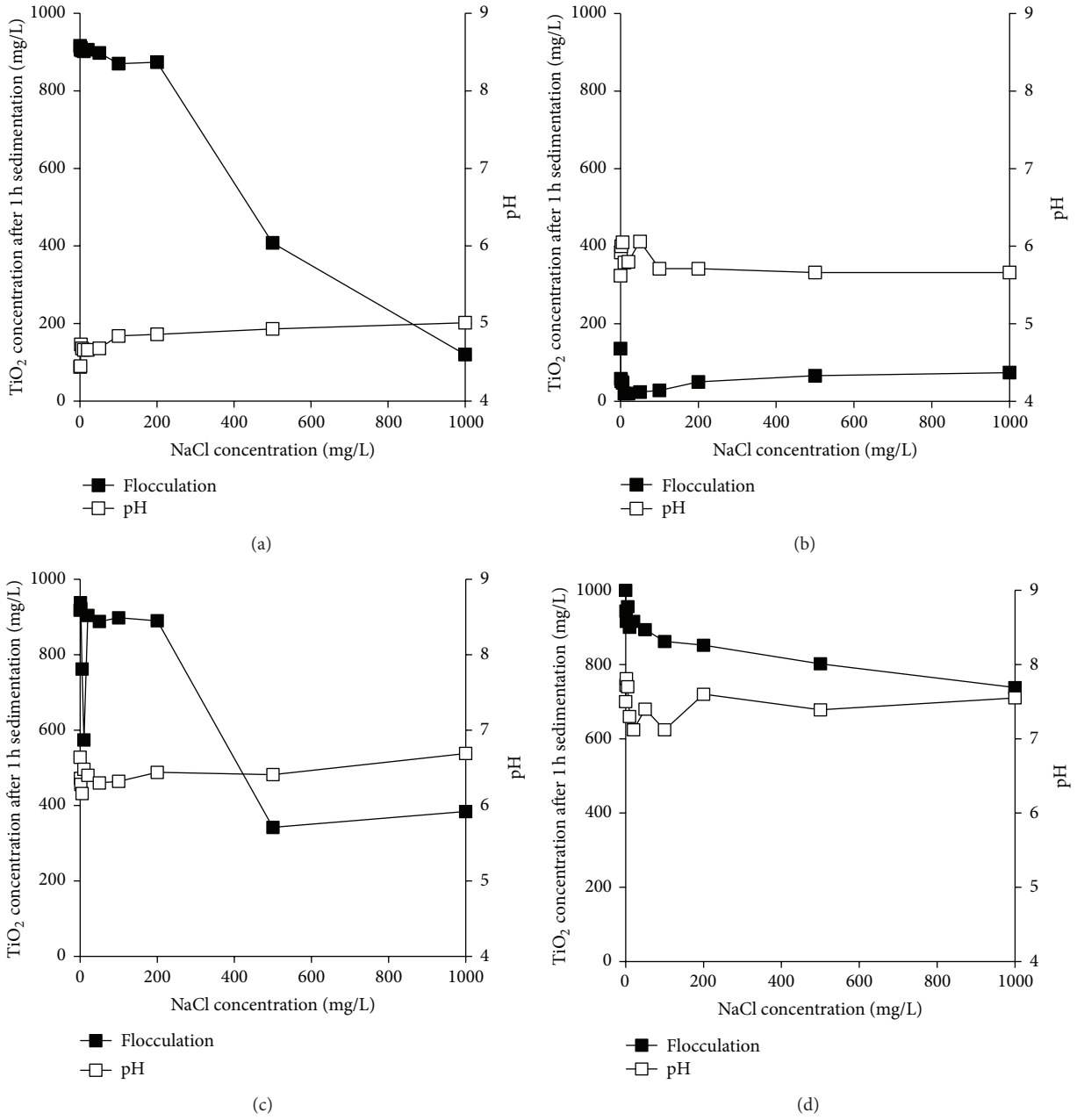

Figure 2: Photocatalyst flocculation and pH in 1 g/L TiO_2 "P25" suspensions in aqueous solutions with no (a), 10 (b), 20 (c), and 50 mg/L (d) humic acid sodium salt, HANa, at different NaCl concentrations.

charges on their surface due to less adsorbed humic acid anions might have been the consequence.

Only a few of the matrices tested in this study led to pronounced flocculation of TiO_2 nanoparticles; in the absence of HANa, only NaCl concentrations in the range of 1000 mg/L (pH ≈ 5) and $NaHCO_3$ concentrations of 10 to 1000 mg/L (resulting in a pH range of 7–8.5) led to flocculation. HANa addition commonly deteriorated flocculation except in NaCl matrices (irrespective of NaCl concentration) when HANa concentrations did not exceed 10 mg/L (Figure 2). However, as PCO leads to removal of humic substances, repulsion of photocatalyst particles caused by humic or fulvic acid anions adsorbed to the photocatalyst is no longer expected in PCO-treated wastewaters. The hydrogen carbonate formed by PCO might enhance flocculation when pH of the suspension is between 6.5 and 8 (Figure 3(a)).

Overall, the impact of organic and inorganic wastewater constituents on photocatalyst flocculation is very complicated and difficult to predict. Flocculation can be expected to affect photocatalyst sedimentation as well as PCO efficiency. A previous study [5] revealed that the relation of PCO rate constants to photocatalyst flocculation was not as unequivocal as the relationship between rate constants and pH. However, most intense flocculation was linked to

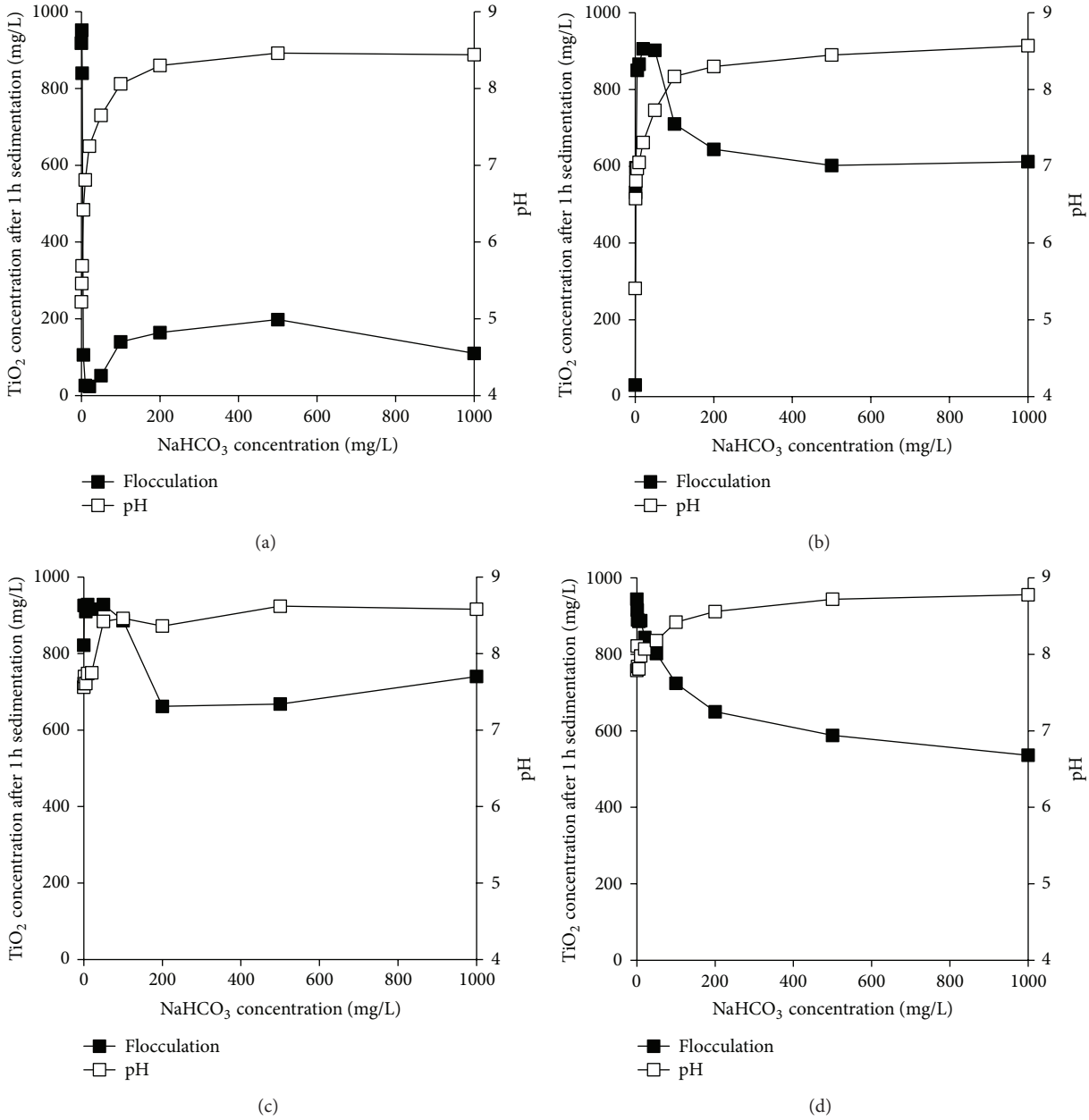

Figure 3: Photocatalyst flocculation and pH in 1 g/L TiO_2 "P25" suspensions in aqueous solutions with no (a), 10 (b), 20 (c), and 50 mg/L (d) humic acid sodium salt, HANa, at different $NaHCO_3$ concentrations.

lowest rate constant while the rate constant was maximum when flocculation was negligible. While it cannot be excluded that TiO_2 photocatalyst flocculation is disadvantageous with respect to PCO efficiency, it is beneficial for photocatalyst recovery by sedimentation and also by sand filtration as recently shown [6].

3.2. Precoat Filtration. The filtrates received by vacuum filtration over the spunbond polypropylene fabrics were turbid in all cases. Without addition of PAC, the filtrates were white opaque suspensions similar to the suspensions before filtration. When PAC was added to TiO_2 suspensions prior to filtration, the filtrates appeared as grey suspensions. However, opacity of the filtrates decreased with increasing PAC dosage prior to filtration. Increasing PAC concentrations led to longer periods of time required for filtering one batch of 50 mL. In Figure 4, total solids (TS) concentrations in mixed TiO_2/PAC suspensions filtered over spunbond polypropylene fabrics are displayed which were corrected by subtraction of total solids of the liquid phases. Figures 4(a) and 4(b) show that TiO_2 "P25" was not retained from 1 g/L suspensions in deionized water when no PAC was added. So, the investigated fabric does not remove the nanoparticles without precoating. However, the addition of increasing amounts of Merck

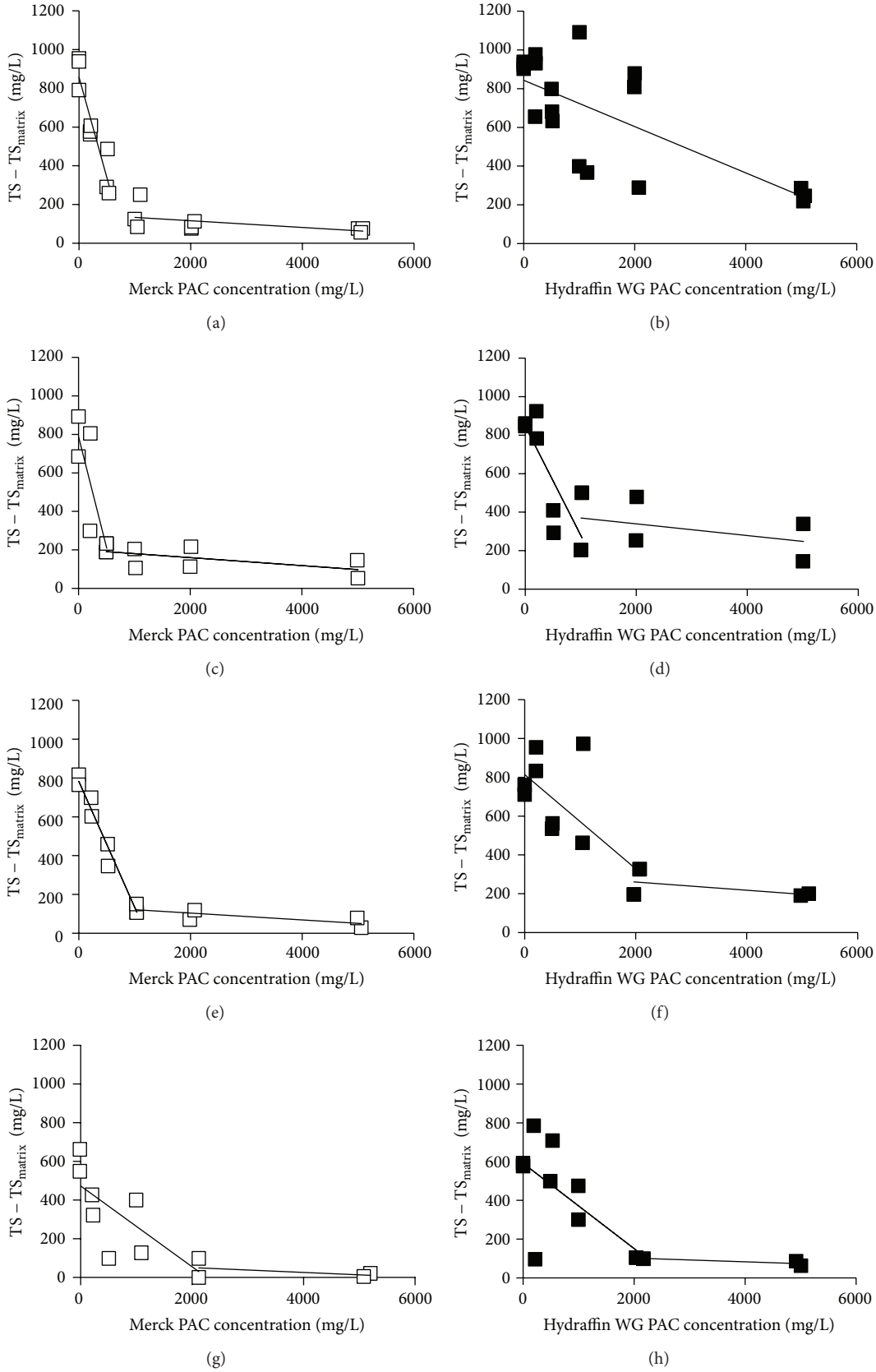

Figure 4: Total solids concentrations (corrected for TS concentrations of the matrices) in 1 g/L TiO_2 suspensions containing different amounts of Merck PAC or Hydraffin WG PAC in different matrices ((a), (b): deionized water; (c), (d): 0.1 g/L NaCl solution; (e), (f): 0.5 g/L NaCl solution; (g), (h): 1 g/L NaCl solution) subsequent to vacuum filtration over spunbond polypropylene fabrics.

PAC led to decreased concentrations of total solids in the filtrate indicating that this PAC type is a feasible precoat (Figure 4(a)). When the added Merck PAC concentration exceeded 1 g/L, further increase of PAC concentration did not result in pronounced reduction of TS concentration in the filtrate (Figure 4(a)). During the experiments with the Merck PAC in the deionized water matrix, the total solids obtained after drying the filtrates were subjected to glowing at 550°C (until weight constancy). While without addition of PAC the total nonvolatile solids concentration in the filtrate was about 800 mg/L, only around 70 mg/L nonvolatile solids were detected in the filtrates subsequent to addition of 2000 mg/L Merck PAC as a precoat (data not shown). This indicates that the particles in those filtrates obtained with sufficient Merck PAC addition consisted of TiO_2 particles for the most part. Nevertheless, precoat filtration with 2000 mg/L Merck PAC resulted in more than 90% TiO_2 removal.

The other investigated PAC type (Hydraffin WG) showed a completely different behaviour as precoat in the deionized water matrix (Figure 4(b)); although solid retention showed an increasing tendency with increasing PAC concentration in the original suspensions, it was less efficient and not as reproducible as with the Merck PAC. Nonvolatile solids determined in one of the filtrates were more than 800 mg/L when 2000 mg/L Hydraffin WG was used as a precoat (data not shown). A conclusion from these results is that the Hydraffin WG PAC is a less efficient precoat than the Merck PAC when the aqueous solutions contain NaCl.

It was not expected from particle size data of the two PAC types (Table 1), that precoat filtration with Hydraffin WG PAC would have resulted in a lower TiO_2 retention than with the Merck PAC; Hydraffin WG consisted of slightly smaller particles than the Merck PAC. So, it was assumed that TiO_2 particles should be retained to a larger extent in the filter cake formed by Hydraffin WG, because it will exhibit smaller pores than the Merck PAC filter cake. Probably, some more Hydraffin PAC particles escaped through the pores of the fabric filter. However, as mentioned above more than 800 mg/L of the solids in the filtrate were nonvolatile, that is, TiO_2. So, the least part of the particles in the filtrate was represented by Hydraffin WG PAC.

Lower precoat efficiency of Hydraffin WG might be caused by a lower extent of interaction of the TiO_2 surface with functional groups on the surface of Hydraffin WG PAC in comparison to the Merck PAC. Coordinative interactions of Ti centers on the TiO_2 photocatalyst surface with particular oxygen-containing carbon-functional surface groups such as carboxylic acids or cyclic ethers were claimed by Matos et al. [14]. Interactions between TiO_2 "P25" and the Merck PAC which was also utilized in this study were indicated by the disappearance of FTIR peaks of the Merck PAC at 3400 cm^{-1} (phenolic PAC surface groups) and at 1000–1200 cm^{-1} (attributed to cyclic ether groups) when it was mixed with TiO_2 [20]. On one hand, this coordination might enable injection of charge carriers from illuminated TiO_2 particles into activated carbon grains. On the other hand, such interactions can also be hypothesized to lead to enhanced adhesion between TiO_2 photocatalyst particles and particular PAC types.

This hypothesis was also supported by results of the precoat filtration experiments with the NaCl solution matrices (Figures 4(c)–4(h)); in all cases, addition of Merck PAC above 2000 mg/L resulted in lower TS concentrations in the filtrates than addition of the Hydraffin WG PAC. Obviously, increase of NaCl concentration in the aqueous phase was beneficial for precoat filtration with both PAC types; especially at PAC concentrations ≥ 2000 mgL, total solids concentrations in the filtrate were decreasing. This might be a consequence of intensified flocculation of TiO_2 nanoparticles caused by compression of the electric double layer. Agglomerated TiO_2 particles are probably more readily retained in the PAC filter cakes.

Replacement of NaCl by $NaHCO_3$ led to similar results of TiO_2 precoat filtration (Figure 5). Both PAC types at concentrations of ≥2000 mg/L clearly reduced particle concentrations in the filtrates. However, precoat filtration with Merck PAC in the $NaHCO_3$ matrix showed slightly worse results than in the NaCl matrix, while precoat filtration with Hydraffin WG at concentrations ≥ 2000 mg/L was a bit more efficient in the $NaHCO_3$ matrix. When $NaHCO_3$ concentration was 0.5 g/L, the Hydraffin WG PAC was an even better precoat than Merck PAC. At $NaHCO_3$ concentrations of 0.1 and 1 g/L, precoat filtration with both PAC types at concentrations above 2000 mg/L wasnearly equally efficient.

In a matrix of biologically treated greywater, more particles escaped through the spunbond polypropylene fabric (Figures 6(a) and 6(b)) than in experiments with aqueous NaCl and $NaHCO_3$ solutions (Figures 4 and 5). Biologically treated greywater contains more salts additional to NaCl [5]. Substances contained in biologically treated greywater might have affected interactions between photocatalyst and PAC particles. Obviously, they deteriorate the precoat filtration. These findings are in contrast with results obtained with TiO_2/PAC suspensions in secondary municipal effluent (Figures 6(c) and 6(d)); in the secondary municipal effluent, precoat filtration with both PAC types was more efficient than in the greywater matrix. Similar to findings in the greywater, the Merck PAC was more suitable than the Hydraffin WG PAC.

Overall, the impact of the wastewater matrix on precoat filtration seems to be quite complex. As mentioned above, it can be hypothesized that there are interactions between TiO_2 nanoparticles and PAC grains such as coordinative complexation of Ti centers on TiO_2 surface by carboxylic acid or cyclic ether functional groups on surfaces of the activated carbon [14, 20]. These interactions are probably influenced by the surrounding aqueous solution similar to interactions between activated carbon surface functional groups and organic adsorptive molecules which have been recently reviewed [21]. The two key factors found in the surrounding aqueous solution which influence activated carbon/adsorbed organic molecule interactions were identified to be pH and ionic strength. While NaCl only affects ionic strength, $NaHCO_3$ influences both pH and ionic strength. The pH has a strong impact on surface chemistry of activated carbon [21]. Except by $NaHCO_3$, the pH of the TiO_2/PAC suspensions is affected by the acidic nature of the TiO_2 itself and the acidity or basicity of the activated carbon (see Table 2). Hydraffin

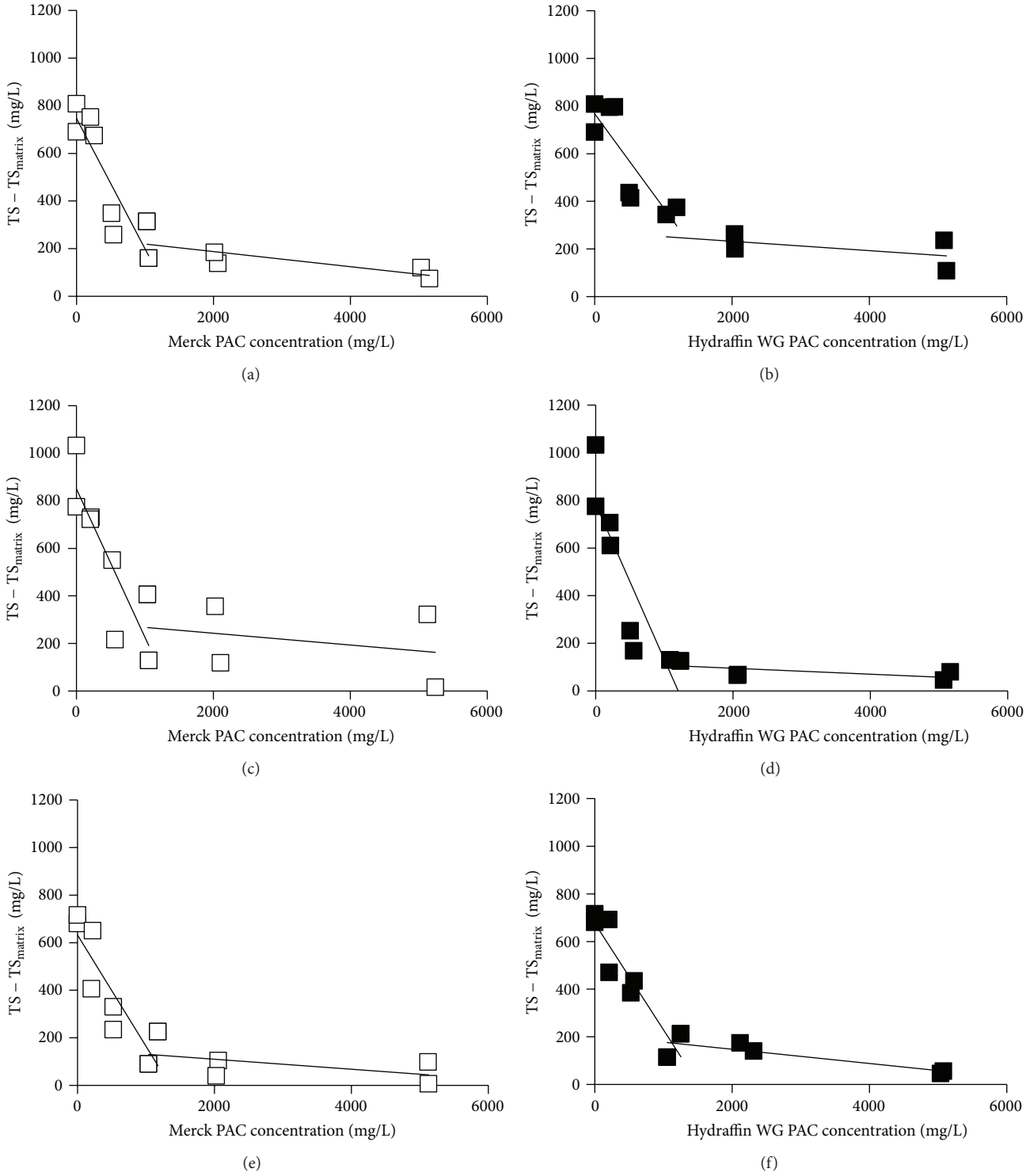

FIGURE 5: Total solids concentrations (corrected for TS concentrations of the matrices) in 1 g/L TiO_2 suspensions containing different amounts of Merck PAC or Hydraffin WG PAC in different matrices ((a), (b): 0.1 g/L $NaHCO_3$ solution; (c), (d): 0.5 g/L $NaHCO_3$ solution; (e), (f): 1 g/L $NaHCO_3$ solution) subsequent to vacuum filtration over spunbond polypropylene fabrics.

WG PAC is more acidic than the Merck PAC (Table 1). When no hydrogen carbonate was added to suspensions containing 1 g/L TiO_2 and 2 g/L PAC, the TiO_2/Hydraffin WG PAC suspensions exhibited a pH of about 3.5, while the pH of the TiO_2/Merck PAC suspensions was in the range of 6.5 to 7 ("Deionized water" and "0.5 g/L NaCl" in Table 2). Replacing the NaCl with 0.5 g/L $NaHCO_3$ increased the pH in the suspensions to 8.0 and 8.4 for Hydraffin WG and Merck

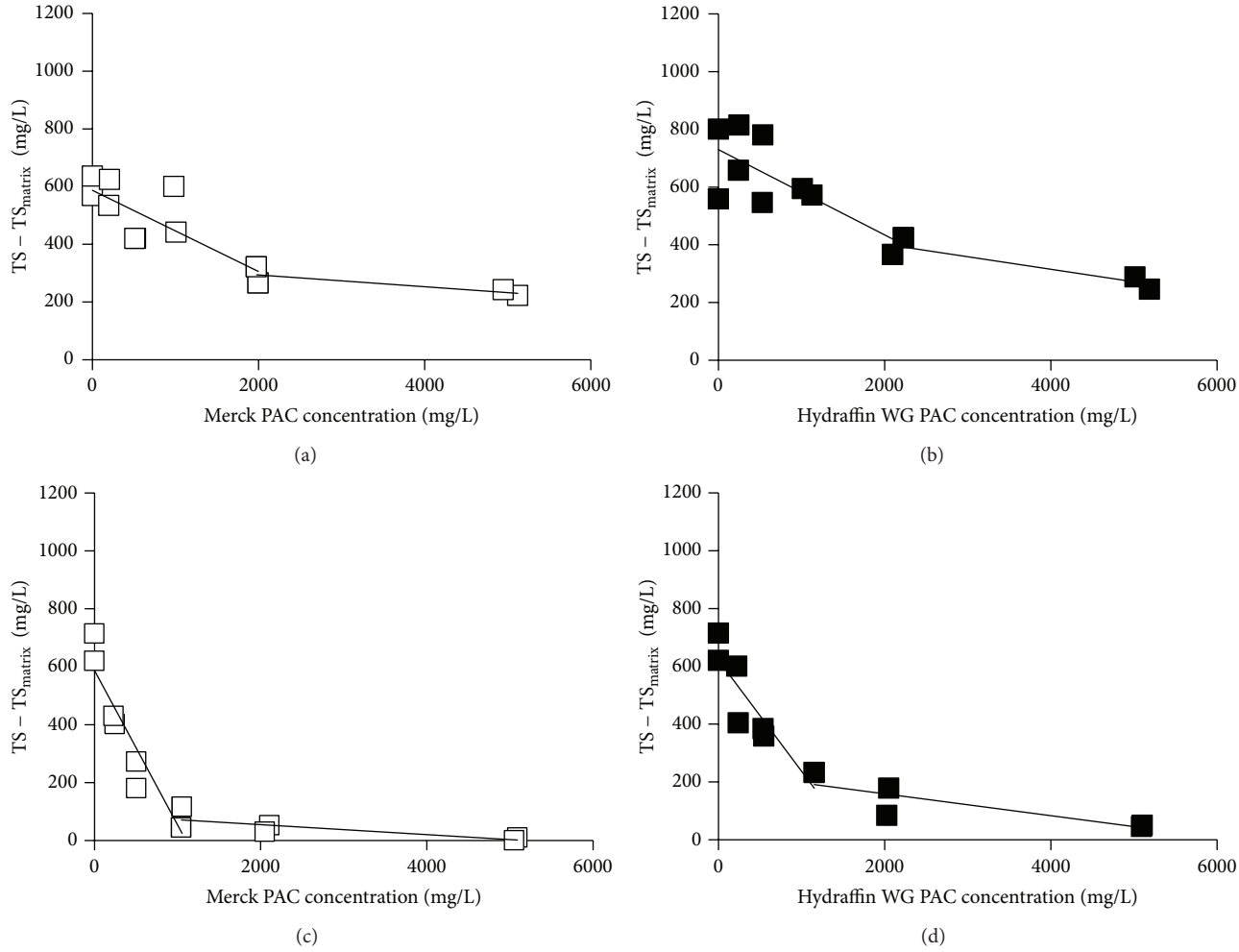

Figure 6: Total solids concentrations (corrected for TS concentrations of the matrices) in 1 g/L TiO_2 suspensions containing different amounts of Merck PAC or Hydraffin WG PAC in a matrix of biologically pretreated greywater ((a), (b)) and secondary municipal effluent ((c), (d)) subsequent to vacuum filtration over spunbond polypropylene fabrics.

Table 2: Impact of aqueous matrix and PAC type on pH of suspensions containing 1 g/L TiO_2 and 2 g/L PAC.

Matrix	pH	
	Merck PAC	Hydraffin WG PAC
Deionized water	6.5	3.5
0.5 g/L NaCl	6.9	3.6
0.5 g/L $NaHCO_3$	8.4	8.0
Biologically treated greywater	8.1	7.4
Secondary municipal effluent	7.7	7.1

PAC, respectively (Table 2). Also in the secondary municipal effluent and in the biologically treated greywater, the pH was above neutral (7.1 to 7.4 for Hydraffin WG and 7.7 to 8.1 for Merck PAC). This is due to some alkalinity in the biologically treated wastewaters predominantly represented by hydrogen carbonate in the pH range of 7 to 8.

Flocculation of the TiO_2 nanoparticles might also have an impact of the wastewater matrix on precoat filtration of nanoparticles. The extent of flocculation is affected by different wastewater constituents as investigated in the first part of this study and also in other studies (e.g., [5]). TiO_2 nanoparticles agglomerated to larger aggregates are retained more efficiently in the PAC filter cake than single nanoparticles. Efficient flocculation of TiO_2 nanoparticles was observed in this study with NaCl concentrations of 1 g/L (Figure 2(a)) and $NaHCO_3$ concentrations between 0 and 1 g/L (Figure 3(a)) when no humic acid was present. Addition of humic acid sodium salt was deteriorating flocculation caused by NaCl or $NaHCO_3$ (Figures 2 and 3) except when pH was between 5.5 and 6.0 (Figure 2(b)). Flocculation impaired by the presence of humic substances might be an explanation for low precoat filtration efficiency in biologically pretreated greywater. However, also secondary municipal effluent contains humic substances formed during biological treatment. As secondary municipal effluent was an excellent matrix for precoat filtration of TiO_2 nanoparticles with Merck PAC in concentrations above 1 g/L (Figure 6(c)), the presence of humic substances cannot be the explanation for deterioration

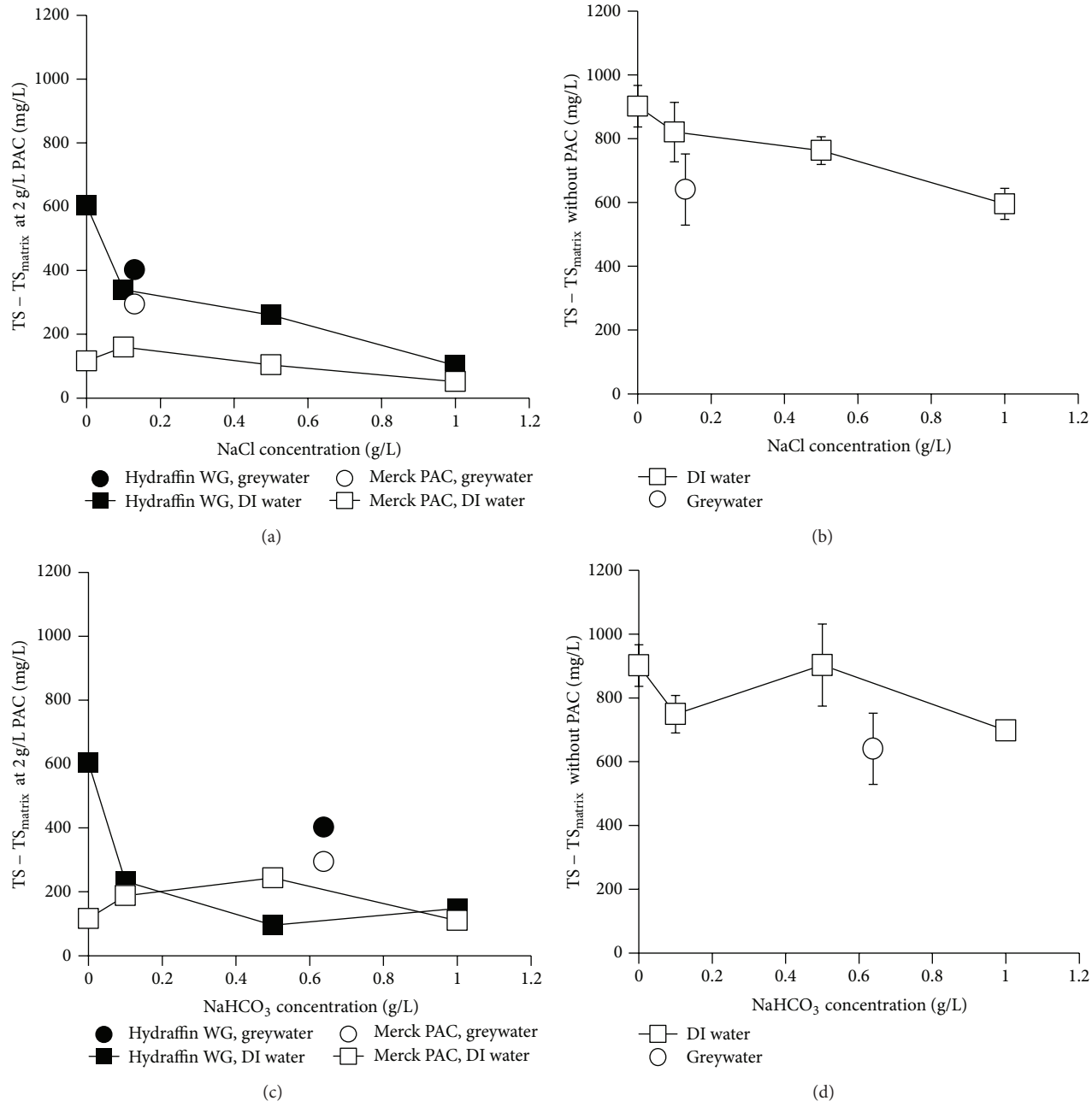

Figure 7: Total solids concentrations (corrected for TS concentrations of the matrices) in 1 g/L TiO_2 suspensions containing 2 g/L PAC ((a), (c)) and in 1 g/L TiO_2 suspensions without any PAC ((b), (d)) at different NaCl ((a), (b)) and $NaHCO_3$ concentrations ((c), (d)) subsequent to vacuum filtration over spunbond polypropylene fabrics.

of precoat filtration. Moreover, TiO_2 flocculation in biologically pretreated greywater was shown to be considerable [5].

Figure 7 summarizes the results displayed in Figures 4, 5, and 6. In Figures 7(a) and 7(c), only the TS concentrations in the filtrates of suspensions containing 1 g/L TiO_2 and 2 g/L PAC are shown depending on the NaCl (Figure 7(a)) and on the $NaHCO_3$ concentrations (Figure 7(c)). As the biologically treated greywater used in this study was not analyzed for chloride or hydrogen carbonate, chloride and alkalinity analyses (2.23 mmol Cl^-/L, 7.6 mmol H^+/L acid-neutralizing capacity) of another biologically treated greywater sample from the same source [5] were used for calculating approximate NaCl and $NaHCO_3$ concentrations. The circles in Figures 7(a) and 7(c) which were based on these approximations indicate that precoat filtration of TiO_2 in a biologically treated greywater matrix is less efficient than in the respective NaCl or $NaHCO_3$ matrices prepared with deionized water. On the other hand, lack of TiO_2 flocculation cannot be looked at as a reason for inefficient precoat filtration with PAC, because in biologically pretreated greywater, TiO_2 flocculation was very

pronounced as shown by the pipet method in another study [5]. Overall, replacement of NaCl with $NaHCO_3$ impaired TiO_2 precoat filtration with the Merck PAC but enhanced precoat filtration with Hydraffin WG PAC. Therefore, in the $NaHCO_3$ matrix, TS concentrations in the filtrates obtained with both PAC types did not differ largely.

When TiO_2 suspensions in different matrices were filtered over the polypropylene fabric without addition of PAC (Figures 7(b) and 7(d)), increasing flocculation due to increased salt concentrations obviously increased particle retention. It has to be noted that in these experiments there was no sufficient time for complete flocculation, because the TiO_2 suspensions in different matrices were filtered over the fabric filters immediately after preparation of the suspensions after a very short stirring period. Nevertheless, with increasing NaCl (Figure 7(b)) and $NaHCO_3$ concentrations (Figure 7(d)) increasing amounts of TiO_2 were retained on the filter. The TiO_2 suspensions in biologically treated greywater showed a better particle retention than expected from the assumed respective NaCl and $NaHCO_3$ concentrations of the greywater when they were not precoated with PAC. This comparably good TiO_2 retention can also be explained by good flocculation of TiO_2 particles in the biologically pretreated greywater.

In a previous study [22] about the hybrid process comprising PCO and PAC adsorption (1 g/L PAC combined with 1 g/L and 5 g/L TiO_2, resp.) with separation and recovery of the photocatalyst/PAC mixture by centrifugation, it was shown that the efficiency for DOC removal from biologically pretreated greywater with a UV dose of 11 W h/L was only slightly decreasing for both TiO_2 concentrations from 84% (with fresh TiO_2/PAC mixtures) to about 71% when the TiO_2/PAC mixtures were reused for the 13th time. It has to be stated that the centrifugation supernatants in that study, although not analyzed for total solids, were similarly turbid by visible inspection as the filtrates in this study when 1 g/L TiO_2 was precoated with 2 g/L PAC. Therefore, the loss of efficiency of the PCO/PAC hybrid process during consecutive solids reuse cycles can be attributed to a slight loss of photocatalyst due to incomplete recovery of photocatalyst by centrifugation.

4. Conclusions

(1) Flocculation of TiO_2 nanoparticles is influenced by ionic strength and pH. In the neutral and slightly basic pH range, humic acid prevents the nanoparticles from agglomeration. Due to complexity of wastewater matrices, the flocculation of TiO_2 particles in real wastewaters is hardly predictable.

(2) Addition of 2 to 5 g/L PAC as a precoat to 1 g/L TiO_2 nanoparticle suspensions substantially increases nanoparticle retention by filter fabrics which are usually not able to retain the nanoparticles.

(3) Efficiency of TiO_2 nanoparticle precoat filtration is also influenced to some extent by selection of the PAC type and by the concentrations and types of constituents of the solution matrix.

(4) Precoat filtration of TiO_2 with PAC is feasible for technical application in the photocatalytic oxidation process, because in the PAC/PCO hybrid process PAC removes organic wastewater constituents by adsorption additional to photocatalytic oxidation.

(5) Precoat filtration with PAC can retain > 90% of TiO_2 nanoparticles. It is thus a suitable pretreatment for further nanoparticle removal, for example, by membrane filtration.

Conflict of Interests

The authors declare that there is no conflict of interests regarding the publication of this paper.

Acknowledgments

The authors greatly acknowledge the support of this study by Kristina Chmelov and Etienne Jepson during their internships at the Institute of Wastewater Management and Water Protection.

References

[1] P. Paraskeva and N. J. D. Graham, "Ozonation of municipal wastewater effluents," *Water Environment Research*, vol. 74, no. 6, pp. 569–581, 2002.

[2] M. Klavarioti, D. Mantzavinos, and D. Kassinos, "Removal of residual pharmaceuticals from aqueous systems by advanced oxidation processes," *Environment International*, vol. 35, no. 2, pp. 402–417, 2009.

[3] A. Dabrunz, L. Duester, C. Prasse et al., "Biological surface coating and molting inhibition as mechanisms of TiO_2 nanoparticle toxicity in daphnia magna," *PLoS ONE*, vol. 6, no. 5, Article ID e20112, 2011.

[4] L. K. Limbach, R. Bereiter, E. Müller, R. Krebs, R. Gälli, and W. J. Stark, "Removal of oxide nanoparticles in a model wastewater treatment plant: influence of agglomeration and surfactants on clearing efficiency," *Environmental Science & Technology*, vol. 42, no. 15, pp. 5828–5833, 2008.

[5] A. Armanious, A. Özkan, U. Sohmen, and H. Gulyas, "Inorganic greywater matrix impact on photocatalytic oxidation: does flocculation of TiO_2 nanoparticles impair process efficiency?" *Water Science & Technology*, vol. 63, no. 12, pp. 2808–2813, 2011.

[6] I. Chowdhury, Y. Hong, R. J. Honda, and S. L. Walker, "Mechanisms of TiO_2 nanoparticle transport in porous media: Role of solution chemistry, nanoparticle concentration, and flowrate," *Journal of Colloid and Interface Science*, vol. 360, no. 2, pp. 548–555, 2011.

[7] W. Pang, N. Gao, Y. Deng, and Y. J. Tang, "Novel photocatalytic reactor for degradation of DDT in water and its optimization model," *Journal of Zhejiang University SCIENCE A*, vol. 10, no. 5, pp. 732–738, 2009.

[8] R. I. Bickley, M. J. Slater, and W.-J. Wang, "Operating experience and performance evaluation of a photocatalytic reactor," *Process Safety and Environmental Protection*, vol. 83, no. 3, pp. 217–223, 2005.

[9] N. Xu, Z. Shi, Y. Fan, J. Dong, J. Shi, and M. Z. C. Hu, "Effects of particle size of TiO_2 on photocatalytic degradation of methylene

blue in aqueous suspensions," *Industrial & Engineering Chemistry Research*, vol. 38, no. 2, pp. 373–379, 1999.

[10] C. Aprile, A. Corma, and H. Garcia, "Enhancement of the photocatalytic activity of TiO_2 through spatial structuring and particle size control: from subnanometric to submillimetric length scale," *Physical Chemistry Chemical Physics*, vol. 10, no. 6, pp. 769–783, 2008.

[11] K. Sopajaree, S. A. Qasim, S. Basak, and K. Rajeshwar, "An integrated flow reactor-membrane filtration system for heterogeneous photocatalysis—part II: experiments on the ultrafiltration unit and combined operation," *Journal of Applied Electrochemistry*, vol. 29, no. 9, pp. 1111–1118, 1999.

[12] T. E. Doll and F. H. Frimmel, "Cross-flow microfiltration with periodical back-washing for photocatalytic degradation of pharmaceutical and diagnostic residues-evaluation of the long-term stability of the photocatalytic activity of TiO_2," *Water Research*, vol. 39, no. 5, pp. 847–854, 2005.

[13] H. Gulyas, A. S. Oria Argáez, F. Kong, C. F. Liriano Jorge, S. Eggers, and R. Otterpohl, "Combining activated carbon adsorption with heterogeneous photocatalytic oxidation: lack of synergy for biologically treated greywater and tetraethylene glycol dimethyl ether," *Environmental Technology*, vol. 34, no. 11, pp. 1393–1403, 2013.

[14] J. Matos, A. Garcia, T. Cordero, J.-M. Chovelon, and C. Ferronato, "Eco-friendly TiO_2—AC photocatalyst for the selective photooxidation of 4-chlorophenol," *Catalysis Letters*, vol. 130, no. 3-4, pp. 568–574, 2009.

[15] N. G. Asenjo, R. Santamaría, C. Blanco, M. Granda, P. Álvarez, and R. Menéndez, "Correct use of the Langmuir-Hinshelwood equation for proving the absence of a synergy effect in the photocatalytic degradation of phenol on a suspended mixture of titania and activated carbon," *Carbon*, vol. 55, pp. 62–69, 2013.

[16] J. Matos, J. Laine, and J.-M. Herrmann, "Synergy effect in the photocatalytic degradation of phenol on a suspended mixture of titania and activated carbon," *Applied Catalysis B*, vol. 18, no. 3-4, pp. 281–291, 1998.

[17] H. Gulyas, M. Reich, and R. Otterpohl, "Organic micropollutants in raw and treated greywater: a preliminary investigation," *Urban Water Journal*, vol. 8, no. 1, pp. 29–39, 2011.

[18] H. Gulyas, C. F. Liriano Jorge, M. Reich, and R. Otterpohl, "Reclaiming biologically pretreated greywater for reuse by photocatalytic oxidation. Qualitative study on the removal of trace rganics," *Journal of Water Resource and Protection*, vol. 5, pp. 568–584, 2013.

[19] L. J. Banasiak and A. I. Schäfer, "Removal of boron, fluoride and nitrate by electrodialysis in the presence of organic matter," *Journal of Membrane Science*, vol. 334, no. 1-2, pp. 101–109, 2009.

[20] J. Matos, J. Laine, J.-M. Herrmann, D. Uzcategui, and J. L. Brito, "Influence of activated carbon upon titania on aqueous photocatalytic consecutive runs of phenol photodegradation," *Applied Catalysis B*, vol. 70, no. 1–4, pp. 461–469, 2007.

[21] C. Moreno-Castilla, "Adsorption of organic molecules from aqueous solutions on carbon materials," *Carbon*, vol. 42, no. 1, pp. 83–94, 2004.

[22] H. Gulyas, P. Choromanski, N. Muelling, and M. Furmanska, "Toward chemical-free reclamation of biologically pretreated greywater: solar photocatalytic oxidation with powdered activated carbon," *Journal of Cleaner Production*, vol. 17, no. 13, pp. 1223–1227, 2009.